PRODUCTION AND BIOMINERALIZATION PERFORMANCE ASSESSMENT OF BIOGRANULES SIMULTANEOUSLY CONDUCTING UREA HYDROLYSIS AND DENITRIFICATION

SİMÜLTANE OLARAK ÜRE HİDROLİZİ VE DENİTRİFİKASYON YAPABİLEN BİYOGRANÜLLERİN ÜRETİMİ VE BİYOMİNERALİZASYON PERFORMANSLARININ DEĞERLENDİRİLMESİ

BEYZA KARDOĞAN

ASSOC. PROF. DR. YUSUF ÇAĞATAY ERŞAN

Supervisor

Submitted to

Graduate School of Science and Engineering of Hacettepe University

as a Partial Fulfilment to the Requirements for the Award of the Degree of Master of Science in Environmental Engineering

2024

to the pursuit of knowledge, driven by curiosity and love

ABSTRACT

PRODUCTION AND BIOMINERALIZATION PERFORMANCE ASSESSMENT OF BIOGRANULES SIMULTANEOUSLY CONDUCTING UREA HYDROLYSIS AND DENITRIFICATION

Beyza KARDOĞAN

Master of Science, Department of Environmental Engineering

Supervisor: Assoc. Prof. Dr. Yusuf Çağatay ERŞAN

June 2024, 150 pages

Biomineralization, particularly calcium carbonate precipitation through microbial pathways, is gaining attention as an environmentally friendly alternative for various applications, including bioremediation, bioconsolidation, and the production of bio-based materials. Calcium carbonate precipitation naturally occurs through various metabolic pathways, such as urea hydrolysis and nitrate reduction. However, most studies have focused on axenic (pure) cultures and single metabolic processes, leaving the potential of combined metabolic activities unexplored. Using single metabolic pathways and axenic cultures resulted in biomineralization performances under either aerobic or anoxic conditions. Urea hydrolysis and nitrate reduction are complementary to achieving biomineralization under both aerobic and anoxic conditions. This should be investigated to enhance the overall biomineralization performance. This thesis presents the production of non-axenic biogranules capable of conducting urea hydrolysis and nitrate reduction metabolisms. These biogranules could extend the occurrence of the biomineralization

process in both aerobic and anoxic conditions and enhance the overall calcium carbonate precipitation. An SBR was operated for 560 days under alternating anoxic-aerobic periods and biogranule production under minimal nutrient conditions was optimized. Produced biogranules were compared with a previously reported nitrate-reducing granular culture in terms of microbial activity and biomineralization performance. Biogranules in the size range of 0.2-0.7 mm could be produced continuously during the steady production period between operation days 270 and 560. Metagenomic analyses revealed a consistent microbial community dominated by ureolytic and denitrifying bacteria, maintaining a high degree of similarity across samples taken at different time intervals from the bioreactor. The produced biogranules achieved maximum specific urea hydrolysis and nitrate reduction activities of 232 mg urea.h^{-1}.g^{-1} VSS and 9.25 mg NO_3-N.h^{-1}.g^{-1} VSS, respectively. In 9-day batch tests, the biogranules precipitated up to 642.5 mg $CaCO_3$ in calcite form, which was significantly higher than the 137 mg $CaCO_3$ obtained by the reference nitrate-reducing granular culture. The desiccated biogranules demonstrated 73% nitrate reduction and 67% urea hydrolysis efficiency on average in the biomineralization test. However, reference nitrate-reducing granular culture showed 34% nitrate reduction and 2% urea hydrolysis efficiency on average. To see the shelf-life effect on MICP performance another biomineralization test was conducted after 1.5 years of storage of the desiccated biogranules. When comparing the yeast-containing batches B1 and C1 with the yeast-free batches B3 and C3, it was found that biogranules exhibited a 30% and 164% higher MICP performance, respectively, compared to the reference nitrate-reducing granular culture in the second biomineralization test. It was observed that the storage period negatively impacted the MICP performance of the desiccated biogranules. Overall, it was revealed that complementary microbial metabolisms could enhance the total amount of $CaCO_3$ precipitated in a single application which can be beneficial for improving the efficiency of biomineralization applications.

Keywords: MICP, nitrate reduction, biodeposition, metagenomics, resuscitation

ÖZET

SİMÜLTANE OLARAK ÜRE HİDROLİZİ VE DENİTRİFİKASYON YAPABİLEN BİYOGRANÜLLERİN ÜRETİMİ VE BİYOMİNERALİZASYON PERFORMANSLARININ DEĞERLENDİRİLMESİ

Beyza KARDOĞAN

Yüksek Lisans, Çevre Mühendisliği Bölümü

Tez Danışmanı: Doç. Dr. Yusuf Çağatay Erşan

Haziran 2024, 150 sayfa

Biyomineralizasyon, özellikle mikrobiyal yollarla kalsiyum karbonat çökelmesi, biyoremediasyon, biyokonsolidasyon ve biyo-bazlı malzemelerin üretimi gibi çeşitli uygulamalar için çevre dostu bir alternatif olarak ilgi görmektedir. Kalsiyum karbonat çökelmesi, doğada üre hidrolizi ve nitrat indirgenmesi gibi çeşitli metabolik yollarla gerçekleşebilmektedir. Ancak, çoğu çalışma saf kültürler ve tekil metabolik süreçler üzerine odaklanmış olup, birleştirilmiş metabolik aktivitelerin potansiyelini araştırmamıştır. Tekil metabolik yollar ve aksenik kültürlerin kullanılması ya aerobik ya da anoksik koşullar altında biyomineralizasyon performanslarının elde edilmesiyle sonuçlanmıştır. Üre hidrolizi ve nitrat indirgenmesi hem aerobik hem de anoksik koşullar altında biyomineralizasyonu gerçekleştirmek için tamamlayıcı yollardır. Bu kombinasyonun araştırılması, genel biyomineralizasyon performansını artırmak için önem arz etmektedir. Bu tez çalışması, üre hidrolizi ve nitrat indirgeme metabolizmalarını kullanabilen aksenik olmayan biyogranüllerin üretimini sunmaktadır. Bu biyogranüller, biyomineralizasyon sürecinin hem aerobik hem de anoksik koşullarda gerçekleşmesini

sağlayarak genel kalsiyum karbonat çökeltme miktarını artırabilmektedir. Bir AKR (Ardışık Kesikli Reaktör), değişen anoksik-aerobik periyotlar altında 560 gün boyunca işletilmiş ve minimal besin koşullarında biyogranül üretimi optimize edilmiştir. Üretilen biyogranüller, mikrobiyal aktivite ve biyomineralizasyon performansı açısından daha önce raporlanan nitrat indirgeyen granül kültürü ile karşılaştırılmıştır. İşletim günleri 270 ile 560 arasında 0.2-0.7 mm aralığında biyogranüllerin kararlı üretimi sağlanmıştır. Metagenomik analizler, biyoreaktörden farklı zaman aralıklarında alınan örneklerde, ürolitik ve denitrifikasyon yapan bakterilerin baskın olduğu tutarlı bir mikrobiyal topluluğu ortaya koymuştur. Üretilen biyogranüller, sırasıyla 232 mg üre.sa^{-1}.g^{-1} UAKM ve 9,25 mg NO_3-N.sa^{-1}.g^{-1} UAKM maksimum spesifik üre hidrolizi ve nitrat indirgeme aktivitelerine ulaşmıştır. Biyomineralizasyon testlerinde 9 gün içerisinde, biyogranüller kalsit formunda maksimum 642,5 mg $CaCO_3$ çökeltirken, referans nitrat indirgen granül kültürü maksimum 137 mg $CaCO_3$ çökeltmiştir. Kurutulmuş biyogranüller, biyomineralizasyon testinde ortalama %73 nitrat indirgeme ve %67 üre hidrolizi verimliliği gösterirken, referans nitrat indirgen granül kültürü ortalama %34 nitrat indirgeme ve %2 üre hidrolizi verimliliği göstermiştir. MICP performansına raf ömrünün etkisini görmek için kurutulmuş biyogranüller 1,5 yıl saklandıktan sonra başka bir biyomineralizasyon testi yapılmıştır. Test sonucunda saklama süresinin, kurutulmuş biyogranüllerin MICP performansını olumsuz etkilediği gözlemlenmiştir Maya özütü içeren B1 ve C1 ile maya özütü içermeyen B3 ve C3 grupları karşılaştırıldığında, biyogranüllerin ikinci biyomineralizasyon testinde referans nitrat indirgen granül kültürüne göre sırasıyla %30 ve %164 daha yüksek MICP performansı sergilediği bulunmuştur. Genel olarak, tamamlayıcı mikrobiyal metabolizmaların, tek bir uygulamada çökeltilen toplam $CaCO_3$ miktarını artırarak biyomineralizasyon uygulamalarının verimliliğini artırabileceği ortaya konulmuştur.

Anahtar Kelimeler: MICP, nitrat indirgenmesi, biyobirikim, metagenomik, canlanma

ACKNOWLEDGMENT

This journey has been a mosaic of contributions from remarkable individuals, each adding a unique piece to the puzzle that is this thesis.

First and foremost, I am immensely grateful to my supervisor, Assoc. Prof. Dr. Yusuf Çağatay Erşan whose expertise and dedication have been integral to the completion of this thesis. His profound knowledge and exceptional skills in engineering have not only guided my research but have also inspired me to strive for excellence. Every discussion with him has been profoundly enlightening, and his unique contributions have significantly shaped the course of this work. His constructive feedback and insightful suggestions have continually pushed me to enhance and refine my research.

I would also like to thank the members of my thesis committee, Prof. Dr. Hülya Yavuz Ersan, Prof. Dr. Tuba Hande Ergüder Bayramoğlu, Prof. Dr. Selim Latif Sanin, and Assoc. Prof. İlknur Durukan Temuge for their constructive suggestions.

I am particularly thankful to LabMInE team members who are Kadir Şekercioğlu, Betül Özbay, Mevlüt Soluk, and Rabia Konakcı for providing a collaborative and stimulating environment, which contributed to the progress of my work.

I would also like to acknowledge the financial support received from The Scientific and Technological Research Council of Turkey (TUBITAK) under project number 120Y291.

Last but not least, I am deeply grateful to my family and my dearest closest Kaan Arda Ünver and Sedanur Çetinkaya for their unwavering support and belief in me. Their encouragement and belief in my abilities have been invaluable, especially during times when I felt overwhelmed or discouraged. Their love and understanding have been a bedrock of stability, enabling me to keep moving forward. This accomplishment would not have been possible without them.

TABLE OF CONTENTS

LIST OF FIGURES

LIST OF TABLES

ABBREVIATIONS

AGS	Aerobic Granular Sludge
BCM	Biologically Controlled Mineralization
BIM	Biologically Induced Mineralization
CA	Carbonic Anhydrase
CAS	Conventional Activated Sludge
COD	Chemical Oxygen Demand
DIC	Dissolved Inorganic Carbon
DO	Dissolved Oxygen
EPS	Extra Polymeric Substances
GFS	Granule-Forming Substrates
MICP	Microbially Induced Calcium Carbonate Precipitation
OLR	Organic Loading Rate
SEM	Scanning Electron Microscope
SRB	Sulfate-Reducing Bacteria
SBR	Sequencing Batch Reactor
SRT	Solid Retention Time
SVI	Sludge Volume Index
UASB	Up-Flow Anaerobic Sludge Blanket

1. INTRODUCTION

The global sustainability crisis is intensifying as the pervasive use of non-biodegradable and contaminating materials increasingly endangers natural environments and biological life. The rise in environmental consciousness along with the adoption of laws that support sustainable and renewable technologies, has led to an increase in interest in biotechnology and foster using biobased products rather than materials produced based on linear economic models.

As a part of the biotechnological perspective, biomineralization, particularly calcium carbonate precipitation through microbial pathways, has been extensively investigated as an environmentally friendly technique in various Environmental and Civil Engineering fields. Biomineralization applications including radionuclide and heavy metal removal, ground improvement, restoration of historical heritages and monuments, carbon dioxide sequestration, bio brick production, and developing self-healing bioconcrete are key tools to achieve sustainable development and combat climate change in cities [1–7]. Thus, microbial-induced calcium carbonate precipitation efficiency should be enhanced and bioagents tailored for biomineralization applications should be stably produced.

The microbial-induced calcium carbonate precipitation (MICP) can occur through numerous distinct metabolic pathways consisting of urea hydrolysis, denitrification, photosynthesis, aerobic oxidation, sulfate reduction, methane oxidation, ammonification, and iron reduction [8,9]. The most extensively researched metabolic pathway of applied MICP so far is urea hydrolysis catalyzed by urease in high calcium concentrations due to its simplicity and reaction rate. In this process, urease (urea amidohydrolase) positive bacteria (*Sporosorcina pasteurii, Bacillus sphaericus, Bacillus megaterium*, etc.) hydrolyze urea and eventually ammonium, bicarbonate, and hydroxide ions are formed [3]. These formed ions increase pH, thus shifting the bicarbonate balance towards carbonate ions. When free calcium ions are available in the environment, $CaCO_3$ minerals with low solubility ($K_{sp} = 3.8 \times 10^{-9}$) are formed and precipitation occurs.

Although significant research efforts have been focused on investigating urea hydrolysis owing to its notable efficiency, it has some disadvantages. Biominerals rapidly precipitate around the cell membrane due to the high ureolysis rate, causing occlusion of bacteria and limitation of nutrient transfer. This phenomenon negatively affects microorganism activities [8]. Furthermore, urease-positive bacteria require oxygen to maintain growth

and urease enzyme production. It was reported that the urease enzyme, produced under aerobic conditions, retained activity for a period under anaerobic conditions, the bacterium could not sustain growth or produce new enzymes in both anoxic and anaerobic conditions. Thus, the amount of precipitated minerals drops significantly when moving from aerobic anaerobic conditions [2,10].

In the metabolism of nitrate reduction, calcium carbonate precipitation can occur even when oxygen is limited or absent, as nitrate serves as the electron acceptor. Consequently, the nitrate reduction mechanism can be presented as an alternative pathway to urea hydrolysis to obtain MICP in the absence of oxygen. In this context, some researchers have explored the application of nitrate reduction metabolism in biomineralization practices such as soil consolidation, the removal of calcium from wastewater, and the development of self-healing bioconcrete [11–13]. In the soil consolidation field, a study conducted by van Paassen et al. employed denitrification metabolism by using *Castellaniella denitrificans* and achieved a yield of 6 grams of $CaCO_3$ per consumed gram of nitrate nitrogen after seven days [13]. Another study by Ersan et al. demonstrated an enhancement in efficiency, reaching 14.1 and 18.9 grams of $CaCO_3$ per consumed gram of nitrate nitrogen within two days, following optimization, using *Pseudomonas aeruginosa* and *Diaphorobacter nitroreducens*, respectively [14].

Overall calcium carbonate yield can theoretically be increased when aerobic and anaerobic metabolisms such as urea hydrolysis and denitrification metabolisms are employed simultaneously. Moreover, in environments with a specific depth (where there is no oxygen limitation at the surface, but oxygen concentration decreases with increasing depth), urea hydrolysis and nitrate reduction metabolisms can be considered complementary mechanisms [15]. In this scenario, simultaneous biomineralization can occur at different oxygen concentrations.

In addition to all studies using axenic cultures, biogranules formed through the non-axenic microbial cultures' granulation have the potential to economically enhance biomineralization capacity through the management of the community within the granule content using a microbial source management approach. The biogranules are mainly used in Environmental and Construction Engineering fields. On the one hand, in the field of Environmental Engineering, biogranules have been applied for the treatment of wastewater from both domestic and industrial sources. The granular sludge-based wastewater treatment system has been developed to decrease the land requirement,

increase process efficiency, and enable resource recovery. On the other hand, in the field of Construction Engineering, biogranules are utilized for self-healing bioconcrete development. The lifespan of the buildings can be increased with self-healing bioconcrete applications. Considering the concrete production carbon footprint, self-healing applications contribute to sustainable development. Therefore, biogranules are crucial microbial agents to extend the use of microorganisms in creating a bio-based circular economy.

2. LITERATURE REVIEW

2.1. Microbially Induced Calcium Carbonate Precipitation (MICP)

Biomineralization refers to the formation of minerals such as carbonates, sulfates, phosphates, and silicates by living organisms through various metabolic pathways. It is a natural occurrence that can be observed in nature, from bacteria to animals, and can take the form of bones, corals, certain rocks, shells, and minerals [16].

The synthesis of biominerals by organisms can be divided into three biological categories based on the formation mechanism: controlled, induced, and influenced mineralization [17,18]. Biologically controlled mineralization (BCM) refers to the process by which an organism exerts precise control over the nucleation, shape, and location of the biominerals [8]. The process occurs at a certain location in or on the cell. Whereas, in biologically induced mineralization (BIM) biominerals are synthesized extracellularly due to the chemical reactions that occur as a consequence of metabolic activity rather than cell control. Biominerals are precipitated through the interaction of microorganisms' metabolic byproducts with ions present in the surrounding environment. In biologically influenced mineralization minerals are generated through the interaction between an organic matrix and various organic and inorganic compounds by external environmental factors. This process does not involve any biological activity, whether it is extracellular or intracellular [18].

The most common biominerals formed through the mechanisms described above are composed of primarily calcium, given its vital role in numerous processes within an organism's cellular metabolism.

Carbonates are particularly noteworthy among the minerals formed in biomineralization and Microbially Induced Calcium Carbonate Precipitation (MICP) is one of the most widely studied kinds of biomineralization phenomena [19].

MICP process initiates in the microenvironment surrounding microbial cells where various metabolic byproducts such as bicarbonate and calcium ions first interact to form $CaCO_3$ minerals. This process is driven by the metabolic activity of microorganisms and can be utilized for a wide range of applications such as sequestration of atmospheric CO_2, soil stabilization, bioremediation, concrete repair, and restoration of heritage structures

[8,20]. Due to its versatility and potential for sustainable development, the study of MICP has become an essential area of research.

2.2 Metabolic Pathways of MICP

The phenomenon of MICP can be initiated through multiple metabolic pathways. These metabolic pathways were summarized with their advantages and disadvantages in Table 2.1. Given their prominence among the metabolic pathways outlined in the table, urea hydrolysis and denitrification are elucidated in detail below.

Urea hydrolysis by ureolytic bacteria is considered one of the most widely used biochemical pathways in MICP due to some reasons such as high reaction rate via urease enzyme, ease of application, and hydrolysis of urea is a common trait of most of the non-pathogenic strains [21].

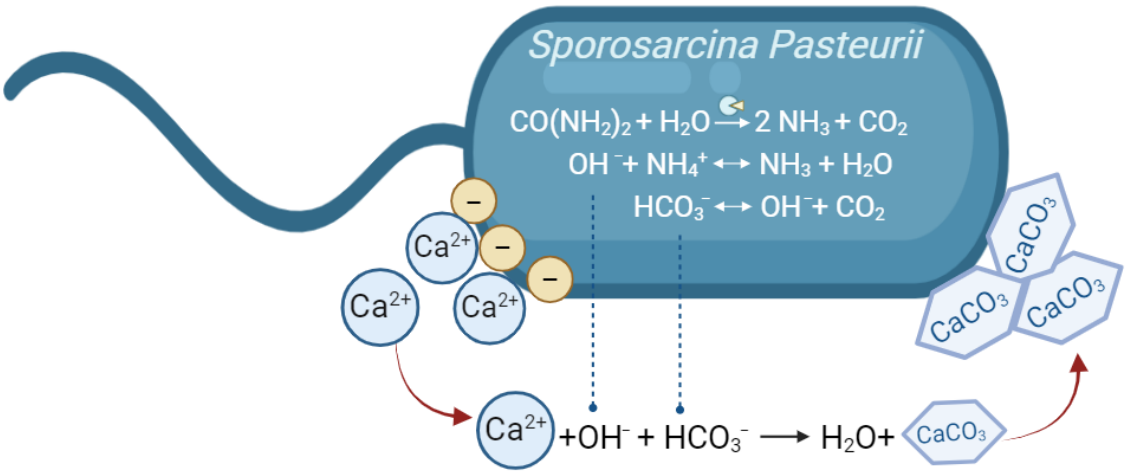

Figure 2.1. Schematic representation of MICP catalyzed by cells of the *S. pasteurii* redrafted after [16]

In this metabolic pathway, urease (urea amidohydrolase) positive bacteria *(Sporosorcina pasteurii (Bacillus pasteurii), Bacillus sphaericus, Bacillus megaterium*, etc.) hydrolyze the urea and first decompose it into one mole of carbamate and ammonium (Equation 1). With continued hydrolysis reactions, one more mole of ammonium and carbonic acid is formed. By balancing these products in water hydroxide ions, bicarbonate and two moles of ammonium are formed. These formed ions cause the pH to rise, and the increase in pH alters the bicarbonate balance, enabling the formation of carbonate ions (Equation 1-6).

Table 2.1. Metabolic Pathways of MICP

Metabolic Pathway	Microorganism	Advantages	Disadvantages	References
Photosynthesis	• Cyanobacteria • (Micro-)Algae	• No toxic by-product	• Limited application due to dependency on sunlight and CO_2	[4,8,22–24]
Urea Hydrolysis	• Ureolytic bacteria	• Fast and straightforward process	• NH_3 and NH_4^+ production (Aquatic toxicity) • Oxygen dependency for bacterial growth	[1,2,21,25,26]
Aerobic Oxidation	• Non-ureolytic aerobic bacteria	• Versatile, simple process	• Oxygen dependency • Dependence on external alkalinity	[1,27,28]
Ammonification	• Myxobacteria	• High versatility in applications	• Poor solubility of reagents • NH_3 and NH_4^+ production (Toxic by-product)	[27,29,30]
Sulfate Reduction	• Sulfate-reducing bacteria (SRB)	• Can be applied in anoxic and extreme environments	• H_2S production (Highly toxic and odorous by-product) • Biogenic corrosion	[24,27,30,31]
Iron Reduction	• Iron-reducing bacteria	• Stable process • No toxic byproduct • Iron leach/corrosion	• Relatively slow precipitation rates compared to other pathways	[32,33]
Methane Oxidation	• Methanotrophs	• Scalability and adaptability of applications	• H_2S production (Type II methanotrophs) (Highly toxic byproduct)	[8,24,25,34,35]
Nitrate Reduction	• Denitrifiers	• Can be applied in anoxic and anaerobic environments	• Relatively slower precipitation rate compared to urea hydrolysis • Possibility of greenhouse gas production • Nitrite ions can accumulate (Harmful to aquatic ecosystems)	[24,25,30,31,36]

If free calcium ions are present in the environment, the cell's negative surface gathers them and serves as the site of nucleation. Then calcium carbonate minerals with low solubility (Ksp = 3.8 x 10^{-9}) are formed and precipitation occurs (Equation 6) [3] .

$$CO(NH_2)_2 + H_2O \rightarrow NH_2COOH + NH_3 \quad (1)$$

$$NH_2COOH + H_2O \rightarrow NH_3 + H_2CO_3 \quad (2)$$

$$H_2CO_3 \leftrightarrow HCO_3^- + H^+ \quad (3)$$

$$2NH_3 + 2H_2O \leftrightarrow 2NH_4^+ + 2OH^- \quad (4)$$

$$HCO_3^- + H^+ + 2NH_4+ + 2OH^- \leftrightarrow CO_3^{2-} + 2NH_4^+ + 2H_2O \quad (5)$$

$$CO_3^{2-} + Ca^{2+} \leftrightarrow CaCO_3 \quad (6)$$

Sporosarcina pasteurii is a gram-positive bacterium that originates from the soil. Its growth necessitates the presence of urea and ammonium and possesses the capacity to produce spores as a survival mechanism when exposed to challenging environmental conditions. Among the cohort of ureolytic microorganisms, *S. pasteurii* emerges as the predominant strain studied in the domain of biomineralization owing to its high urease activity [21].

Although urea hydrolysis is an effective microbial pathway that has been extensively studied in MICP, it has some drawbacks. The reaction rate causes $CaCO_3$ minerals to rapidly precipitate around the cell membrane, which restricts microbial activity and may eventually lead to the microorganism's vital activities' termination [8]. In addition, since urease-positive bacteria are not omnipresent in certain environmental conditions, microbial activity is adversely affected in some situations, such as oxygen and nutrient deficiencies, highly alkaline pH, and elevated salt concentrations [2,25]. In a study conducted by Li et al., the impact of available oxygen levels on the quantity of $CaCO_3$ precipitated through microbial means in urea hydrolysis metabolism was systematically investigated. The research, which focused on ground improvement utilizing *S. pasteurii*, scrutinized the amount of $CaCO_3$ precipitation in columns subjected to aerated, open, and air-restricted conditions. The findings revealed a substantial reduction in the precipitated $CaCO_3$ quantity as the level of air restriction increased. After the biomineralization process, the percentage $CaCO_3$ contents of the sand samples were determined as 4.03-9.88%, 2.9-4.5%, and 1.4-1.9% in aerated, open, and air-restricted conditions, respectively [10].

In a separate investigation carried out by Jain et al., the biomineralization test using *S. pasteurii*, as a result of 72 hours of incubation, 32.24 ± 3 mg, 17.38 ± 3 mg, 7 ± 2 mg $CaCO_3$ precipitation was observed in 100 mL biomineralization solution under aerobic, anoxic, and anaerobic conditions, respectively. It has been reported that the amount of precipitated minerals drops significantly when moving from aerobic to anoxic conditions and is negligible in the anaerobic condition [2].

The process of biomineralization facilitated by ureolytic bacteria results in the substantial generation of ammonia as a consequential byproduct. Due to the aquatic toxicity of the latter, urea hydrolysis might raise environmental concerns in MICP applications near water resources[26]. Furthermore, depending on the type of the urease enzyme, the accumulation of ammonia can impede the MICP process, leading to suboptimal precipitation. Optimum performances could only be achieved with strains possessing non-suppressive urease enzyme [37]. If the produced ammonia is further oxidized on site, it results in a local pH decrease and dissolution of the precipitated $CaCO_3$ [1].

The nitrate reduction process, known as denitrification, plays a crucial role in the global nitrogen cycle by enabling the conversion of fixed nitrogen back into nitrogen gas, thereby facilitating its return to the atmosphere. By accomplishing this crucial transformation, denitrification is essential in closing the global nitrogen cycle and maintaining the balance in the ecosystems. Most denitrifying microorganisms conduct complete nitrate reduction when organic carbon and nitrate coexist under anoxic conditions. Recent studies also revealed the possibility of autotrophic denitrification and aerobic denitrification [38]. Among these processes, MICP through autotrophic denitrification is unlikely due to its dissolved inorganic carbon consumption. MICP through aerobic denitrification on the other hand remains unknown.

In anoxic denitrification, anaerobic microorganisms classified within taxonomic genera such as *Pseudomonas*, *Diaphorobacter*, *Denitrobacillus*, *Alcaligenes*, *Thiobacillus*, *Micrococcus*, and others are involved in the consecutive enzymatic conversion of nitrate (NO_3^-) into elemental nitrogen gas (N_2) during the oxidation of organic carbon (Equations 7-10) [24,25]. In the presence of dissolved calcium ions (Ca^{2+}), the reduction of NO_3^- culminates in the precipitation of $CaCO_3$ (Equation 11).

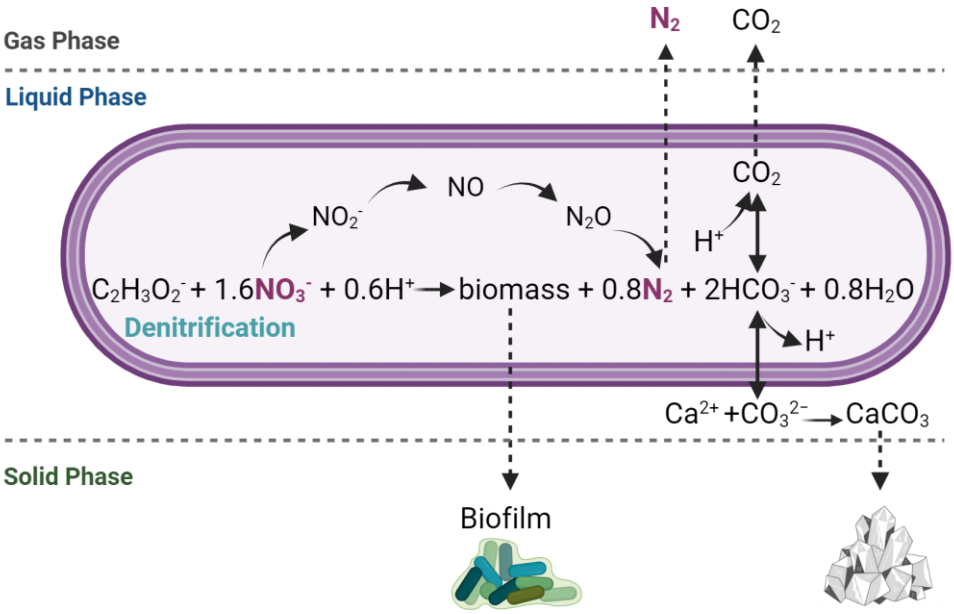

Figure 2.2. The complete denitrification reactions for MICP redrafted after [25]

$$4NO_3^- + 2HCOO^- + 2H^+ \xrightarrow{nitrate\ reductase} 2NO_2^- + 2CO_2 + 2H_2O \quad (7)$$

$$2NO_2^- + HCOO^- + 3H^+ \xrightarrow{nitrate\ reductase} 2NO + CO_2 + 2H_2O \quad (8)$$

$$2NO + HCOO^- + H^+ \xrightarrow{nitric-oxide\ reductase} 2N_2O + CO_2 + 2H_2O \quad (9)$$

$$2N_2O + HCOO^- + H^+ \xrightarrow{nitrous-oxide\ reductase} N_2 + CO_2 + 2H_2O \quad (10)$$

$$Ca^{2+} + CO_2 + H_2O \rightarrow CaCO_3 + 2H^+ \quad (11)$$

Denitrification has been considered a prospective and auspicious metabolic way for MICP applications within subsurface environments. This preference is attributed to its advantageous characteristics compared to alternative microbial metabolic processes. Denitrification is noted for its thermodynamic favorability, outperforming all other metabolic pathways with the exception of aerobic respiration. In contrast to oxygen-dependent microbial metabolic processes like urea hydrolysis and aerobic respiration, denitrification occurs in oxygen-depleted subsurface environments where nitrate is present [25]. In the utilization of particular microbial strains, denitrification can take place even in the absence of micronutrients [12]. In contrast to aerobic respiration, MICP via denitrification does not rely on external alkalinity, as the process can generate adequate alkalinity autonomously (Equations 33-36) [25]. However, the principal drawbacks

associated with denitrification are the relatively low calcium carbonate precipitation rates compared to urea hydrolysis and the limited $CaCO_3$ precipitation under aerobic conditions [36].

2.3 MICP Through Complementary Metabolic Pathways

Combining metabolic pathways can theoretically enhance MICP yield, and some studies investigated this possibility. In a study [15], *Ralstonia eutropha* H16 bacteria was used to enhance MICP yield by combining urea hydrolysis and nitrate reduction pathways. Despite challenges such as restricted nitrate reduction of H16 by high Ca^{2+} ion in the medium, optimizing these pathways improved $CaCO_3$ precipitation by 20-30%, and a yield of 14 $g.L^{-1}$ was reached. *Ralstonia eutropha* H16 showed potential for activating multiple pathways. In another study, non-anexic biogranules capable of hydrolyzing urea and reducing nitrate were produced to increase the performance of self-healing bioconcrete [39]. A similar approach was used by [40] to produce non-axenic calcium carbonate precipitating biomass which enabled healing of cracks and inhibition of reinforcement bar corrosion in self-healing bioconcrete.

In another non-anexic granular study [41], nitrate-reduction and sulfate-reduction metabolisms were combined to maximize self-healing and mitigate Microbially Induced Concrete Corrosion (MICC). Utilizing the synergetic effect between sulfate reduction, sulfate oxidation, and nitrate reduction bacteria is advantageous to combat corrosion in sewer systems effectively. However, the $CaCO_3$ precipitation capacity of the biogranules was not tested in these biogranule development studies.

2.4 Factors Affecting MICP

Microbially induced calcium carbonate precipitation has four major drivers: (i) available nucleation sites, (ii) pH of the environment, (iii) DIC concentration, and (iv) dissolved calcium ions in the solution. Firstly, MICP is a chemical process necessitating the presence of an adequate concentration of calcium ions and carbonate ions, and it is imperative that the saturation state (Ω) of the system. If the saturation state of the system (Ω) > 1, the system becomes oversaturated and culminates in precipitation (Equation 12-13) [4,24].

$$Ca^{2+} + CO_3^{2-} \leftrightarrow CaCO_3 \quad (12)$$

$$\Omega = [Ca^{2+}]\,[CO_3^{2-}] / K_{sp\ calcium\ carbonate} \quad (13)$$

The solubility product constant of $CaCO_3$ (K_{sp}) is 2.8 x 10^{-9} at a temperature of 25°C [24].

In addition to calcium ions, the biomineralization of calcium carbonate is driven by these three crucial factors: dissolved inorganic carbon (DIC) amount, the system's pH level, and available nucleation sites. The quantity of carbonate ions is contingent upon the concentration of DIC and the pH of the system. Furthermore, the DIC concentration is tied to environmental variables, such as the atmospheric pressure of carbon dioxide (CO_2) and ambient temperature [24].

2.4.1 Dissolved Inorganic Carbon

Several pivotal elements influencing the concentration of DIC encompass parameters such as temperature, pH, atmospheric CO_2 levels, the geological composition of the local surroundings, the decomposition of organic materials, and the influence of microbial activity [42].

$$DIC = [CO_2] + [H_2CO_3] + [HCO_3^-] + [CO_3^{2-}]$$

The equilibrium reactions and associated constants that govern the dissolution of carbon dioxide in aqueous solutions at standard conditions (25°C and 1 atmosphere) are shown in Equations 14-18 [4].

$$CO_{2(g)} \leftrightarrow CO_{2(aq)} \ (pK_H = 1.468) \quad (14)$$

$$CO_{2(aq)} + H_2O \leftrightarrow H_2CO_3^* \ (pK = 2.84) \quad (15)$$

$$H_2CO_3^* \leftrightarrow H^+ + HCO_3^- \ (pK_1 = 6.352) \quad (16)$$

$$HCO_3^- \leftrightarrow CO_3^{2-} + H^+ \ (pK_2 = 10.329) \quad (17)$$

$$\text{With } H_2CO_3^* = CO_{2(aq)} + H_2CO_3 \quad (18)$$

According to the studies conducted to analyze DIC in aquatic environments, the following results have been obtained. Elevated temperatures typically result in diminished solubility of DIC in aqueous environments [43]. This phenomenon can be attributed to the diminished capacity of water to retain dissolved gases, most notably carbon dioxide, under conditions of increased temperature. The metabolism of aquatic plants and microbial activities influence DIC behavior. In photosynthesis, marine flora actively assimilates carbon dioxide, which, in turn, instigates a reduction in the concentration of DIC. Conversely, the biological process of respiration elevates the concentration of DIC [42]. Variations in pH significantly have an impact on the dissolved inorganic carbon.

Under acidic pH conditions carbon dioxide bicarbonate balance shifts towards the carbon dioxide gas, potentially resulting in a decrease in DIC concentration. Conversely, under alkaline pH, bicarbonate carbonate balance shifts towards the carbonate ions bringing more carbon dioxide to the solution increasing overall DIC levels [44]. The elevation of atmospheric CO_2 levels leads to a rise in the presence of DIC within aquatic environments.[45].

Since DIC is primarily controlled by microbial activity in MICP, parameters such as pH, temperature, salinity, nutrient availability, and oxygen availability affect microbial activity also influence DIC.

The pH level affects the microbial community and enzyme activity. According to studies conducted using *Bacillus* species, it was revealed that *B. pasteurii* and *B. sphaericus* optimum growth pH ranges are 7-9 and 8-9, respectively. *B. cereus* was unable to survive at pH levels above 9.0 whereas *B. sphaericus* demonstrated survival within the pH range of 8.0 to 12.5. *B. megaterium* can survive up to a pH of 8.9 [46]. Based on the other findings, it was found that the most favorable pH for the function of the urease enzyme falls between 7.5 and 8.0. Notably, they found a gradual enhancement in urease activity as the pH of the environment shifted from 6.0 to 8.0 [47]. This pH rise was attributed to the generation of ammonia as a byproduct of urea hydrolysis. Additionally, microbial respiration generated carbon dioxide, which acted as a buffering agent, counteracting the rise in pH within the reaction medium [48].

Temperature assumes a pivotal role in the growth and metabolic activity of microorganisms, thereby exerting a substantial influence on the MICP process. The optimum temperature for bacterial activity differs from that for calcite precipitation. Within a defined temperature range, elevations in temperature yield heightened microbial proliferation and metabolic activity. This phenomenon is rooted in the principle that chemical and enzymatic reactions show increased rates at elevated temperatures. According to the studies in this field, carbonate precipitation was observed across a temperature range from 2 to 32 °C [49]. Notably, an elevated rate of precipitation was observed at higher temperatures. However, calcite precipitation experiences a considerable decline within the temperature range of 30-50 °C, reaching its lowest point at 50 °C. In addition to its impact on the quantity of crystalline structures generated, the temperature has also exhibited an impact on the morphology of the biological crystals [48].

The salt concentration of the medium is among the most critical factors affecting carbonate precipitation. Salinity levels can significantly affect the formation of carbonates. In a study [50], *Halobacillus trueperi* was used as a halophilic bacterium to test the salinity effects on MICP since halophilic bacteria are capable of thriving across a broad spectrum of osmotic concentrations. In this study, 2.5%, 7.5%, 15%, and 20% salinity levels were used. According to the results, the amount of biodeposits and the size of the formed bioliths decreased as salinity levels increased. Additionally, higher salinity concentrations were associated with longer precipitation times. The precipitation occurred at various growth stages, but it happened during the death phase in the test group with a 20% salt concentration.

Providing an ample, suitable, and essential nutrient supply to bacteria is vital to ensure spore germination and sustain the viability of bacteria, thereby enabling MICP to persist for an adequate duration, thus facilitating the attainment of the intended structural performance objectives [48,51,52]. The production of calcium carbonate is found to exhibit a positive correlation with the nutrient solution concentration within a specified interval; however, elevated concentrations have been observed to impede the formation of $CaCO_3$. When nutrient solution concentrations are maintained at lower levels, the microbial-induced formation of $CaCO_3$ is comparatively diminished [53]. A study has demonstrated that changes in the nutrient solution content exhibit a discernible impact on the rate of nucleation and the dimensions of calcium carbonate precipitates. Notably, the influence of the nutrient solution varies across different environmental contexts [54]. In certain situations, such as under low-temperature environments, adding urea into the medium can enhance the $CaCO_3$ precipitation rate and overcome solidification inhibition [55]. This addition not only enhances urease activity but also alkalizes the environment, which inhibits microorganism growth. However, a high urea content can lead to uneven distribution of precipitation crystals and weak soil strength. As the nutrient solution concentration rises, there is an initial increment in the internal friction angle, followed by a subsequent decline, ultimately reaching its optimal point at a concentration of 1.60 $mol.L^{-1}$ for the nutrient solution [53]. According to another study, the addition of ammonium chloride nutrient broth and sodium bicarbonate to the nutrient solution effectively enhances the MICP performance and the mechanical properties of bio-cemented sand. Furthermore, sand solidified with a nutrient compound solution had a

significantly higher calcium carbonate content than sand solidified with an essential nutrient solution [56].

The availability of oxygen in the MICP process has been a subject of increased attention, and conflicting perspectives have emerged. Aerobic bacteria are responsible for the majority of the MICP processes. Therefore, oxygen availability plays a critical role in MICP treatment [10]. It was reported that anoxic conditions did not impede urease activity in *S. pasteurii*, demonstrating similar or even more significant urea degradation than aerobic conditions. However, anoxic cultures showed significantly higher increases in conductivity, suggesting the potential for MICP treatments in environments with limited oxygen, provided a sufficient ureolytic bacterial population is injected [57]. In contrast, Martin et al. [58] found that *S. pasteurii* cannot grow anaerobically and that urease activity observed under anoxic conditions results from pre-existing enzyme content. This discrepancy raises doubts about the efficacy of MICP in situ reinforcement, especially where oxygen availability is constrained.

2.4.2 Dissolved Calcium Ions

Calcium ion is an indispensable factor in the formation of calcium carbonate. Nonetheless, as the concentration of Ca^{2+} rises, an increasing quantity of Ca^{2+} ions becomes affixed to the surfaces of bacterial cells, leading to a deceleration in the diffusion of nutrients and, consequently, a diminished precipitation rate. Moreover, an excess of Ca^{2+} can elicit a toxic response in bacteria, as their requisite amount for regulating essential biological processes is limited. [51]. The impact of Ca^{2+} concentration on bacterial precipitation exhibits noteworthy characteristics. The source of calcium ions in the environment of biocementation exerts a controlling influence over the characteristics of the resulting crystals, encompassing their type, size, morphology, and degree of crystallinity. Specifically, calcium chloride instigates the development of calcite crystals with a rhombohedral structure, calcium acetate prompts the formation of aragonite crystals characterized by a lamellar or needle-like morphology, while calcium lactate engenders the production of intricate vaterite crystals exhibiting a hexagonal lattice configuration [48].

2.4.3 Nucleation Site Development and Crystal Growth

Crystallization is typically associated with two primary processes: nucleation site development and crystal growth. In these processes, both bacterial and abiotic (non-living) nucleation sites can play crucial roles under specific circumstances.

From the biotic perspective, the development of nucleation sites and crystal growth is influenced by various factors such as bacterial metabolic activities, bacterial cell structure, extra polymeric substances (EPS) concentration, and bacterial concentration [59].

Bacteria itself serve as the primary nucleation sites for calcium carbonate, subsequently facilitating in-situ growth. Carbonate nucleation initiation occurs on the cell wall, either via the membrane or through particular anionic functional groups such as biopolymers and biofilms capable of attracting Ca^{2+} [60,61]. The exopolymers, which are secreted by bacteria to form biofilms, are crucial for the adsorption of ions due to charge neutralization, mineral nucleation, and growth. Also, these biopolymers and biofilms have a notable influence on the morphology and mineralogy of carbonate sediments. Studies have shown that the extracellular polymeric secretions framework influences the precipitation of $CaCO_3$ by serving as a suitable surface for precipitation through successive stratification [60,62]. Additionally, the particular proteins found in EPS formed by various bacteria control the selection of calcite or aragonite polymorphs. Accordingly, higher concentrations of EPS led to a significant increase in calcium carbonate precipitation due to the provision of more nucleation sites for MICP [63]. In a similar vein, higher bacterial concentrations can provide more nucleation sites in the solution. This can result in a more effective transformation of minerals in the solution into crystal nuclei [64].

From the abiotic perspective, nucleation and crystal growth occur through the involvement of non-living factors and constitute a multifaceted process shaped by various factors. This process typically begins when the dissolved substances' concentration in a solution surpasses a certain threshold. The progression of abiotic nucleation and crystal growth is intricately linked to calcium and carbonate ions, which are fundamental constituents for crystal formation in MICP [20]. When the saturation state of the system (Ω) > 1, it indicates that the solution can no longer accommodate further dissolution, the system becomes oversaturated and culminates in precipitation. This marks the point

where molecules in the solution begin to adopt a specific order. Additionally, elevated initial supersaturations lead to a more evenly distributed nucleation across all grains, whereas lower initial supersaturations culminate in more isolated patterns, thereby influencing crystal growth in porous media [65].

Abiotic nucleation generally involves the aggregation of certain molecules in the solution to form crystal nuclei. These nuclei initiate the gathering of additional molecules from the solution onto their surfaces. These sites can be observed on mineral surfaces, where certain minerals provide an ideal location for crystal formation to commence. Additionally, foreign particles or impurities present in the environment, such as dust or sediment, can also function as abiotic nucleation sites by serving as a surface for calcium carbonate precipitation. In laboratory experiments, the walls or surfaces of containers utilized in MICP are capable of acting as abiotic nucleation sites. This is due to the interaction between the solution and the container surfaces, which triggers crystal formation. Pre-existing crystals or substances present in the solution or on surfaces can also function as templates for abiotic nucleation, providing a foundation for ion arrangement and subsequent crystal growth. Moreover, chemical gradients within the solution, characterized by localized variations in concentration, are also known to contribute to abiotic nucleation. These gradients create conditions that are conducive to the initiation of crystal formation.

2.5 Biomineralization Applications

The biomimetic study of $CaCO_3$ formation by microorganisms has been systematically studied and yielded applications in diverse subfields such as medical, construction, environmental, pharmaceutical, agricultural, and industrial biotechnology [66]. MICP has been tested in numerous applications, with variations in the bacterial species used depending on the specific application. The commonly used bacteria were summarized in Table 2.2. Due to the challenging conditions of MICP applications, such as high pH, shear stress, and shrinking pores, methods like encapsulation and immobilization have been developed to protect the bacteria. Additionally, bacterial spores, known for their resistance to harsh conditions, are used as bio-agents [41]. On the other hand, biogranules which have layered non-axenic cultures present several advantages over axenic bacterial cultures, particularly as microbial healing agents. A key benefit of biogranules is their layered structure composed of minerals and extra polymeric substances. Therefore, the

use of biogranules eliminates the necessity for protective carriers. This layered structure substantially boosts the durability of biogranules in challenging environments, thereby enhancing their utility, longevity, and cost-effectiveness compared to axenic cultures [14].

Table 2.2. Biomineralization Applications

Biomineralization Applications	Metabolic Pathway	Bacterial Strain	References
Biocementation	Urea Hydrolysis	*Sporosarcina pasteurii* *Bacillus sphaericus* *Bacillus megaterium* *Bacillus cereus*	[16,32,67]
	Nitrate Reduction	*Diaphorobacter nitroreducens* *Pseudomonas aeruginosa*	[14,68,69]
	Sulfate reduction	Sulfate-reducing bacteria	[41]
	Aerobic oxidation of organic carbon	*Bacillus halmapalus* *Bacillus cohnii* *Bacillus subtilis* *Bacillus pseudofirmus*	[28,70–72]
Soil stabilization	Urea Hydrolysis	*Bacillus sp. strain VS1* *Sporosarcina pasteurii*	[73,74]
	Nitrate Reduction	*Pseudomonas denitrificans*	[25,75]
Bio-immobilization	Urea Hydrolysis	*Sporosarcina pasteurii* *Kocuria flava*	[16,76]

2.6 Biogranulation

Anaerobic granules, also known as methanogenic granules, were first observed in the 1950s but formally recognized in the 1970s [77]. These granules are typically found in an up-flow anaerobic sludge blanket (UASB), where wastewater introduced from the bottom promotes microbial aggregation. Anaerobic granules enable high-rate anaerobic digestion (AD), consisting of hydrolysis, acidogenesis/fermentation, acetogenesis, and methanogenesis, converting complex organic substances to methane (Figure 2.3).

The development of Aerobic Granular Sludge (AGS) in a sequencing batch reactor (SBR) was initially observed in 1997 [78]. Aerobic granules consist of densely packed microbial communities with excellent settling properties, facilitating biomass retention, and extending solids retention times. Typically cultivated in SBR with aeration, aerobic granules facilitate the heterotrophic degradation of organic pollutants, along with concurrent processes of nitrification-denitrification and improved biological phosphorus removal. The structure of these granules includes aerobic bacteria in the outer layers and often an anoxic core, making them highly effective in various treatment processes (Figure 2.3) [79].

Anammox granules are integral to the nitrogen cycle, directly converting ammonium and nitrite to molecular nitrogen, thereby bypassing the energy-intensive nitrification and denitrification processes (Figure 2.3). Although the anammox process was first noted in the 1920s, its practical applications were realized in the mid-1990s. These granules support efficient nitrogen removal without the need for oxygen or carbon supplementation, overcoming early biomass retention challenges. By significantly reducing the energy and carbon footprint of wastewater treatment, anammox systems have provided a revolutionary approach to managing nitrogen in wastewater [79].

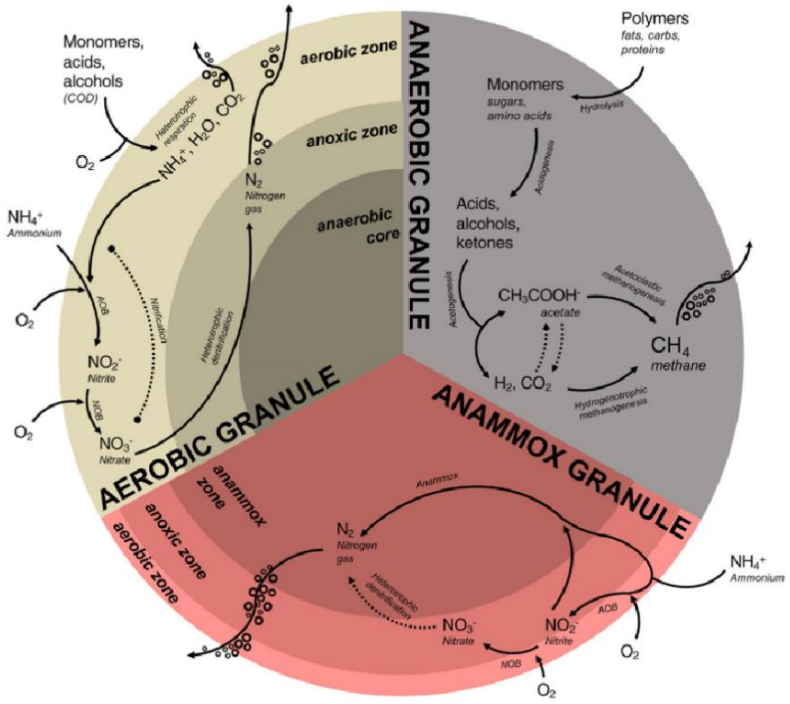

Figure 2.3. Distinct activity zones and biochemical processes of anaerobic, aerobic, and anammox granules [79]

The formation of biogranules occurs through the physical, chemical, and biological interaction of microorganisms similar to the formation of biofilms. This interaction leads to the creation of dense, spherical aggregates with a diameter of around 1-5 mm (Figure 2.4). Within these aggregates, the microbial cells are immobilized within a matrix of extracellular polymeric substances (EPS) [80]. Scientific research indicates that certain operating parameters are crucial for initiating and improving the self-immobilization of bacteria leading to biogranulation [81]. Flocs are prevalent and frequent components of the AGS system. Biogranules exhibited a higher degree of mass diffusion restriction compared to flocs, primarily due to their larger size and denser structure [82]. This led to the creation of distinct microenvironments as aerobic, anoxic, and anaerobic within the granules, enabling the concurrent removal of COD, nitrogen, and phosphorus in a single reactor [83–85]. Furthermore, the biogranules have superior resilience compared to flocs, displaying enhanced resistance to the detrimental impacts of hydrogen sulfide, heavy metals, and aromatic contaminants often present in wastewater. Previous studies have shown that a certain quantity of flocs coexisted after achieving stable sludge settleability and nutrient removal. This quantity ranged from 3% to 20% and varied depending on different operational factors [82,86]. In order to maintain granulation in the system selective pressure should be applied to wash out flocs from the system.

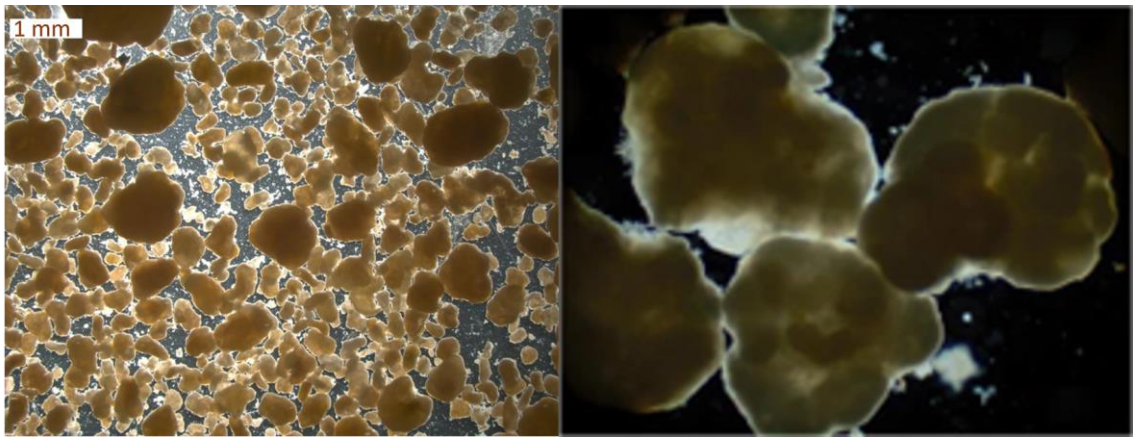

Figure 2.4. Microscopic images of aerobic biogranules [80,87]

Biogranulation is a biotechnological improvement in wastewater treatment that involves the formation of thick three-dimensional biofilms, called granular sludge or biogranules, in reactors with certain environmental conditions [81,88].

The distinct attribute highlights the promise of biogranulation as a highly efficient and resilient approach for addressing issues in wastewater treatment. Recently biogranules

have been employed in diverse applications, including the production of bio-based composites as well as the cultivation of biogranules that are suitable for the development of microbial self-healing concrete [89–91]. In these studies, biogranules were used for MICP in concrete, and investigations were mostly focused on the resuscitation time of the core community, compatibility with the cementitious matrix, and crack closure performance [90,92]. Although the studies presented some information about the microbial activity of biogranules, the calcium carbonate precipitation yield of the biogranules, and the limitation of this approach remain unknown.

2.6.1 Factors Affecting Aerobic Granule Formation

Aerobic granulation is a step-by-step progression starting from seed sludge, then forming compact aggregates, followed by the development of granular sludge, ultimately resulting in mature granules. The process of cell aggregation in a culture can be influenced by multiple factors [93].

Substrate Composition

The granulation process is profoundly affected by the composition of the substrate, which selectively supports and enriches specific bacterial species. This, in turn, impacts the size, settling ability, and microbial activity of the resulting granules [94]. Aerobic granules can develop on a diverse range of organic substrates including glucose, phenol acetate, ethanol, and simulated and actual wastewater in sequencing batch reactors [93].

According to a study, acetate-fed granules exhibited a dense and regular microstructure, which, however, led to disintegration at an intermediate Organic Loading Rate (OLR) of 9 kg COD $m^{-3}.d^{-1}$ due to diffusion limitation and anaerobiosis. On the contrary, glucose-fed granules with a loose filamentous matrix demonstrated improved settling and strength characteristics, allowing them to sustain higher OLRs, reaching up to 15 kg COD $m^{-3}.d^{-1}$. Despite having a lower Specific Sludge Volume (SVI) and being more compact than acetate-fed granules, the irregular morphology of glucose-fed granules facilitated enhanced nutrient penetration and shorter diffusion distances [94].

In addition, the granulation process can be affected by the ratio of COD/N in the feeding solution because it can cause microbial selection that favors either heterotrophic bacteria or nitrifying species and granule properties [95]. A study discovered that aerobic granules were effectively developed in a system that functioned only under aerobic conditions, with C/N ratios of 1:1 and 2:1. However, no granules were generated in reactors that had

no carbon added or had a C/N ratio of 4:1 over a 30-day operation [96]. According to another study, the stability of aerobic granules was greatly compromised when the C/N ratio was as low as 2 or 1 primarily due to a substantial decrease in extracellular polymer substances (EPS) [97]. In a different study, it was observed that a COD/N ratio between 2 and 5 resulted in the formation of stable, compact granules with a high concentration of slow-growing nitrifiers and also determined that the optimum COD/N ratio for efficient removal of both COD and nitrogen was 7.5 [98].

Organic Loading Rate

The organic loading rate (OLR) is an essential factor that influences the formation of granules, as the presence of substrate is vital for the development of microorganisms. Previous studies have indicated that AGS can be successfully grown within a wide range of organic loading rates between 0.6 and 30 kg COD $m^{-3}.d^{-1}$ [99]. Granules produced with low-strength wastewater and low organic loading rates grow more slowly and are smaller in size than high-strength ones. Generally, high OLRs are implemented to promote rapid granulation. However, this practice may result in the proliferation of filamentous microorganisms which can negatively impact the morphology, efficiency, and functionality of AGS [100]. For instance, when OLR was kept at 8 kg COD $m^{-3}.d^{-1}$ aerobic granulation was seen after 18 days of operation. However, the granules showed instability and broke down after two weeks [99]. In another study on the growth of salt-tolerant AGS, different OLRs of 2.4, 3.6, 4.8, and 7.2 kg COD $m^{-3}.d^{-1}$ were tested. The higher OLRs resulted in a faster formation of AGS, but they also led to the development of unstructured and fluffy filamentous granules [101].

Sludge Retention Time

The SRT means the average duration that microorganisms reside in a bioreactor thus it is a significant parameter that may regulate the existence of microbial communities by considering their overall growth rate. To survive in the reactor, a specific organism must have a net growth rate equal to or greater than 1/SRT. If not, it will be flushed out from the reactor, unless it is introduced with the influent stream at a high dispersion rate. Therefore, the microbial aggregates of varying sizes correspond to distinct settling conditions with varying solid retention times [102]. Due to the separation of biomass and selective withdrawal of excess sludge, flocs experience a shorter solids retention time (SRT) in contrast to granules [103].

The slow-growing bacteria were more abundant in granules compared to flocs, mostly because of their high SRT. Regarding this matter, cultivating microorganisms in granules may offer advantages in comparison to flocs [102].

In a study, in the AGS SBR, it was found that SRT fluctuated significantly, ranging from 1 to 40 days in the process of granulation [104]. Similarly, in another study it was recorded a rise in SRT from 2 days to 30 days, followed by a decrease to 17 days, and ultimately stabilization at 9 days, corresponding with the development and maturation of aerobic granules in the SBR [105]. In a different study, AGS reactors were built with varying SRTs to promote the concentration of functional microorganisms and the formation of granules. The findings indicated that the reactor operating with a 6-day SRT had superior total nitrogen removal efficiency and the formation of dense granules. In addition, *Xanthomonadaceae*, *Rhodobacteraceae*, and *Hyphomonadaceae*, which could produce AHL (acyl-homoserine lactone) and secrete EPS (extracellular polymeric substances), were also shown to be abundant with 6 days of SRT [106]. As a result, granulation can occur under different SRTs based on the operational parameters and desired microbial community.

Presence of Cations

The partial neutralization of negative charges on bacterial cell surfaces by cations such as Ca^{2+}, Mg^{2+}, Fe^{2+}, and Fe^{3+} has been identified as a factor that can trigger the granulation process. It was observed that the addition of some divalent cations led to a noteworthy decrease in sludge granulation time (from 32 to 18 days) and a more compact and denser aerobic granule structure [107]. Aerobic granules grown with Ca^{2+} exhibited superior physical properties, while granules grown with Mg^{2+} demonstrated accelerated substrate biodegradation and more microbial diversity [108].

Also, changes in the concentration of Ca^{2+} have a substantial impact on the generation of EPS which is a binding material. In a study, the EPS content demonstrated an increase from 116.4 $mg.g^{-1}$ VSS to 150.0 $mg.g^{-1}$ VSS when the Ca^{2+} concentration raised from 0 to 150 $mg.L^{-1}$ [109].

Extracellular Polymeric Substances Formation

Extracellular polymeric substances (EPS) refer to sticky compounds such as nucleic acid, polysaccharides, and proteins released by cells [110]. EPS a crucial constituent of AGS exerts discernible influence on the surface attributes of sludge, encompassing

flocculation, hydrophobicity, surface charges, and sedimentation dynamics [111]. Thus, EPS has a significant role in adhesion phenomena, the creation of matrix form, microbial physiology, and the enhancement of the long-term stability of granules [81]. The diverse forms and constituents of EPS, including dissolved (S-EPS), loosely bound (LB-EPS), tightly bound (TB-EPS), protein (PN), and polysaccharide (PS), have been substantiated to assume distinct functions in the granulation process. It was indicated that TB-EPS played a pivotal role in the development of AGS, with the PN in EPS being the primary factor in encouraging AGS formation and enhancing its ability to aggregate [111].

Under standard cultural conditions, microorganisms do not necessitate the secretion of surplus EPS. The heightened EPS production witnessed in biogranules is incited by conditions characterized as stressful conditions. Thus, under stressful operating conditions such as elevated hydrodynamic shear force, abbreviated settling time/hydraulic retention time, and periodic feast-famine cycles, bacteria exhibit a pronounced inclination to synthesize a greater quantity of EPS [81].

Feast and Famine Cycle

In the formation of aerobic granules, an SBR is operationalized through a sequential cycle involving feeding, aeration, settling, and supernatant discharge. The aeration period of the SBR has two distinct phases, an initial degradation phase depleting the substrate to a minimum level and an aerobic starvation phase wherein external substrate availability diminishes. Microorganisms within the SBR experience a cyclical regime characterized by periodic feasting and famine, referred to as periodic starvation [93].

It was observed that under periodic feast-famine conditions, bacterial hydrophobicity tends to increase, and heightened cell hydrophobicity facilitates the aggregation of microorganisms. This periodic starvation stimulates the formation and utilization of EPS, hence facilitating the aggregation of microorganisms and the creation of suitable gradients of substrate and oxygen within the granule [80].

Additionally, it was shown that extending the duration of the feast time by increasing the availability of nutrients often led to the scattering of granules or biofilms in a structural manner. In contrast, a prolonged period of starvation tended to produce granules with enhanced structural stability [112]. In a study, the feast and famine ratio effect on granulation was investigated using series-connected completely stirred tank reactors as plug flow reactor without changing HRT and OLR. According to the results, aerobic

granulation was unsuccessful when the feast/famine ratio exceeded 0.5 [112]. Similarly, aerobic granulation has been achieved successfully in sequencing batch reactors (SBRs) with feast/famine ratios of 0.16, 0.25, 0.33, and 0.42 [112–114]. According to another study, the duration of the feast time shouldn't exceed 25% of the total cycle length to optimize the stability of granules and improve the quality of the effluent [100].

Settling Time and Exchange Ratio

The settling time is a crucial factor in the selection of granules. A high exchange ratio (low hydraulic retention time), coupled with a short discharge phase, promotes the selection of granules in the reactor and accelerates the process of granulation [80]. The use of SBRs with a short settling time typically 2–10 min enables the rapid selection of microbial aggregates that settle quickly, whereas sludge with poor settling properties is effectively washed out [115]. In a study, different strategies were compared to enhance AGS development, and results revealed that the fastest granulation was observed in 11 days when using a short settling time (gradually decreasing from 15 to 1 min). Also, these granules had improved settling characteristics, enhanced stability, and high levels of EPS and protein content [116]. Similarly, in a different study, rapid granulation was achieved by reducing the settling time to 2 minutes by using a 50-70% volume exchange ratio. Moreover, selection pressure created by settling time was found more significant than hydraulic retention time. The investigation showed that varying HRT did not impact the speed of aerobic granulation when a short initial settling time of 2 minutes was applied [117].

Hydrodynamic Shear Forces

Shear forces play a pivotal role in determining the morphology and configuration of aerobic granules although hydrodynamic shear force is not considered a primary instigator of aerobic granulation. In laboratory-scale AGS reactors commonly configured as bubble columns, shear forces are induced by the aeration rate, quantified as up-flow superficial velocity, typically ranging between 1 and 2 $cm.s^{-1}$. An investigation revealed that increased shear force promoted the development of more condensed, tightly bound, rounder, smaller, and stronger aerobic granules. Additionally, the enhancement of extracellular polysaccharide synthesis and microbial activity was seen under high-shear force conditions [93].

In a study, the formation of stable granules was achieved by decreasing the aeration rate to 0.55 $cm.s^{-1}$ during the starvation phase [118]. In another study, granules were formed at an aeration rate of 0.8 $cm.s^{-1}$. However, these granules have a more porosity and less stable structure [119].

Seed Sludge

The parameters of the seed sludge also impact the development and structure of aerobic granules. Granulation relies on crucial parameters such as the settling characteristics, hydrophobicity, microbial community, and biological activity of the seed sludge [120]. Studies showed that when stored aerobic granules were used as seed sludge in an AGS system the start-up time may be effectively reduced [121]. In instances where the introduction of stored aerobic granules is unfeasible, the utilization of anaerobic granular sludge as a seeding strategy has been explored to augment granulation by establishing an anaerobic core [122].

In a study, it was revealed that seed sludge with rapid settling characteristics could expedite the granulation process [123]. Also, another study elucidated that the acceleration of granulation in AGS systems is attainable through the introduction of seed sludge having a high level of hydrophobicity [120]. In a different study, conventional activated sludge (CAS) and aerobic granular sludge (AGS) were used as a seed in two other reactors. The results showed that the reactors seeded with AGS achieved complete granulation faster (28 days) and exhibited a larger granule size (496 μm) than those seeded with CAS (65 days, 210 μm) [124].

Dissolved Oxygen and pH

The amount of dissolved oxygen (DO) present in the reactor influences granular stability and structure in addition to microbial activity. Aerobic granules have been reported to develop in an SBR even when the DO concentrations are low, typically ranging from 0.7-1.0 $mg.L^{-1}$ [125]. However, insufficient DO concentration can lead to the generation of gas through anaerobic metabolism within particles. Concurrently, the proliferation of filamentous bacteria in low DO conditions may contribute to the susceptibility of AGS to internal disintegration [126]. Also, research indicates that aerobic granules can effectively develop at dissolved oxygen concentrations ranging from 2-6 $mg.L^{-1}$ [127]. According to the research, if there is enough aeration, it seems that the concentration of DO may not be a decisive factor in the aerobic granulation process.

The pH level has a substantial impact on the growth rate of microorganisms in the reactor. When there are large amounts of organic matter, oxidation results in the production of significant quantities of CO_2, which causes a decrease in pH in solutions that do not have the buffering capacity. Fungi, which flourish in acidic environments, have a significant impact on the early formation of granulation. In a study, it was discovered that the existence of fungi promoted the development of granules of around 7 mm at pH 4.0. Conversely, when bacteria were responsible for controlling granulation under pH 8.0 conditions, the size of the granules only reached 4.8 mm [128].

In a study, it was discovered that AGS has excellent structural stability and sedimentation performance under weakly acidic (pH = 5.5) and neutral conditions. In addition, a very low pH (pH = 3.0) might lead to the breakdown of EPS, causing the AGS to become unstable and disintegrate, and a very high pH might lead to irreversible detrimental effects quickly [126]. Although these observations have provided valuable knowledge, there is still ongoing research to fully comprehend the impact of pH on aerobic granulation.

2.6.2 Granule Formation Mechanisms

The granulation process often experiences a lag period (pre-maturation), during which there is minimal alteration in the proportion of biomass in the granules. Following the lag phase, the granulation phase comes and can be defined by the appearance of granules in the reactor, resulting in an enhancement of granule quality (Figure 2.5).

In a study, it was proposed that six primary processes are crucial for achieving effective granulation: (i) microbial selection, (ii) selective wasting, (iii) maximizing transport of substrate into the biofilm, (iv) selective feeding (v) using substrates that may or may not form granules, and (vi) the breakdown of granules [129].

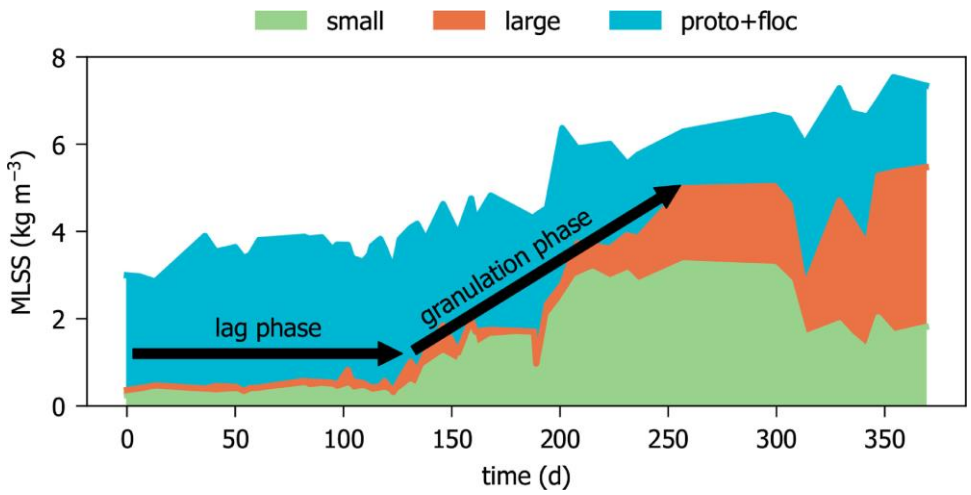

Figure 2.5. Typical granulation period. The colors represent the size of the microbial aggregates. Illustrating proto-biogranules and flocs, tiny biogranules, and large biogranules represent respectively <200 µm, >200 µm, and >1000 µm. The data originates from the Nereda® reactor in the Netherlands [129].

Microbial selection plays a crucial role in the development of granules. Research has demonstrated that the most effective way to establish a solid and compact biofilm is by ensuring that the pace at which substrates are absorbed is slower than the rate at which they are transported into the granules [130]. This optimization is achieved by favoring organisms that capture easily degradable substrates under anaerobic conditions, metabolizing them into storage compounds, and subsequently utilizing these compounds for growth in aerobic environments. This process effectively segregates nutrient absorption and proliferation into two distinct processes termed "feast and famine." Species such as phosphate-accumulating organisms (PAO) and glycogen-accumulating organisms (GAO) exemplify the ability to bifurcate these processes and are commonly found in full-scale AGS processes [102]. These substrates are identified as non-granule-forming substrates (n-GFS). Conversely, substrates that foster the growth of aerobic granules, including volatile fatty acids and readily biodegradable substrates convertible through anaerobic processes, are termed granule-forming substrates (GFS) [129].

Physical selection plays another essential part in the development of aerobic granular sludge [131]. AGS has superior settling characteristics in comparison to activated sludge flocs. Flocs are consistently present in AGS reactors to a certain degree, as not every carbon substrate found in sewage can be transformed into storage polymers during anaerobic feeding. Hence, it is necessary to selectively eliminate the flocculent sludge portion containing the surplus sludge to provide granules with a competitive edge. This is accomplished by using the disparity in settling velocity between flocculent and granular

sludge [132]. The phenomenon is referred to as the physical selection pressure (Table 2.3).

Another renowned driver is maximizing the transportation of substrate into the biofilm. The substrate penetrates the biofilm more extensively when concentrations of the substrate in the bulk liquid are increased. This promotes the development of and sustains a denser biofilm. In AGS reactors, a greater substrate concentration can be attained through either initial pulse feeding or, in a more practical context, plug-flow feeding from the bottom of the reactor [131,133]. This provides a competitive edge to bigger granules because larger granules have a faster settling rate compared to smaller granules and flocs [132]. Consequently, feeding from the bottom leads to an extended duration of interaction with the incoming flow and exposure to greater concentrations of substrate for the bigger granules. In addition, when a granule fractures into smaller components, some will be dispersed while others as a seed will catalyze the formation of new granules, thereby initiating the granule life cycle once again. Granules of a size greater than 1000 µm are more prone to fragmentation [134]. Granulation theories were summarized in Table 2.3.

2.6.3 Granule Properties

Stability

The stability of granules refers to the ability of microbial aggregates to maintain their structural integrity and functional characteristics under various operational conditions. In the context of aerobic granular sludge (AGS) technology, granule stability is crucial for the efficient and sustainable performance of the applications. The structural integrity of granules is often enhanced by the existence of a compact core, and the proliferation of microorganisms across the whole depth of the granules is a critical component in determining their stability [135]. Because of the more compact and well-defined structure, good settling characteristics, diverse microbial community, and resilience to fluctuations granules are more stable than flocs [82].

Granule stability relies on physical, chemical, and microbial characteristics. Physical attributes such as settling properties, density, and physical strength, particularly influenced by granule size, are crucial for stability. Chemical characteristics, including hydrophobicity, pH, and EPS content, also contribute to stability. Additionally, the microbial community and activity greatly influence stability [136].

Table 2.3. Granulation theories

Theory	**Brief Mechanism**	**Reference**
Selection Pressure-Driven Theory	The settling time is a crucial factor in the hydraulic selection process. In SBR operations, inspired by biological evolution theory a screening process selects biomass adapted for rapid settling.	[110,137]
EPS Bonding Theory	Extracellular polymers play a dual role in facilitating both cell cohesion and adhesion, while concurrently altering the surface's negative charge.	[110,111,137,138]
Phase Formation Theory	Aerobic granule formation theories include a four-phase model, involving stochastic cell aggregation, particle formation, EPS-mediated gathering, and maturation via hydrodynamic forces. There is also a three-stage model that emphasizes aggregate emergence, shaping by hydrodynamic forces, and final stabilization.	[110,139]
Core Theory	The EPS hypothesis posits that β-D-glucopyranose polysaccharides form the core of stable aerobic granules, accumulating proteins and heterotrophs for effective contaminant removal. The dark anaerobic core hosts young granules growing on dead cells, maturing over time.	[110]
Hydrophobicity Theory	Alterations in physico-chemical characteristics, such as elevated hydrophobicity and zeta potential allow immature granules to improve their interaction with other particles.	[140,141]
Filamentous Theory	Filamentous bacteria at low or moderate levels can act as cohesive agents that uphold the structural stability of aerobic granular sludge.	[100,110]
Quorum Sensing Theory	Cell-to-cell communication (quorum sensing) and signal molecules affect gene expression, EPS regulation, and microbial community dynamics, all of which contribute to the formation and stability of aerobic granules.	[106,110]

Size

The microbial aggregates are typically defined as granules exceeding 200 μm in size, although the smaller aggregates, particularly those below this size, may exhibit similar granular characteristics. These diminutive aggregates are occasionally referred to as "baby granules" [132].

In general, larger granules offer enhanced settling properties and biomass retention, contributing to the efficiency of wastewater treatment processes. The specific size criteria for optimal granule performance may be influenced by factors such as the type of microorganisms present, reactor design, and the characteristics of the wastewater being treated. Aerobic granules exhibit a range of sizes, spanning from approximately 0.2 to 5.0 mm in diameter. Research findings have elucidated that the optimal dimension for aerobic granules typically falls below 1600 μm [142].

Settling Velocity-SVI

The Sludge Volume Index (SVI) and the settling velocity have been used to determine the sedimentation dynamics of microbial aggregates [132]. The settling performance of the microbial aggregates is a crucial factor directly linked to its ability to retain biomass and the efficiency of separating solids from liquids in the reactor. In aerobic granular systems, the settling velocity of granules ranges from 18 to 90 $m.h^{-1}$ with occasional peaks reaching up to 130 $m.h^{-1}$ as documented by various studies. These values closely align with those recorded for anaerobic granules and notably surpass the settling velocities typically observed in flocculent-activated sludge, which typically range from 7 to 10 $m.h^{-1}$ [143]. In SBRs utilizing AGS, granules typically exhibit an SVI ranging from 30 to 50 $mL.g^{-1}$ and may decrease as low as 20 $mL.g^{-1}$. Also, AGS has an SVI_5/SVI_{30} ratio approaching unity. In contrast, flocculent sludge demonstrates a higher SVI_{30}, exceeding 100 $mL.g^{-1}$, and an SVI_5/SVI_{30} ratio typically falls within the range of 1.6 to 2.0 [144].

2.6.4 Biogranulation Applications

According to the literature it has seen that biogranules have two main areas of use: in the field of Environmental Engineering, in domestic and industrial wastewater treatment, and in the field of Construction Engineering, in the context of microbially induced self-healing concrete.

The application of biogranules in wastewater treatment has advantages, encompassing superior settleability, heightened biomass retention, concurrent nutrient removal, reduced spatial requirements, robust resistance to organic loading rates, and diminished energy consumption throughout the process [145]. However, structural instability problem was reported in the long-term operation [95,135]. Biogranules are also used for removing heavy metals or other toxic products from wastewater through biosorption. However, it is important to note that while biosorption can effectively remove toxic pollutants from water, there is a limit to the capacity of biogranules to adsorb these contaminants [146]. In order to increase toxicity resilience, heavy metal removal, and support the long-term structural stability of biogranules, integrating biomineralization strategies into biogranules can be beneficial.

Although the biomineralization activity of biogranules was observed in wastewater treatment, studies were not conducted to report the biomineralization capacity of the biogranules. In a study conducted by Şekercioğlu, biogranules that can use urea hydrolysis and denitrification mechanisms were produced for metal recovery through biomineralization but the biomineralization activity of biogranules was not determined [147].

The use of granular sludge in self-healing bioconcrete introduces a biological component that enhances the material's ability to heal cracks over time through biomineralization. The utilization of biogranules in self-healing concrete applications has several benefits, such as the simultaneous restoration of cracks and enhanced resistance to corrosion [148].

In self-healing bioconcrete applications, axenic cultures are more widely studied in the literature than non-axenic cultures such as biogranules. However, using axenic cultures is very costly due to the need for encapsulation and special conditions such as nutrient-rich medium and adjected physical parameters for cultivation. It was reported that using non-axenic cultures incurs a cost reduction of 40 times compared to axenic cultures [149]. Consequently, to mitigate the expenses associated with axenic culture production, the research orientation has pivoted toward the utilization of non-axenic cultures, characterized by simplified and cost-effective production and culturing methods. Also, using a single axenic culture and a sole metabolic pathway is disadvantageous than using combinations of different metabolic pathways in terms of $CaCO_3$ precipitation efficiency. Thus, using non-axenic cultures containing different bacterial strains and metabolic pathways can be beneficial. There are limited studies on non-axenic biogranules

developed and used for self-healing concrete application in the literature, the existing studies had been carried out using either only nitrate reduction metabolism or nitrate reduction and sulfate reduction mechanisms together [41,150]. In addition to them, biogranules that can conduct urea hydrolysis and the denitrification mechanism simultaneously have been produced by Özbay, and crack healing has been analyzed for the first time by using these biogranules in cement composites under different environmental conditions [39].

The current state of large-scale studies in self-healing concrete applications faces challenges, including a limited understanding of long-term performances and a lack of systematic evaluation methods specifically for MICP experiments, self-healing performance, and cost assessment. Also, the sporulation and germination processes of bacteria within the granular matrix are pivotal for the sustained efficacy of bioconcrete over an extended operational timeframe [41].

2.7 Research Needs and The Scope of The Thesis

In the biomineralization applications, most studies have predominantly been conducted on pure cultures, leading to the evaluation of biomineralization performances solely within the context of a single metabolism. Additionally, mostly studied two metabolisms urea hydrolysis and nitrate reduction occur in aerobic and anoxic conditions respectively. Thus, the oxygen content in the environment influences biomineralization performances. Nonetheless, it is hypothesized that simultaneous occurrences of these two metabolisms could enhance biomineralization performance and enable biomineralization in both aerobic and anoxic conditions. In the literature, there are few studies to use this hypothesis.

The non-axenic biogranules enable the concurrent utilization of multiple metabolic pathways and are more cost-effective compared to pure cultures. The studies on biogranules developed and utilized for specific biomineralization applications are limited in the literature. The existing studies have been conducted by using i) only nitrate reduction metabolism, ii) nitrate reduction combined with sulfate reduction mechanisms, or iii) nitrate and urea hydrolysis mechanisms together [148]. In some of these existing studies, microbial community analysis was conducted [39,147,148,150]. However, specifically, the biomineralization capacity of the biogranules and analyzing the MICP performance of them remained unclear.

Considering the aforementioned needs in the literature, it seems that there is a need to clarify the biomineralization-oriented biogranule production and conduct studies on the biomineralization capacity of the produced biogranules. Thus, the production of biogranules capable of concurrently urea hydrolysis and nitrate reduction metabolisms and the assessment of the MICP performance of these biogranules has been determined as the scope of the thesis.

In this context, bacteria capable of urea hydrolysis and nitrate reduction were cultivated within a sequential batch reactor. This cultivation was performed using a microbial resource management approach. As a result of this study, biogranules with enhanced biomineralization capacity were produced. This was achieved by integrating both ureolytic and nitrate-reducing bacteria within a single granule. The microbial activity and biomineralization capacity of the produced granules were determined. Then, the produced biogranules were compared to a previously reported nitrate-reducing granular culture in terms of microbial activity and biomineralization performance.

3. MATERIALS AND METHODS

The methods used to set up the bioreactor, analytical methods to observe nutrient consumption, the production of nitrate-reducing and urea hydrolyzing biogranules, and assessment of microbial activity and biomineralization capacity are explained in detail in this chapter.

3.1 Production of Biogranules Incorporating Bacteria with Nitrate-Reduction and Urea Hydrolysis Capabilities

3.1.1 Seed Sludge

In order to be used in MICP applications, the production of the biogranules can conduct urea hydrolysis and nitrate reduction, are resilient to high pH and osmotic stress, and can grow on a minimal nutrient medium was planned. Previously, urea hydrolyzing and denitrifying biogranules were successfully produced by Şekercioğlu [147]. These biogranules had been cultivated under neutral pH conditions without considering any osmotic pressure and nutrient limitation. In order to produce nitrate-reducing and urea-hydrolyzing biogranules with the pre-defined features, two types of inoculums were used. First inoculum was a mixture of flocs and granules taken from the previously operated biogranule reactor. The floc-granule mixture was allowed to settle for 30 minutes. Settled solids were used as the primary inoculum source for starting the bioreactor operated in this thesis study.

The second inoculum source was used for cross-inoculation of the bioreactor during the cultivation of new granules. The major purpose of this cross-inoculation was to provide bacteria capable of withstanding extreme conditions such as high temperature and high pH. Therefore, the second inoculum was prepared by using the final process water (pH 10, 80°C) obtained from Ankara Sugar Factory (Figure 3.1).

Process water was further enriched with urea and NO_3^- to have initial urea and nitrate concentrations of 100 mM and 10 mM, respectively. The mixture was incubated at 28 °C on a shaker at 100 rpm for 48 hours. After the incubation period, the mixture was pasteurized at 80°C in a water bath for 30 minutes to kill any vegetative bacteria. After pasteurization, the mixture was incubated again by replacing 90% of the volume with a fresh nutrient solution. The process was repeated three times for selective enrichment of urea hydrolyzing and nitrate-reducing spore-forming bacteria.

Figure 3.1. The second inoculum source obtained from Ankara Sugar Factory

At the end of the selective enrichment process, 90% of the solution (500 mL) was centrifuged at 3045*g* for 5 minutes. The separated bacteria were then added to the bioreactor as the first cross-inoculation. The remaining 10% of the volume was used to continue the selective enrichment process as described above. Cross-inoculation was regularly repeated every other day with the same procedure until the 169th day of the bioreactor operation.

However, considering the negative impact of cross-inoculation on the settling behavior of the biogranules, as detailed in the Suspended Solid section, the cross-inoculation was terminated on the 169th day of the biogranule reactor operation.

3.1.2 Sequential Batch Reactor Characteristics and Operating Parameters

The biogranules were produced within a cylindrical SBR which is 76 cm in length, 4.5 cm in diameter and has a volume of 1.2 L. The representation and photo of the bioreactor are shown in Figure 3.2. SBR was operated with four identical cycles per day as outlined in prior research on the production of granular sludge [14,90,147,148]. Reactor operation involved sequential anoxic/aerobic periods to enable the simultaneous cultivation of nitrate-reducing and urea-hydrolyzing bacteria during granulation.

Each cycle was operated with a 120-minute anoxic feeding/withdrawal period, an additional 60-minute anoxic period, and an aerobic period ranging between 150 and 180 minutes, depending on the settling time (which varied between 0 and 30 minutes according to the granulation process).

In the anoxic stage growth of denitrifying bacteria was favored and in the subsequent aerobic phase, growth of aerobic ureolytic bacteria could be achieved [10].

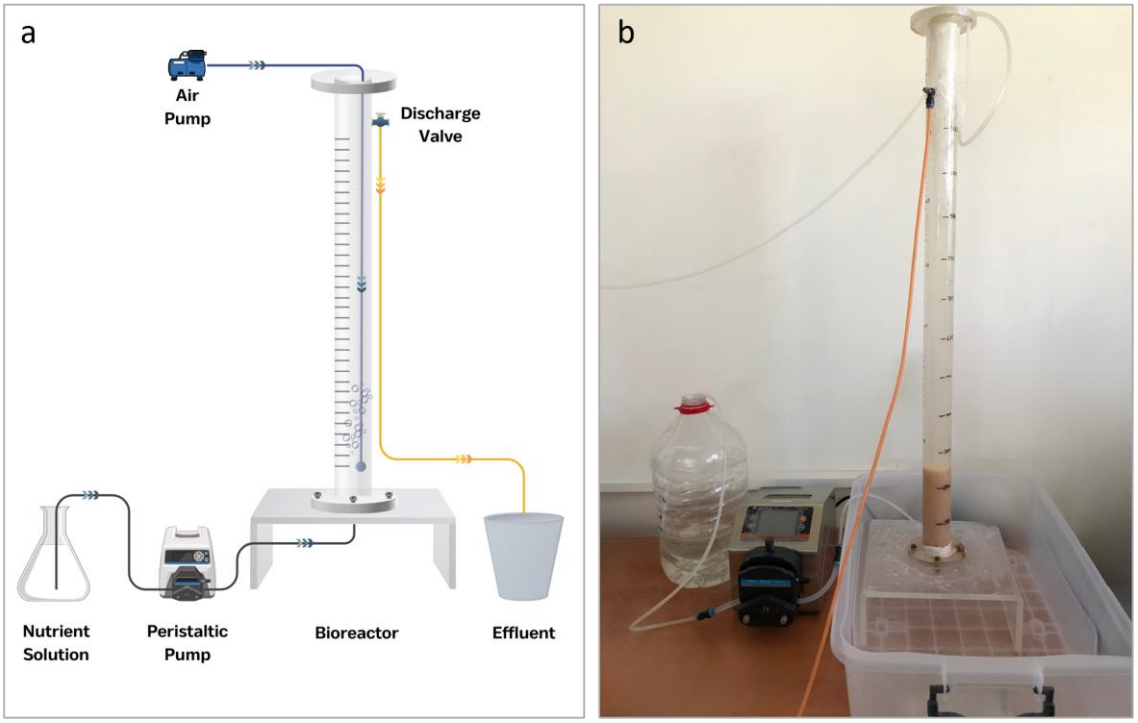

Figure 3.2. Biogranule production reactor a) Schematic representation of the bioreactor b) Photo of the bioreactor

During the anoxic feeding period, the nutrient solution was fed from the bottom of the reactor using a peristaltic pump at a rate of 5 $mL.min^{-1}$ for two hours. During this feeding period, effluent from the previous cycle was discarded from the top of the reactor at a rate of 5 $mL.min^{-1}$ providing a 50% volume exchange ratio in each cycle. The hydraulic retention time was 12 hours. A slower feeding rate compared to previous granulation studies was applied [39,147]. The presence of more stress parameters in the environment, such as alkaline pH, high urea concentration, salinity, and low yeast extract can affect the mass transfer into the biogranules.

Granule properties, microbial activity, and the abundant microbial community were monitored throughout the operation. The feed solution was modified at different stages of the operation to optimize the monitored parameters. The changes in the operational parameters during the bioreactor operation are summarized in Table 3.1.

Table 3.1. Operational parameters in different stages

Parameters		Operational Stages (days)						
		Stage I	Stage II	Stage III	Stage IV	Stage V	Stage VI	Stage VII
		0-31	32-40	41-106	107-168	169-222	223-263	264-560
Nutrients ($mg.L^{-1}$)	Chemical Oxygen Demand	655	655	655	740	740	740	1460
	Nitrate Nitrogen	50	50	50	100	100	100	185
	Calcium Formate	200	100	100	0	0	0	0
	Sodium Formate	1100	1100	1100	1600	1600	1600	2200
	Methanol	235	250	250	250	250	250	634
	Urea	6000	6000	1000	1000	1000	1000	1000
	Yeast Extract	4	4	100	100	100	50	50
	Sodium Chloride	2000	2000	2000	2000	2000	2000	500
	Potassium Dihydrogen Phosphate	10	10	10	10	10	10	10
Other parameters	Settling Period (min)	30	5	5	0	0	0	0
	HRT (hours)	12	12	12	12	12	12	12
	pH of the nutrient solution	~9.75	~9.75	~9.75	~9.75	~9.75	~9.75	~9.75
	Cross-inoculation	+	+	+	+	-	-	-

Stage I (0-31 days): During the initial stage, the two types of inoculum were utilized. The operation was conducted for the production of biogranules that could be used under alkaline pH conditions (pH 9.5-10), high urea concentration (6 $g.L^{-1}$), moderate salinity (2 $g.L^{-1}$ NaCl), and low yeast extract (4 $mg.L^{-1}$).

Stage II (32-40 days): The amount of $Ca(HCOO)_2$ was halved in this operational stage to reduce the dissolved Ca^{2+} related mineralization problem. The settling period was decreased from 30 minutes to 5 minutes.

Stage III (41-106 days): The amount of yeast extract was increased to boost the activity and the urea amount was decreased in order to regulate F/M ratio.

Stage IV (107-168 days): The nitrate nitrogen (NO_3-N) amount was increased to enhance anoxic urea hydrolysis instead of aerobic urea hydrolysis. $Ca(HCOO)_2$, the sole Ca^{2+} source in the nutrient solution, was replaced with NaHCOO to prevent mineralization of the biomass in the reactor without causing any changes in Chemical Oxygen Demand (COD) of the feed. The settling period was completely removed on the 107^{th} operating day to ensure that the flocs washed out from the bioreactor during the feeding/withdrawal period.

Stage V (169-222 days): Cross-inoculation was terminated.

Stage VI (223-263 days): The yeast extract concentration was reduced from 100 $mg.L^{-1}$ to 50 $mg.L^{-1}$ to decrease reliance on yeast extract in biomineralization applications.

Stage VII (224-560 days): COD and NO_3-N amount were increased to increase daily biogranule yield. Osmotic pressure was decreased by decreasing the NaCl content of the feed.

In all stages, KH_2PO_4 was used in the nutrient solution as 10 $mg.L^{-1}$, and the pH of the nutrient solution was adjusted to values ranging between 9.5 and 10.0 by using NaOH.

3.2 Analysis of Biogranulation Performance and Microbial Activity

The formation of biogranules in the granulation process was observed through the analysis of parameters such as total suspended solids (TSS), volatile suspended solids (VSS), sludge volume index (SVI), and wet granule size distribution. Furthermore, microscopic examination was conducted to assess the surface characteristics of flocs and granules.

During the reactor operation, regular samples were taken from the feed solution and at two-time points; (i) at the end of the anoxic period and (i) at the end of the aerobic period. Samples were analyzed for pH, dissolved oxygen concentration, COD concentrations, NO_3-N concentrations, and total ammonium nitrogen (TAN) concentrations. Results were used to monitor urea hydrolysis and nitrate reduction activities in the reactor.

Monitoring microbial activity involved tracking denitrification, organic carbon consumption, and urea hydrolysis efficiencies of biogranules at the end of the anoxic and aerobic periods with samples taken at different time intervals during a single cycle. Samples were obtained at three distinct time points: from the feeding solution (t=0), the effluent of the preceding cycle (t=0), the anoxic effluent of the new cycle (t=180 min), and the aerobic effluent of the new cycle (t=360 min).

The analytical techniques employed for the systematic monitoring of the biogranulation reactor are summarized as follows.

pH: Measurements were conducted on a daily basis using a Hanna HI98190 pH meter.

DO: Measurements were conducted on a daily basis using a Hanna HI98193 DO meter.

TSS & VSS: Tests were performed to analyze the amount of total suspended solids and volatile suspended solids, following the guidelines outlined in standard methods 2540 D and E [151].

SVI: The SVI_{30} measurements were obtained following the standard procedure 2710 D. As previously reported by Liu et al. [163], the duration of the method was adjusted to 5 minutes for the determination of SVI_5.

Granule Percentage and Mean Granule Size: The ratio of SVI_{30} to SVI_5 serves as a valuable indicator for approximating the proportion of granules present in the reactor.

$$\text{Granulation Percentage} = \frac{SVI_{30}}{SVI_5} x100 \quad (19)$$

The formula expressed by Liu et al. [152] and presented in Equation 19 was utilized to determine the granule percentage in the reactor during the granulation period. After obtaining the granular system, granule samples taken from the reactor were measured under a microscope at 100 μm intervals for each size. Samples for wet granule size determination were obtained during the fully mixed aerobic period. Samples were dropped onto a glass surface and observed under 40x and 100x magnification with a light microscope. Micrographs were captured with a 25-megapixel camera. Subsequently, 8-9 granules were randomly selected from each micrograph using ImageJ software, and their sizes were measured. The same process was applied to 20 photographs to determine the wet size distribution of granules.

COD: Soluble COD was determined in the range of 100-1000 $mg.L^{-1}$ by using EPA-approved HACH LCI 400 test kits and prepared kits in the laboratory. The calibration curve for the prepared kits was attached as Figure Annex 1. Absorbance values were read spectrophotometer at 620 nm wavelength (Dr. Lange CADAS 200).

Total Ammonium Nitrogen (TAN): TAN analyses were undertaken to assess the efficiency of urea hydrolysis induced by microbial activity. According to the urea hydrolysis overall equation, 2 moles of TAN are obtained from the hydrolysis of 1 mole of urea (Equations 1-5). Samples were filtered through 0.45 μm PTFE syringe filters to remove all the solids. Then, filtered samples were diluted up to 20 times when necessary and analyzed according to the instructions given in standard methods 4500-NH3 Step-B, C, using 0.02 N sulfuric acid as the titrant. The distillation step was conducted by using the BUCHI K-350 Distillation Unit.

NO_3-N and NO_2-N (Nitrate and Nitrite Nitrogen): The levels of nitrate nitrogen in filtered samples were quantified in the range of 5-35 $mg.L^{-1}$ NO_3-N utilizing HACH LCK 340 test kits. Additionally, nitrite nitrogen levels were quantified in the range of 0.6-6.0 $mg.L^{-1}$ NO_2-N utilizing HACH LCK 340 test kits. The samples were diluted up to 10 times when necessary. Absorbance values were read by spectrophotometer by the kit code (Dr. Lange CADAS 200).

3.3 Monitoring of Nutrient Consumption in a Single Cycle

To explore the nutrient consumption by biogranules at a single cycle and to determine the microbial activity of these granules, samples were collected at 15-minute intervals throughout the entire cycle (from t=0 to t= 360 min). Collected samples were analyzed to determine changes in total ammonium nitrogen (TAN), chemical oxygen demand (COD), and nitrate nitrogen (NO_3-N) concentrations. In typical operational conditions, the granulation reactor received feeding from the bottom part at a rate of 5 $mL.min^{-1}$ over 120 minutes, facilitating the passage of the nutrient solution through the sludge layer. While fresh nutrient was supplied from the bottom, nutrients consumed in the previous cycle were discharged from the top of the reactor simultaneously. In experiments focusing on the monitoring of a single cycle, the reactor was operated in a completely mixed batch reactor mode. Therefore, any heterogeneity that might happen due to the up-flow feeding of the reactor was avoided. The completely mixed batch operation was only applied for observation of the changes in nutrient concentrations with respect to time in a single cycle. In order to switch to this mode, after the completion of the previous cycle, half of the reactor volume was replaced with the fresh nutrient solution. This moment was defined as t=0 and samples were collected at every 15 minutes until the end of the cycle. Before taking the samples, the reactor content was thoroughly mixed to ensure homogeneity. In this mode, the anoxic period was from t=0 min to t=180 minutes and the aerobic period was between t=180 min to t=360 minutes.

3.4 Examination of Possible Dissimilatory Nitrate Reduction to Ammonia (DNRA) Occurrence within the Bioreactor

DNRA is another nitrate reduction metabolism and might be more favorable compared to denitrification under certain conditions. The presence of dissimilatory nitrate reduction to ammonia in the reactor was exclusively checked by simulating the anoxic period of a single reactor cycle in a separate 100 mL batch reactor (Figure 3.3). The batch reactor was set up to have the same VSS concentration as the SBR. In order to achieve the latter, granule samples were collected from the SBR during the aeration period (close to the end of the cycle) and further centrifuged at 3045 *g* for 5 minutes for separation of the biomass. Collected biogranules were rinsed twice by using tap water to get rid of any soluble matter, urea in particular, coming from the SBR. Therefore, any potential interference with the batch analysis was minimized. In rinsing procedure, centrifuged solids were

resuspended in tap water by using a vortex machine and then centrifuged again. Collected and rinsed biogranules were re-suspended in a urea-free nutrient solution to achieve a similar VSS concentration with the SBR. The nutrient solution used in this batch reactor was urea-free in order to distinguish any TAN production through DNRA metabolism. Nutrient solution was composed of 90 $mg.L^{-1}$ of NO_3-N and 730 $mg.L^{-1}$ of COD creating conditions for any type of nitrate reduction. This batch reactor was operated under anoxic conditions for three hours to simulate the anoxic period of a single cycle of SBR under urea-free conditions. Samples were collected every half hour and analyzed for TAN and NO_3-N to ascertain the occurrence of nitrate ammonification.

Figure 3.3. DNRA batch reactor

3.5 Detecting Whether the Urease Enzyme in Biogranules Is Suppressive or Non-Suppressive

In order to determine whether the urease enzyme in biogranules is suppressive or non-suppressive, high urea-containing batch reactors were established. Biogranule samples were taken from the reactor with the same procedure as the DNRA test. The effect of initial biogranule concentration under similar nutrient conditions was also assessed in this setup. Recorded VSS concentrations whilst reactor operation were considered while deciding the two different initial biogranule concentrations in the batch reactors. Accordingly, high, and low biogranule concentrations were set as 6.5 g $VSS.L^{-1}$ and 2 g $VSS.L^{-1}$, respectively. Additionally, to assess the impact of yeast extract on activity, two different concentrations of yeast extract were used in the nutrient solution (0.05 $g.L^{-1}$ and 5 $g.L^{-1}$). The nutrient solution, containing 10 $g.L^{-1}$ urea, 10 $g.L^{-1}$ NaHCOO, 3 $g.L^{-1}$ $NaNO_3$, 0.01 $g.L^{-1}$ KH_2PO_4, and 0.09 $g.L^{-1}$ $MgSO_4.7H_2O$, was prepared with two different concentrations of yeast extract (0.05 and 5.00 $g.L^{-1}$ yeast extract) and used in the test conducted at room temperature. According to the SBR loading rates, urea was 4 times higher in this test. Thus, the anoxic period time was adjusted to 12 hours, and

the aerobic period was adjusted to 18 hours because of no additional air supply. Serum bottles with a volume of 100 mL were utilized for the setup of batch reactors (Figure 3.4). Throughout the 30-hour operation of the batch reactors, aeration was restricted for the initial 12 hours to achieve anoxic conditions, while aeration was unrestricted for the remaining 18 hours. During the operation of the batch reactors over 30 hours, samples were collected at 3-hour intervals during the first 12 hours, with the last two samples taken at the 26th and 30th hours.

Table 3.2. Batch reactors used in the determination of the form of urease enzyme test

Batch Name	VSS (g.L^{-1})	Yeast Extract (g.L^{-1})
A	6.5	5
B	6.5	0.05
C	2	5

Figure 3.4. Used batch reactors during the anoxic period in the determination of the form of urease enzyme test (Table 3.2)

3.6 Ensuring the Consistent Production of Similar Biogranules

In order to determine the microbial composition of the biogranules metagenomic analyses were conducted. After achieving granulation on day 270th, three samples were taken from the bioreactor on days 347, 469, and 498. In order to analyze the microbial composition of the biogranules in wet and desiccated form, on the 469th day, wet and desiccated samples were prepared. Wet biogranule samples were taken from the bioreactor under completely mixed conditions during aeration. Taken biogranules on day 469 were rinsed as described in section 3.4 and a portion of them were dried at 60°C for two days.

Biogranules were regarded as specimens of environmental origin, and the retrieval of DNA was accomplished utilizing the GeneMATRIX Environmental DNA RNA Purification Kit (Gdańsk, Poland). Subsequent to DNA extraction from wet and desiccated samples, the quality assessment of the extracted DNA was performed using the Thermo Scientific NanoDrop-One spectrophotometer. The 16S rRNA gene was amplified from the DNA using the R341F (-CCTACGGGNGGCWGCAG-) and 850R (-ACTACHVGGGTATCTAA-) primers, followed by purification.

Subsequently, illumina binary indexes and adapters were incorporated through the utilization of the Nextera XT index kit in the index PCR step. The libraries produced via real-time PCR were quantified for concentration and standardized to 4nM. These standardized samples underwent pooling for combination. After the completion of library preparation, the sequencing by synthesis technique was utilized, facilitating the optical detection, and recording of the fluorescent emission corresponding to each newly introduced deoxyribonucleoside triphosphate (dNTP).

The sequencing output underwent conversion into raw data formatted in FASTA for subsequent analysis. Evaluation of the obtained raw data's quality was carried out utilizing FastQC, followed by the assessment of read quality using QIIME2. Subsequently, chimeric reads were identified and eliminated using DADA2, alongside the filtration of reads with Phred scores below 20, as well as primers and barcodes. Taxonomic classification was performed for each sample through QIIME2, involving the clustering of similar sequences and their assignment to respective taxonomic units (OTUs). The analysis steps applied to the raw data obtained after amplification of the 16S rRNA gene are provided in Figure 3.5.

3.7 Comparison of Produced Biogranules and Reference Granular Culture for MICP

In this study, since the biogranules produced are intended for biomineralization applications, a comparison was made with a reference granulated culture produced for this purpose. The first biogranules on this subject were Activated Compact Denitrifying Core (ACDC) reported by [69,148], and these granules were taken as reference in comparisons.

The reference granulated culture (ACDC) was produced as denitrification-oriented in a minimal nutrient medium without using yeast extract. The reference granular culture was

desiccated at 60°C for two days and the sizes of desiccated biogranules had a range of 0.45-2.00 mm [148].

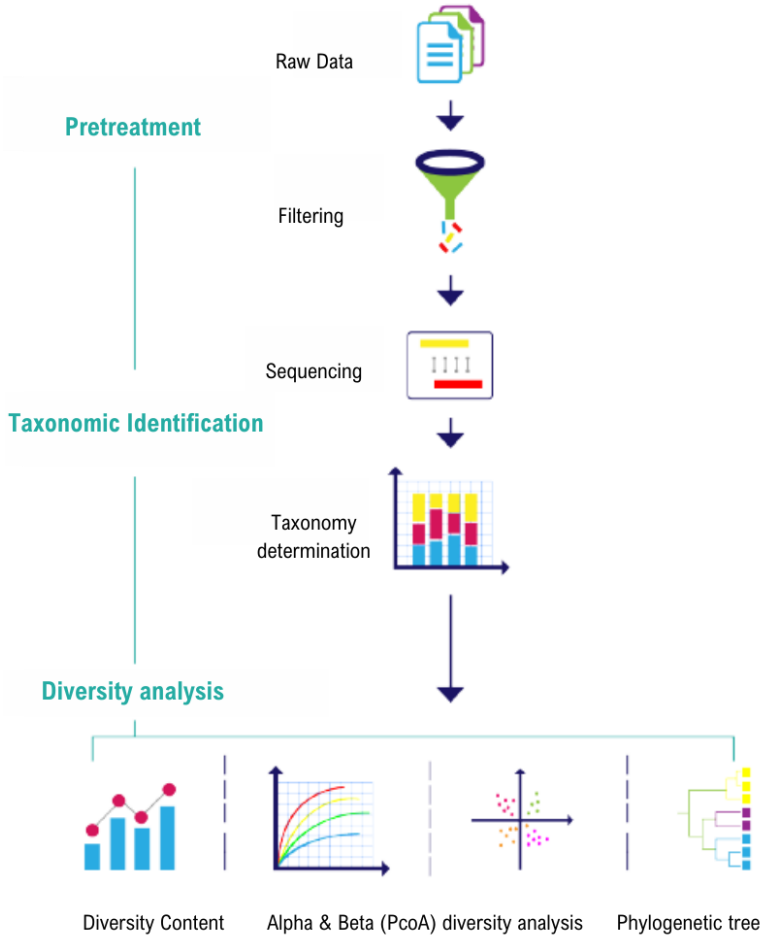

Figure 3.5. Analysis steps of the raw data obtained by amplification of the 16S rRNA Gene

3.7.1 Comparison of Specific Activity of Produced Biogranules and the Reference Granular Culture

In order to compare the specific activity of biogranules in terms of urea hydrolysis and denitrification, separate batch reactors were set up. The produced biogranules in SBR were evaluated in both wet and desiccated forms. For the preparation of wet and desiccated samples, the biogranules were harvested at the end of an aerobic period of a cycle before settling and then centrifuged at 3045 *g* for 5 minutes. Harvested biogranules were rinsed as described in Section 3.4 and a portion of them was desiccated at 60°C for two days. Thus, both wet and desiccated granules could be achieved for further tests. Similarly, previously dried, and stored reference granular culture, prepared using a similar

procedure, were also tested in desiccated form. The initial bacterial concentration in the reactors was adjusted to 0.5 g VSS.L^{-1} in the form of wet or desiccated biogranules.

Batch tests were conducted by using 100 mL serum bottles with rubber stoppers and 100 mL erlenmeyer flasks. Before use, all glassware and equipment were autoclaved at 1 bar and 121 °C for 20 min. The tests were conducted at room temperature and lasted for 48 hours. In the first 24 hours, 100 mL serum bottles were tightly closed with rubber stoppers restricting air access and enabling the anoxic conditions (Figure 3.6a). In the subsequent 24 hours of operation, the reactor contents were transferred to 100 mL flasks and plugged with cotton enabling air access to the headspace. The batch reactors were placed in a shaker at 100 rpm during the air-contact conditions to enhance air access (Figure 3.6b). Samples (5 mL each) were taken at six-hour intervals. Immediately upon sampling, the samples were filtered and stored in a refrigerator at +4°C until analysis. The nutrient solution content and important parameters used in microbial activity tests were summarized in Table 3.3.

Table 3.3. The content of the nutrient solution used in microbial activity tests

Chemical	**Concentration (g.L^{-1})**	**Important Parameters**	**Concentration (g.L^{-1})**
CH_4N_2O (Urea)	10.00	Urea	10.00
$NaNO_3$	0.69	NO_3-N	0.11
NaHCOO	2.50	COD	1.16
$MgSO_4.7H_2O$	0.09	Ca^{2+}	-
Yeast Extract	0.05	Yeast Extract	0.05
KH_2PO_4	0.01	PO_4-P	0.02
CH_3OH	0.39	COD:N ratio (unitless)	10.27

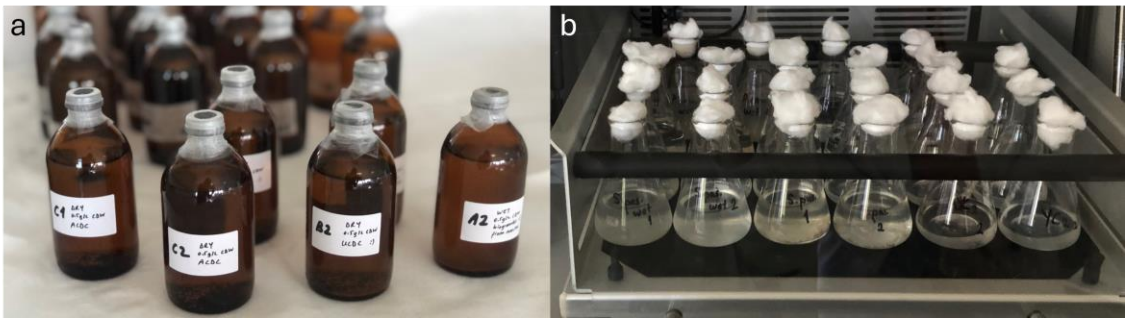

Figure 3.6. Batch reactors used in the Comparison of Specific Activity of Produced Biogranules and ACDC test a) Under anoxic condition b) Under open condition

3.7.2 Assessment of Biomineralization Capacity of Produced Biogranules and The Reference Granular Culture

To analyze the biomineralization capacity of the produced biogranules in this study and previously produced nitrate-reducing granular culture (ACDC), biomineralization tests were conducted. The biogranules to be used in the biomineralization tests were prepared using the same method employed in Section 3.7.1. The nutrient solution content and important parameters used in the biomineralization test were provided in Table 3.4. Since the aim was biomineralization, much higher amounts of urea and nitrate were used in this test compared to the SBR operation. Similarly, the initial bacterial concentration in each reactor was adjusted to 0.5 g VSS.L^{-1} in the form of wet and desiccated biogranules. Since yeast extract is not desired in some biomineralization applications such as self-healing bioconcrete, some reactors were set up without yeast extract in order to observe its effects.

Table 3.4. The content of nutrient solution used in biomineralization tests

Chemical	Concentration (g.L^{-1})	Important Parameters	Concentration (g.L^{-1})
CH_4N_2O (Urea)	10.00	Urea	10.00
$Ca(NO_3)_2.4H_2O$	2.11	NO_3-N	0.25
$Ca(HCOO)_2$	7.33	COD	1.94
Maya Özütü	0.05	Ca^{2+}	2.61
CH_3OH	0.11	COD:N ratio (unitless)	7.76

It was reported that the reference granular culture (ACDC) was resuscitated approximately 1 week after the pH dropped to 10 in the mortar [14]. In the biomineralization test, due to the use of desiccated biogranules, the test duration was adjusted to 9 days considering the resuscitation time of biogranules. The batch reactors used in the biomineralization test were operated for a total of nine days, with the first six days under anoxic conditions followed by three days under open conditions. Samples of 5 mL were collected daily, passed through a syringe filter, and stored in a refrigerator at +4°C until subsequent analysis. The total amount of precipitated $CaCO_3$ was determined by using the carbon dioxide volume exchange method described in previous biomineralization studies [52,153]. The test setup for measurements was given in Figure 3.7. As depicted in Equation 20, the amount of precipitated calcium carbonate was calculated from the volume of gas released by dissolving the biominerals using 10 M H_2SO_4.

$$CaCO_3 + H_2SO_4 \rightarrow CaSO_4 + CO_2\uparrow + H_2O \quad (20)$$

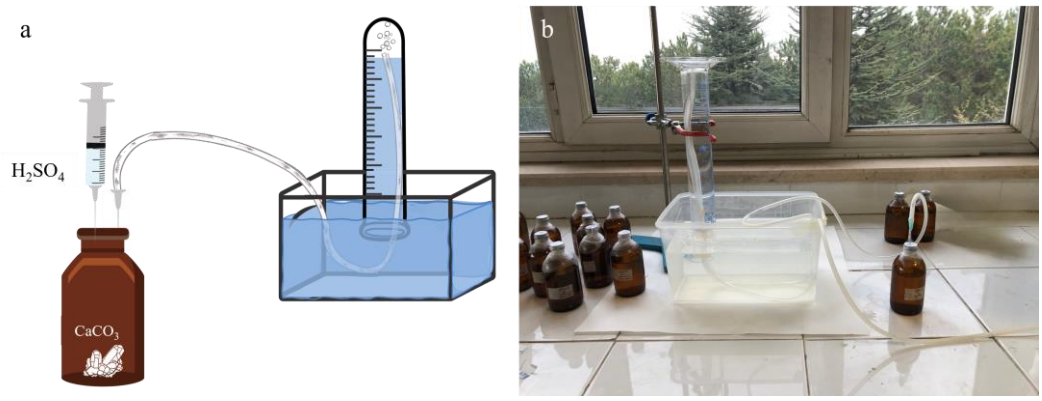

Figure 3.7. Carbon dioxide volume exchange method used for measuring calcium carbonate a) Schematic representation b) Experimental setup

3.8 Investigation of the Morphology and Chemical Composition of Precipitated Minerals

In order to investigate the precipitated minerals a batch reactor containing desiccated biogranules was set up with the same procedure in Section 3.7.2. The precipitates in this batch reactor were coated with a thin layer of gold and then analyzed by scanning electron microscopy (SEM) (GAIA3+Oxford XMax 150 EDS). The analysis was conducted under 5 kV under vacuum and 10 mm working distance. Furthermore, energy dispersive x-ray spectroscopy (EDX) analysis was done to determine the chemical composition of the precipitates.

4. RESULTS AND DISCUSSION

4.1 Granulation of the enrichment culture under minimal nutrient conditions

Biomineralization applications require resilience against certain stress conditions such as osmotic stress, alkali pH, and minimal nutrient conditions. Therefore, in this thesis study, the SBR was operated to selectively enrich a non-axenic microbial community that can be used in biomineralization applications. The ultimate purpose was to facilitate the granulation of the enrichment to benefit from the resilience of a granulated culture.

Optimization of the enrichment and the granulation under minimal nutrient conditions required fine-tuning of several operational parameters and the nutrient solution. Therefore, the bioreactor was operated for a total of 560 days covering seven distinct operational stages. The seventh stage was between the operational days 264 and 560 was the steady period for granulation and granule production. After the optimization of operational parameters, the bioreactor achieved stable granule production.

4.1.1 Variations due to the modifications in operational conditions and the nutrient solution

The operational conditions are more or less well-defined in the literature, so no crucial changes were made to the operational parameters. In order to optimize the granulation of the microbial community within the bioreactor and its microbial activity, modifications were made to the reactor's nutrient solution at different times as detailed in Table 3.1. Modifications made at each stage and their consequences were summarized in this section.

Stage I (0-31 days): In the first stage, corresponding to the initial days of operation, the reactor was operated with the inoculum containing floc-granule mixture and continuously cross-inoculated with a heat- and alkali-tolerant microbial culture. The operation was conducted under alkaline pH conditions (pH 9.5-10), high urea concentration (6 $g.L^{-1}$), moderate salinity (2 $g.L^{-1}$ NaCl), and low yeast extract (4 $mg.L^{-1}$). However, the acclimation could not be achieved under these operating conditions, because the microbial activity in the reactor induced a significant amount of calcium carbonate precipitation. Precipitation of minerals around the microorganisms negatively affected the microbial activity and the production of biomass. Moreover, the accumulated minerals

caused abrasion and fragmentation in the floccule-granule mixture. Consequently, no further granulation could be achieved during this stage.

Stage II (32-40 days): During Stage II, to decrease the feeding of dissolved calcium into the reactor and suppress the further formation of $CaCO_3$ minerals, the concentration of $Ca(HCOO)_2$ in the nutrient solution was halved. As a result, the Ca^{2+} content of the feed decreased from 60 $mg.L^{-1}$ to 30 $mg.L^{-1}$. However, due to the high mineral precipitation in the reactor in the first 30 days (Stage I), decreasing the Ca^{2+} of the feed was not enough to recover microbial growth and activity. Therefore, on Day 40, to get rid of the precipitated minerals in the reactor and to mitigate the impact of accumulated $CaCO_3$ on microbial activity, a solid-liquid mixture was extracted from the reactor and the pH was lowered to 6.5 using acetic acid, dissolving the $CaCO_3$ minerals. After settling the solids, the liquid was discarded thus removing the dissolved Ca^{2+}. However, this harsh procedure also caused the loss of some of the active microbial biomass which was detected by VSS-TSS analysis.

Stage III (41-106 days): The loss of a portion of the active microbial biomass caused an increase in the food-to-microorganism (F/M) ratio. The latter worsened the already low urea hydrolysis activity. Therefore, on the 41st day, the urea concentration in the nutrient composition was decreased from 6 $g.L^{-1}$ to 1 $g.L^{-1}$. Additionally, to promote the growth of microorganisms, the concentration of yeast extract was raised from 4 $mg.L^{-1}$ to 100 $mg.L^{-1}$.

Stage IV (107-168 days): Due to the low anoxic urea hydrolysis in the third stage, the nitrate nitrogen (NO_3-N) amount was increased from 50 $mg.L^{-1}$ to 100 $mg.L^{-1}$ to enhance anoxic urea hydrolysis instead of aerobic urea hydrolysis. Also, the COD amount was increased from 655 $mg.L^{-1}$ to 740 $mg.L^{-1}$ to regulate the C:N ratio. Since the $CaCO_3$ minerals formed due to MICP increase the amount of TSS, it reduces the VSS:TSS ratio. In this stage, VSS:TSS ratio was below 0.30 which is the critical level for this parameter. In order to increase VSS:TSS ratio, mineral production should be limited. Thus, $Ca(HCOO)_2$, the sole Ca^{2+} source in the nutrient solution, was substituted with NaHCOO to minimize the MICP occurrence within the reactor. It was determined by AAS analysis that the tap water used in feed preparation contained 50 $mg.L^{-1}$ Ca^{2+}, and this amount was thought to be sufficient.

Stage V (169-222 days): To date in operational stages, the desired VSS:TSS ratio of 0.5 and recovery could not be attained. Thus, new modifications were made for recovery. On the one hand, considering the total urea hydrolysis efficiency, which increased from the first to the fourth operating stage and reached over 50%, and nitrate reduction efficiency which was above 90% in the fourth operating stage, it was thought that selective enrichment was achieved. Thus, due to the negative impact on settling characteristics, the cross-inoculation process was terminated on the 169th day. On the other hand, a quantity of 6 grams of powder containing denitrifying spores, previously utilized in [89], was added to the bioreactor in order to promote the VSS amount. During the fifth operational stage, due to the stable level of VSS, recovery in microbial activities was observed. With the decreasing trend in TSS values, the beginning of an increase in the VSS: TSS ratio was observed.

Stage VI (223-263 days): Recovery was successfully achieved as a result of the changes made in Stage V, focused on the application areas of the produced biogranules in Stage VI. Therefore, a modification was made towards biomineralization applications by reducing the yeast extract concentration from 100 mg.L^{-1} to 50 mg.L^{-1}. This change did not create any adverse effects, and the recovery in VSS quantity, microbial activities, and the VSS:TSS ratio observed from the fifth stage onwards continued during this stage as well. Stage VII (264-560 days): In order to promote granule formation and increase the amount of VSS produced in a day (biomass yield), the concentrations of COD and NO_3-N in the feed were increased. Biogranules were exposed to salt stress for 42 days since recovery was achieved at the end of Stage 5. Since this period was thought to be sufficient for the enrichment of bacteria with osmotic stress tolerance the stress from the saline environment was reduced from 2000 to 500 mg.L^{-1}. Following these recent changes, no adverse effects were encountered, and granule production in the reactor continued successfully. The optimization of operational conditions continued until the 264th day. The recovery in the reactor started on the 169th operational day, with granulation achieved around the 270th day. After achieving granulation, starting from Day 300, selective pressure was applied once a week to promote further granulation in the system. This involved a three-minute settling period followed by removing half of the reactor content to wash out flocs. Upon all the modifications, optimum key operational parameters were defined as given in Table 4.1.

Table 4.1. Optimum key operational parameters for granulation and production of urea hydrolyzing-nitrate reducing culture

Loading Rates ($kg.m^{-3}.day^{-1}$)			**Nutritional Supplement** ($mg.L^{-1}$)		**Period Time** (min)**	
COD	**NO_3-N**	**Urea**	**Yeast Extract**	**Calcium***	**Anoxic**	**Aerobic**
2.92	0.37	2	50	50*	180	180
*Only 50 $mg.L^{-1}$ of calcium was provided to the system through tap water used for nutrient preparation. **There is no settling period.						

4.1.2 Variations in the monitored parameters throughout the optimization and steady operation stages of the biogranule reactor

pH

In certain biomineralization applications such as self-healing concrete and repair mortar, alkali-resistant bacteria are required due to the high pH conditions. Therefore, after preparing a nutrient solution, for the selection of alkali-resistant bacteria, the pH was adjusted to a value between 9.5 and 10.0. The reactor pH was monitored at regular intervals by conducting measurements at the end of each period (i.e. anoxic and aerobic) and illustrated in Figure 4.1. The pH values of the nutrient solution varied between 8.2 and 10.0 although it was adjusted to approximately 9.75. Under alkaline pH, bicarbonate carbonate balance shifts towards the carbonate ions bringing more carbon dioxide to the solution and increasing overall DIC levels. Over time, this resulted in a decrease in the pH of the nutrient solution. However, throughout the operation of the bioreactor, the pH fluctuated between 9.0 and 9.5 at the end of the aerobic and anoxic periods. Consequently, the necessary environmental conditions were established in the bioreactor for the selection of bacteria capable of operating under alkaline conditions and/or showing tolerance to alkaline conditions [147].

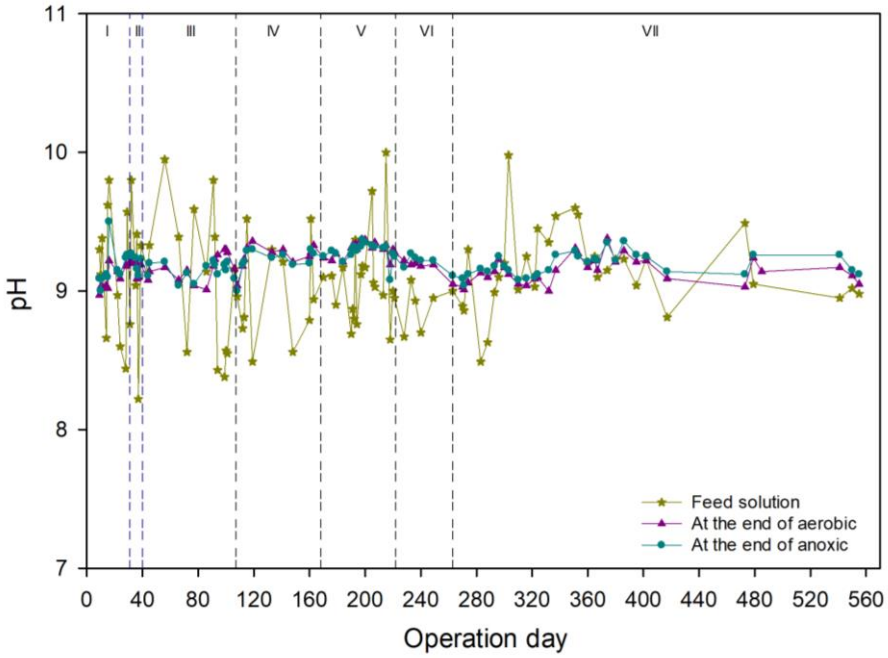

Figure 4.1. pH values monitored in the reactor

Dissolved Oxygen (DO)

The dissolved oxygen (DO) values were measured at the end of the anoxic and aerobic periods during the operation of the bioreactor and presented in Figure 4.2. According to the obtained data, dissolved oxygen was completely depleted during the anoxic period, while values ranging between 3 and 7 $mg.L^{-1}$ were observed during the aerobic period. These results suggest that the anoxic and aerobic periods were achieved as planned. However, the low DO values during the aerobic period indicate a low carbon consumption efficiency of the anoxic period, with carbon consumption continuing in the aerobic phase. This indirectly indicates that the famine period, an important parameter for granulation, was not adequately achieved during these periods (i.e., Stage II). Although long-term nutrient limitation is not essential for granulation according to the literature, it has been reported that granulation accelerates under nutrient-limited conditions [154,155]. Additionally, due to denitrification being dominant over DNRA at lower COD:N ratios, part of the carbon might have remained for the aerobic period. In the feed solution, the COD:N ratio is 13 (Stage I, II and III) and ~ 7.5 (Stage VI, V, VI and VII), and under minimal nutrient conditions, denitrification might have been more dominant at this COD:N ratio [156].

Periodically obtained DO values of 5 $mg.L^{-1}$ and above during the aerobic periods (Stage I, III, IV, V, VI, VII) serve as an indirect indicator that carbon limitation was achieved

during the aerobic phase in the bioreactor. This indication is particularly meaningful in reactor operations where aerobic processes such as nitrification are absent. Indeed, this phenomenon has been previously reported in kinetic analyses conducted on similar granulation reactors [148].

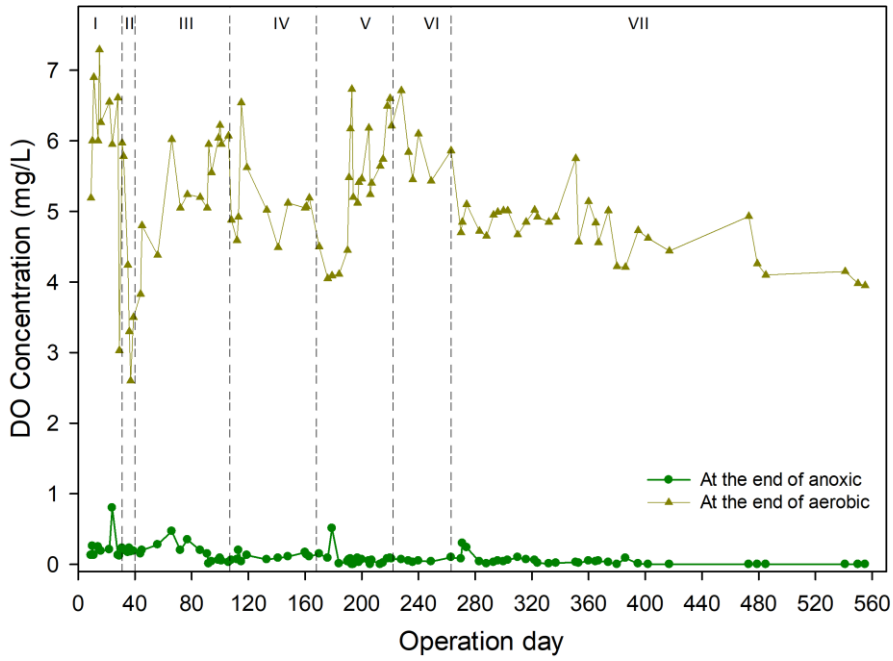

Figure 4.2. DO values monitored in the reactor

Total and Volatile Suspended Solids Concentrations (TSS-VSS)

Analyses were conducted at regular intervals to monitor the total suspended solids (TSS) and volatile suspended solids (VSS) in the bioreactor, and the results were presented in Figure 4.3. According to the results, a significant increase in the amount of TSS was observed during Stage I, while the VSS remained nearly constant. This phenomenon was attributed to the MICP due to the continuous activity of the inoculum (granule-floc mixture obtained from [147]. Considering the carbonate-pH balance, when the pH exceeds 9, carbonate formation increases. Dissolved inorganic carbon formed as a result of urea hydrolysis and denitrification converts to carbonate form in the alkaline environment, and in the presence of dissolved calcium, this leads to rapid precipitation. Considering the previously reported urea hydrolysis and denitrification efficiencies of the inoculum [147], the observed rapid mineral precipitation at pH 9 in a nutrient solution containing 6 $g.L^{-1}$ urea and 0.05 $g.L^{-1}$ NO_3-N was meaningful.

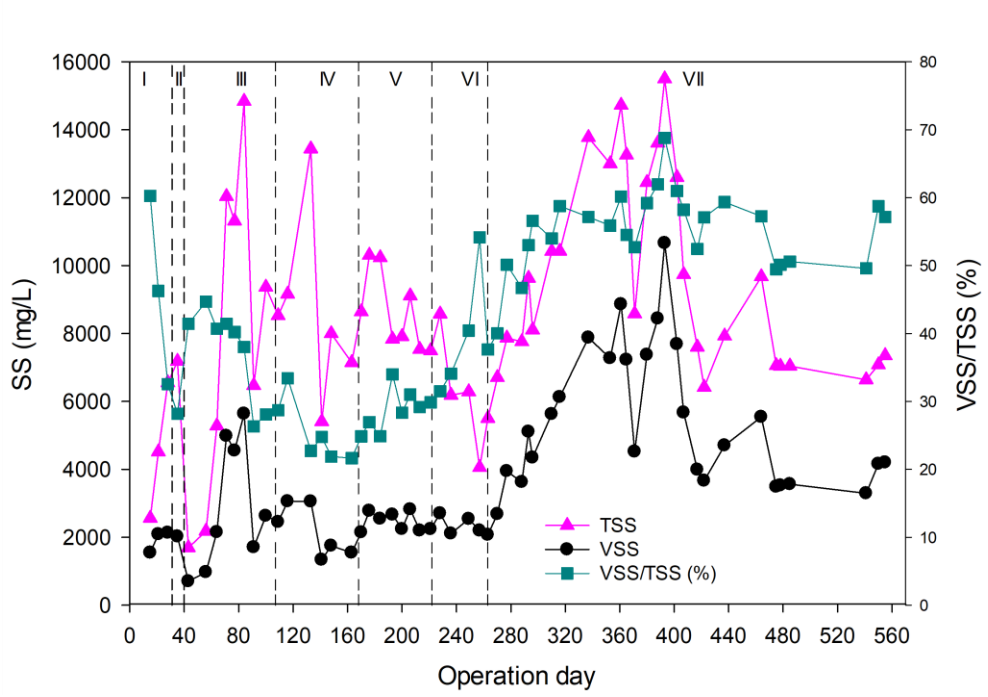

Figure 4.3. The amounts and ratios of suspended solids monitored in the reactor

During the initial stage of the bioreactor operation, the presence of abundant minerals was also observed under the microscope. In Figure 4.4a, the greenish powder like particles seen abundantly alongside the flocs under pink light were minerals. Granule-like microbial agglomerates appeared in pink/purple under the same light.

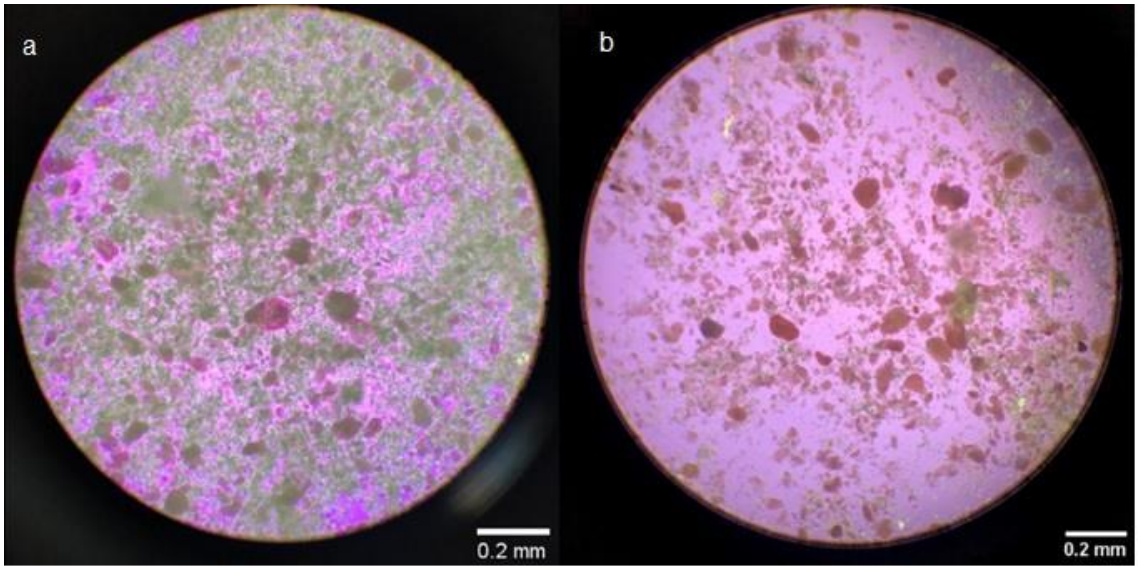

Figure 4.4. Micrographs of the biomass within the reactor: a) Biomass rich in minerals at the end of Stage I; b) Biomass washed with an acetic acid solution at the end of Stage II.

While the high presence of minerals adversely affected the operation, it also disrupted the structure of granules within the reactor. It as previously reported that during aeration

periods, minerals caused abrasion and fragmentation of the granules due to the generated shear stress [157].

In order to mitigate this adverse effect, it was aimed to prevent the excessive precipitation of minerals. Therefore, as the system passed to the second operational stage, the concentration of calcium in the nutrient solution was halved. Although this strategy could decrease the formation of new minerals, it did not provide a solution for the minerals that had already accumulated in the reactor during Stage I. During the second operating phase, the VSS:TSS ratio decreased to less than 30% as a result of the significant mineral accumulation in the reactor.

In an effort to reduce the mineral density within the reactor, on the 40th operational day, a solid-liquid mixture was extracted from the reactor content, and the pH was lowered to 6.5 using acetic acid. This process dissolved the $CaCO_3$ minerals, and the dissolved calcium was removed from the system along with the liquid mixture. The resulting composition was captured under the microscope, as shown in Figure 4.4b. It was evident from this intervention that minerals around the granules and within the reactor environment decreased considerably. Additionally, as shown in Figure 4.3, a significant decrease in TSS in stage II confirmed that a large portion of the minerals was dissolved and removed from the system. As a result of this intervention, at the end of stage II, the VSS:TSS ratio increased to over 40% (Figure 4.3). However, the washing process caused the decrease of VSS concentration from 2000 mg.L^{-1} to 700 mg.L^{-1}. This decrease was attributed to the disintegration of the flocs and granules which further caused washout of the bacteria. Due to their resilience to toxic effects and drastic changes in environmental conditions, and their denser extracellular polymer matrix, bacteria loss from granules was less pronounced compared to flocs, hence granules were more abundant under micrographs (Figure 4.4b).

The decrease in VSS caused an increase in the food to microorganism (F/M) ratio and negatively affected microbial activity. Hence, on the 41st day (Stage III), the urea content in the nutrient was reduced from 6 g.L^{-1} to 1 g.L^{-1}, and yeast extract was increased from 4 mg.L^{-1} to 100 mg.L^{-1} to support microbial growth. Cross-inoculation was continued using the culture enriched from the sugar factory process water. Despite the increase in VSS due to the changes made and cross-inoculation, the increase in TSS was greater than the increase in VSS over time. This eventually led to the washout of the freshly grown bacteria and a decrease in the VSS:TSS ratio in Stage III (Figure 4.3). These results

indicated the ongoing accumulation of minerals in the reactor during the third operational stage. Thus, the Ca^{2+} source was removed entirely from the nutrient solution in Stage IV.

During the cross-inoculation process, VSS values remained stable at levels between 2000-2500 $mg.L^{-1}$ until the middle of Stage IV (Day 133). Although cross-inoculation is important for enriching microorganisms capable of urea hydrolysis, it was found that the continuous addition of planktonic bacterial culture to the granulation reactor had a negative impact on the settling performance of the overall microbial community. As the settling period was completely removed after Day 133, any disruption in settling performance led to VSS loss from the reactor (Figure 4.3). Subsequently, as the negative effects of cross-inoculation began to outweigh the positive effects, the cross-inoculation process was stopped before Stage V (from day 169 onwards).

Additionally, the increase in TSS during Stage IV raised concerns about the potential presence of calcium in the tap water used in the nutrient solution. Subsequent analyses confirmed the presence of 50 $mg.L^{-1}$ of Ca^{2+} in the tap water used for preparation of the nutrient solution.

In Stage IV, the increase in NO_3-N in the nutrient content did not increase anoxic urea hydrolysis. Thus, at the beginning of Stage V, a quantity of 6 grams of desiccated biomass containing denitrifying spores, previously produced in [89], was added to the bioreactor. The purpose of this addition was to enhance the levels of VSS concentration and promote anoxic urea hydrolysis. Following these modifications, the precipitation of minerals in the reactor stopped and the TSS amount was reduced by applying 3 minutes of selective pressure. There was a consistent increase in the VSS:TSS ratio from 24% to 40% (Figure 4.3). The concentration of VSS remained constant at about 2500 $mg.L^{-1}$ from Stage V to Stage VI, which lasted for 96 days (Days 168-264). The stability of VSS levels in the reactor indicated the complete recovery of the granulation reactor during this stage.

The decline in the VSS values during Stage VII was due to the harvesting of biogranules from the reactor for experiments. A significant amount of granule was harvested from the reactor on day 362 (3.2-gram biogranule), on day 402 (3.6-gram biogranule), on day 417 (2-gram biogranule), and on day 470 (2-gram biogranule). To ensure rapid recovery of granule production and microbial activities in the reactor following the granule harvests, granule harvesting was conducted by maintaining the minimum VSS concentration of 4000 $mg.L^{-1}$ in the reactor.

Sludge Volume Index (SVI)

In order to determine the settling characteristics of the microbial culture within the bioreactor and to ascertain whether granulation occurred, the sludge volume index (SVI_{30} and SVI_5) values were measured at regular intervals, and the obtained data were presented in Figure 4.5. It was observed that the SVI_{30} and SVI_5 values of the biomass within the bioreactor varied between 7-80 $mL.g^{-1}$ and 9-131 $mL.g^{-1}$, respectively.

Previous studies reported that granules have a more compact structure than flocs and planktonic bacteria, and a 5-minute duration is sufficient for separation from water [152]. Therefore, several studies have reported using the SVI_{30}:SVI_5 ratio to calculate the granulation percentage [148,152,158]. However, meaningful evaluation of the SVI_{30}:SVI_5 ratio requires consideration of two key parameters. The first is the VSS:TSS ratio and the second is the SVI_{30} value itself. In systems where the VSS:TSS ratio is above 50%, if the SVI_{30} value falls below 50 $mL.g^{-1}$, the system is considered a complete granular system [159,160]. In these systems, the SVI_{30}:SVI_5 ratio mostly varies according to the compactness and size distribution of the granules [132,133,158]. Disruptions in granule structure and size distribution may lead to significant changes in the SVI_5 value, while there is usually no significant change in the SVI_{30} value as long as the granular system remains intact. However, in systems where the VSS:TSS ratio is below 50% the SVI_{30}:SVI_5 ratio cannot be used for the granulation percentage [133,152,161]. In these systems, the mineral density is high in both flocs and granules, rendering SVI data unsuitable for monitoring granulation [109]. In such cases, analyzing the size distribution and surface properties of granules is of paramount importance for granulation monitoring.

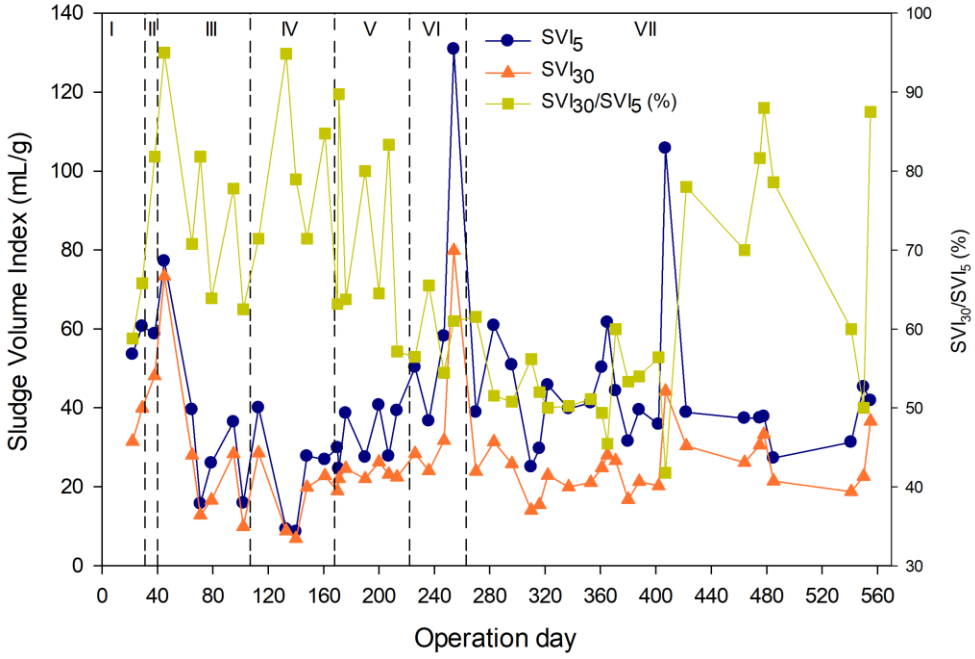

Figure 4.5. SVI values monitored in the reactor

When evaluating the SVI data presented above in conjunction with the VSS and TSS values (Figure 4.3), it was evident that a granular system was not achieved in the bioreactor for 270 days during the optimization of operating parameters, and the mineral content was abundant in total suspended solids (VSS:TSS ratio < 0.5). Throughout the bioreactor operation, SVI values were affected by mineral precipitation and the addition of planktonic bacteria with the cross-inoculation process. The mineral content decreased the SVI values and planktonic bacteria addition adversely affected the settling performance of the biomass. Thus, SVI values fluctuated during the first four stages. After preventing mineral precipitation and terminating the cross-inoculation, an increase in the VSS:TSS ratio has been observed from Stage V onwards (Figure 4.3), and parallel to this increase, an increase in SVI_5 values was observed (Figure 4.5). Particularly from Day 270 onwards, the VSS:TSS ratio passed the 50% threshold (Figure 4.3). Meanwhile, SVI_{30} values remained below 50 $mL.g^{-1}$ (Figure 4.5). These results indicated that in Stage VII, the VSS content in the reactor increased due to the enrichment of a microbial community capable of both urea hydrolysis and denitrification and SVI_{30} values remained below 50 $mL.g^{-1}$ as the enriched culture was granulating. SVI_{30} values below 50 $mL.g^{-1}$ with a VSS:TSS ratio over 50% represented the achievement of a granular biomass system.

The SVI_{30}:SVI_5 ratio could not be used to determine the granule percentage in the bioreactor because of the mineral precipitation and the sudden changes in SVI_5 values.

Size Distribution

In the first studies on granules in the literature, bacterial aggregates up to 200 µm were classified as floc, and larger than 200 µm were classified as granules [152,162,163]. During the reactor operation, examinations were conducted at regular intervals under a microscope to determine the wet-size distribution of the biogranules. Micrographs presented in Figure 4.7 revealed that the granules, which began forming around day 200, gradually increased in size and compactness over time. Following all modifications made to the reactor operation and nutrient solution, size distribution analyses conducted during the days 324-362 indicated that approximately 82±7% of the granules were larger than 200 µm. Analysis of the size distribution of the sample collected from the reactor on day 362 revealed that 94% of the granules in the sample were larger than 200 µm (Figure 4.6).

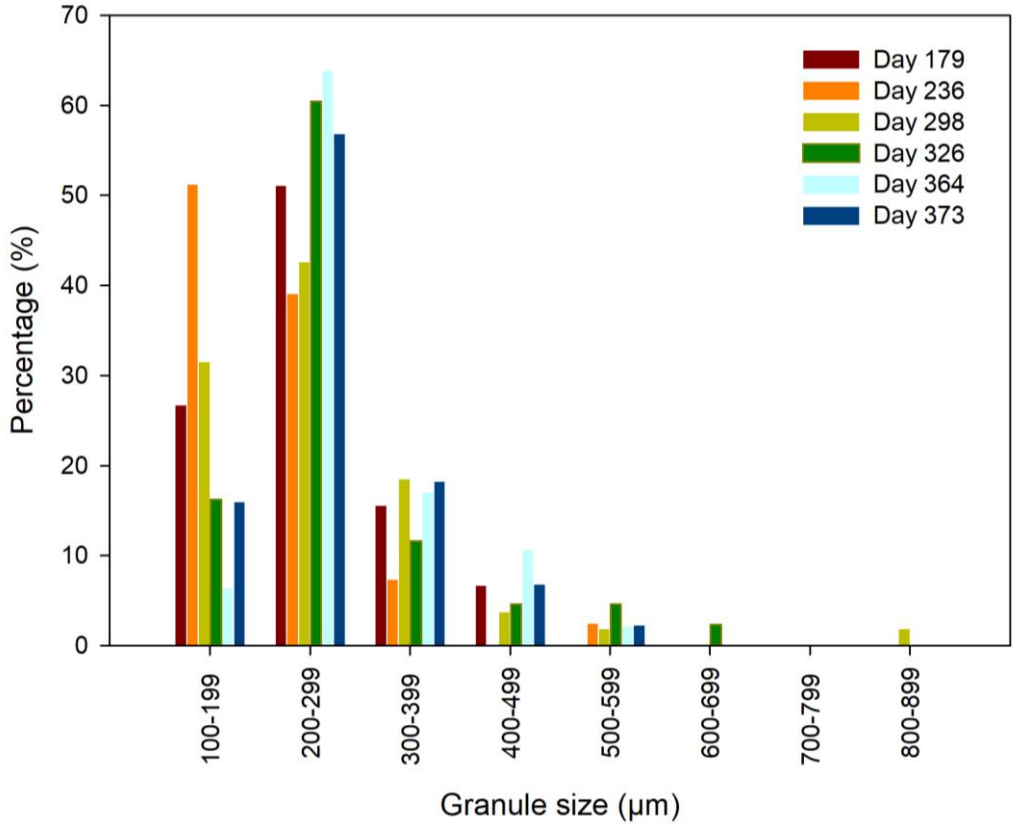

Figure 4.6. Size distribution of biogranules at different times

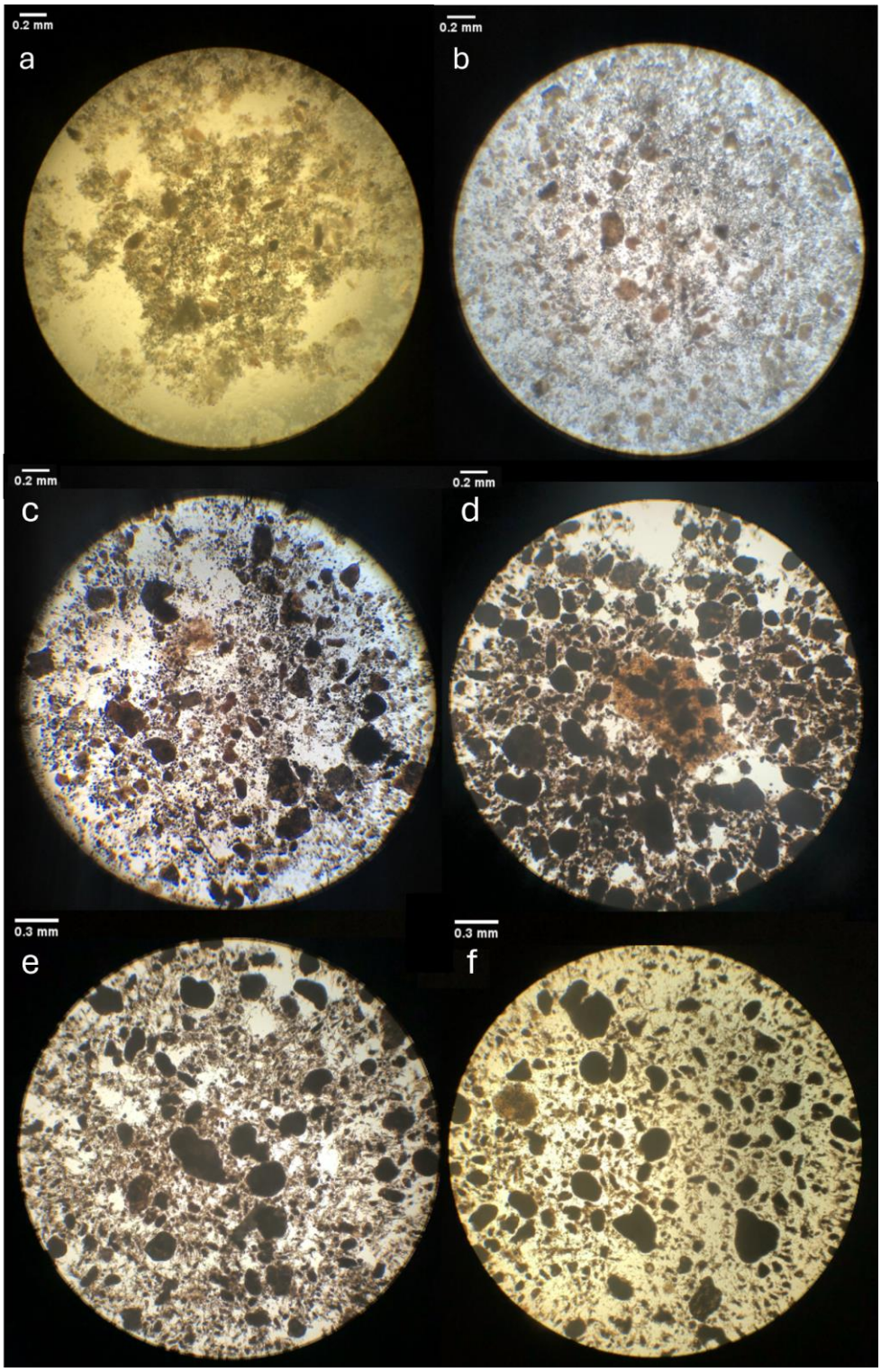

Figure 4.7. Granule micrographs in the bioreactor a) Day 201 (Stage V), b) Day 229 (Stage VI), c) Day 270 (Stage VII), d) Day 315 (Stage VII) e) Day 340 (Stage VII), f) Day 373 (Stage VII)

Following the optimization of operating parameters, the granular system was maintained throughout Stage VII. After the biogranule harvest from the reactor (Figure 4.3) on days 400, 417, and 470, it was observed that the reactor recovered, new granules formed, and the existing ones kept growing as shown in Figure 4.8. According to the sample taken on day 560, 54% of the granules in the sample were larger than 200 µm (Figure 4.8).

In granules and biofilms, parameters such as mass transfer, concentration gradient, and shear force affect biofilm thickness and granule size [136]. In studies defining the 200-µm threshold, the wastewater used was nutrient-rich, containing high levels of nitrogen, COD, and other components, which promoted rapid growth and the formation of larger granules [162,164]. Conversely, granules produced with low-strength wastewater were reported to grow at a slower rate and thus became smaller in size [100]. Due to certain characteristics that distinguish granules from flocs, such as compactness, settling characteristics, and a smooth outer surface, it was possible to obtain granules smaller than 200 µm [132]. Additionally, an extra selective pressure was applied once a week by settling from the midpoint of the reactor for 3 minutes. This factor also played a role in obtaining granules with smaller particle sizes. If this process had been performed more frequently, larger granules could have been obtained. In studies found in the literature, small and fragmented granules were removed from the system much more frequently. In this study, settling pressure was applied once a week, which resulted in smaller granules being retained in the system Therefore, considering the effects of extra hydraulic selection pressure and the minimal nutrient conditions, obtaining smaller-sized granules was meaningful [165].

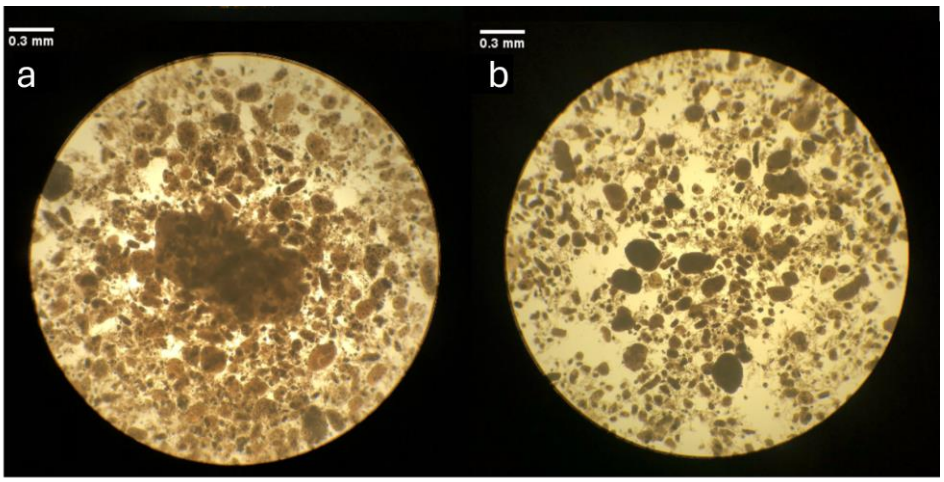

Figure 4.8. Granule micrographs in the bioreactor a) Day 466 (Stage VII), b) Day 560 (Stage VII)

During the Stage VII, the SVI_5 and SVI_{30} values were measured as 40±9 $mL.g^{-1}$ and 24±6 $mL.g^{-1}$, respectively. According to the settling performance, microscopic analysis, and VSS:TSS ratio, results revealed that the bioreactor operation had achieved the production of stable biogranules resilient to alkaline pH, high urea concentration, salinity, and minimal nutrient conditions in biomineralization applications.

Microbial Community of Produced Biogranules

The biogranules produced in this thesis study were intended for use in biomineralization applications as a product. Therefore, understanding the variations in the microbial community of the granules harvested at different periods was crucial. To investigate these variations, metagenomic analyses were performed on granules harvested at various intervals.

According to the obtained results from the metagenomic analysis, it was determined that at least 99% of the genetic material in the produced biogranules belongs to bacteria (Figure 4.9).

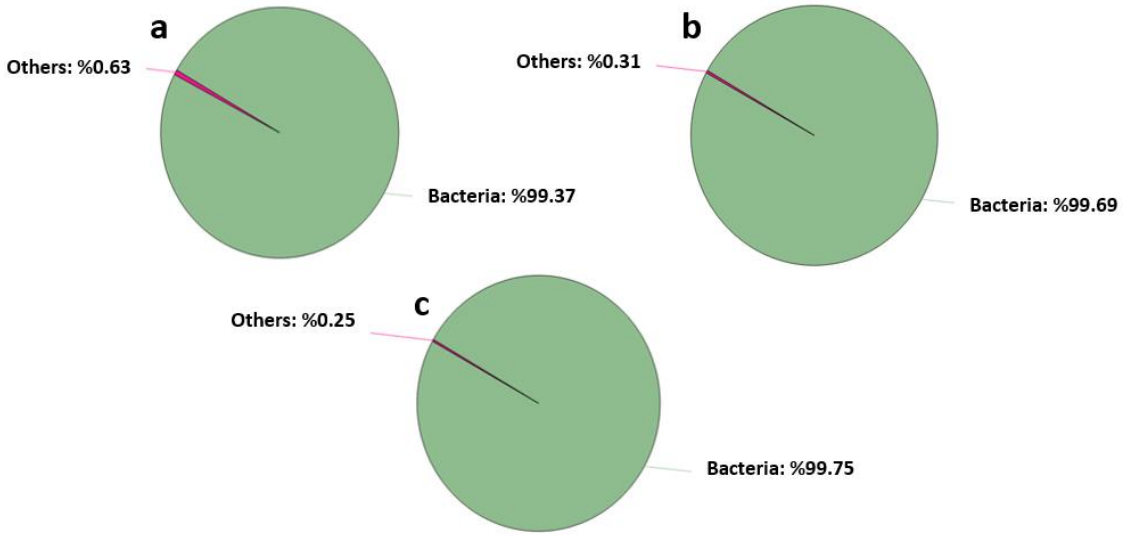

Figure 4.9. The taxonomic distribution of the biogranule samples in the kingdom level, a) Sample taken on day 347, b) Sample taken on day 469, c) Sample taken on day 498

Biogranule samples taken from the reactor at different operational times underwent metagenomic analyses in both wet and desiccated forms. The results obtained at the genus level were subjected to beta diversity analysis to examine the similarity of microbial communities in biogranules produced at different times in the reactor. According to beta diversity analysis, all granule samples taken at different times appeared similar to each

other. The three axes with the highest differences are presented in Figure 4.10. Additionally, wet, and desiccated forms of the obtained granules showed the highest similarity (Figure 4.10).

The presence of a consistent microbial community in biogranules produced at different times was considered advantageous for converting these granules into products and served as a quality control parameter. A similar microbial community ensured that comparable performance could be achieved in biomineralization applications, which was important for standardization.

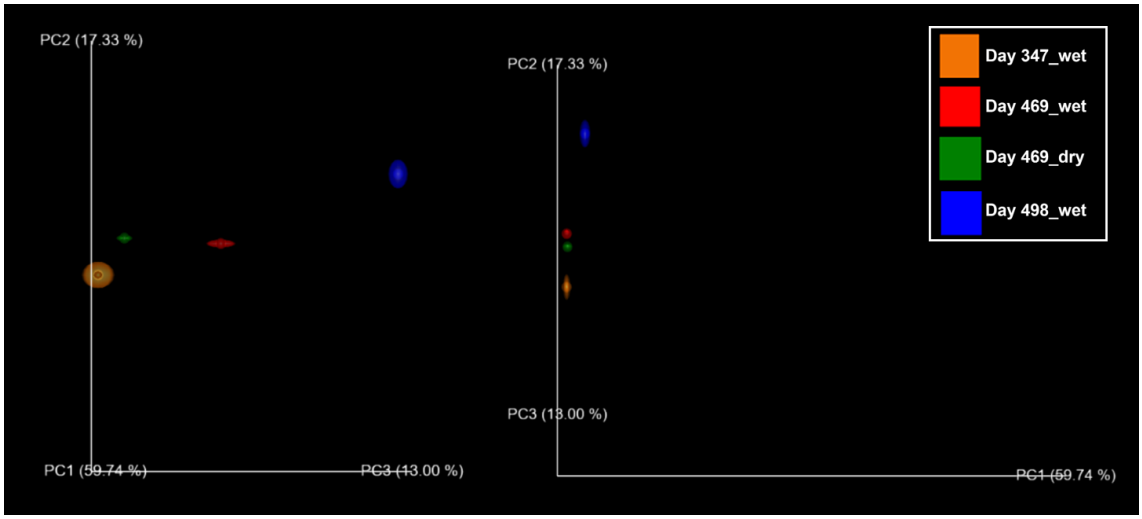

Figure 4.10. The differences observed in beta diversity analysis conducted at the genus level in granule samples. Orange, red, and blue: Wet granule samples were taken in January (347th day), May (469th day), and June 2022 (498th day) respectively; Green: Granule sample was taken on the 498th day and desiccated

The taxonomic analysis achieved a high level of sensitivity up to the genus level; however, the sensitivity significantly decreased at the species level. Therefore, the presence of ureolytic and nitrate-reducing bacteria in granules produced in the bioreactor was evaluated at the genus level. The top 10 dominant genera in each analyzed sample are presented in Table 4.2. It was determined that the dominance of the community capable of denitrification in granule samples taken during periods of stable operation of the bioreactor exceeded 84% in all samples (Table 4.2). In the sample taken on the 347th day when granulation continued in the bioreactor, the dominance of the community capable of urea hydrolysis was 72.3%, while in mature granules taken on the 469th and 498th days, it was 78.6% and 63.1%, respectively (Table 4.2). Bacteria that did not fall within the top 10 dominant species in the granules were labeled as "Others," and their proportion was below 16% in all samples (Table 4.2)

Table 4.2. The dominance of urea-hydrolyzing and denitrifying bacteria in samples taken at three different periods from the bioreactor

Bacterial Genus	**Urease**	**Nitrate reductase**	**The existence within the community (%)**			
			Day 347	**Day 469**	**Day 498**	**References for the enzymes**
Hyphomicrobium sp.	+	+	4.5	20.0	24.7	[166–168]
Paenalcaligenes sp.	+	+	15.9	2.7	1.8	[169,170]
Petrimonas sp.	-	+	11.9	9.9	18.3	[171]
Chryseobacterium sp.	+/-	+/-	17.7	16.0	11.2	[172,173]
Aquamicrobium sp.	+/-	+	10.8	7.4	10.2	[174,175]
Pseudoxanthomonas sp.	+/-*	+	2.7	5.8	7.5	[176–180]
Bosea sp.	+	+/-	14.9	6.8	2.5	[181,182]
Anoxybacillus sp.	+	+/-	0.01	14.5	0.03	[183,184]
Brevundimonas sp.	+	+	4.7	1.3	1.0	[185]
Propioniciclava sp.	+	+	0.1	4.1	3.2	[186]
Pseudofulvimonas sp.	-	+	1.1	3.4	4.0	[187]
Other			15.7	8.1	15.6	
*+/- It indicates that the activity varies from species to species within the community.						

When evaluating the microbial composition of granules produced in the bioreactor while considering the variability in the data separately, it was determined that the dominance of the denitrifying community ranged from 51.7% to 70.7% at different times (Table 4.2). Similarly, when assessing the dominance of the urea-hydrolyzing community with variable bacteria excluded, it was found to range from 34.2% to 49.4% at different times (Table 4.2). Furthermore, the dominance of the community capable of both denitrification and urea hydrolysis varied from 25% to 33% at different times (Table 4.2). The results of beta diversity analysis, alongside the predominant genus in granules collected at different time intervals from the reactor, indicate a high degree of similarity. This demonstrated that stable granule production of consistent quality can be achieved in the bioreactor with optimized operational parameters.

Furthermore, within the microbial community, the pathogenicity class of most bacterial genera was rated as 1, meaning the microorganism is not associated with any known pathogenic species that affect humans, animals, or plants. Only two genera were found to contain pathogenic species belonging to class 2, comprising 12.2% of the community on sample day 498 [188,189].

4.1.3 Continuous and kinetic evaluation of the activity parameters in biogranule production reactor

Nitrate Reduction

In the denitrification process, nitrate is gradually reduced (Equation 7-11). In some cases, instead of complete nitrate reduction (denitrification), partial nitrate reduction and nitrite accumulation occur. Particularly in alkaline environments, nitrite accumulation is a more frequently observed phenomenon [190]. Throughout the operation, NO_2-N accumulation neither in the aerobic phase nor in the anoxic phase was observed in any operational stage. Hence, the nitrate reduction efficiencies in the reactor can also be defined as complete nitrate reduction (denitrification) efficiencies. According to the results, anoxic nitrate reduction efficiency was measured as 87±9% between the 160th and 263rd days (Stage IV, V, VI) as shown in Table 4.3. In Stage VII, the NO_3-N loading rate was increased to 0.37 g $N.L^{-1}.day^{-1}$. Following this increase, a decrease in denitrification efficiency was observed during the initial days, due to the adaptation of microorganisms to the new F/M ratio as shown in Figure 4.11. Nonetheless, following the adaptation of the biogranules to the new nutrient levels, complete denitrification of the fed NO_3-N could be achieved until day 362. Subsequently, significant reductions in VSS concentrations were observed following biogranule harvesting on days 362, 402, 417, and 470 (Figure 4.3), resulting in temporary decreases in denitrification activities. Despite regular granule harvesting from the system, the average denitrification efficiency in the anoxic phase of the reactor was measured as 78% during Stage VII (Table 4.3).

Table 4.3. Average denitrification efficiencies obtained at different NO_3-N loading rates in the reactor

Operational Days	NO_3-N Loading Rate (g. L^{-1}. day^{-1})	Denitrification Efficiency (%)	
		Anoxic	Total
160-263	0,20	87±10	91±8
264-560	0,37	78±14	81±15

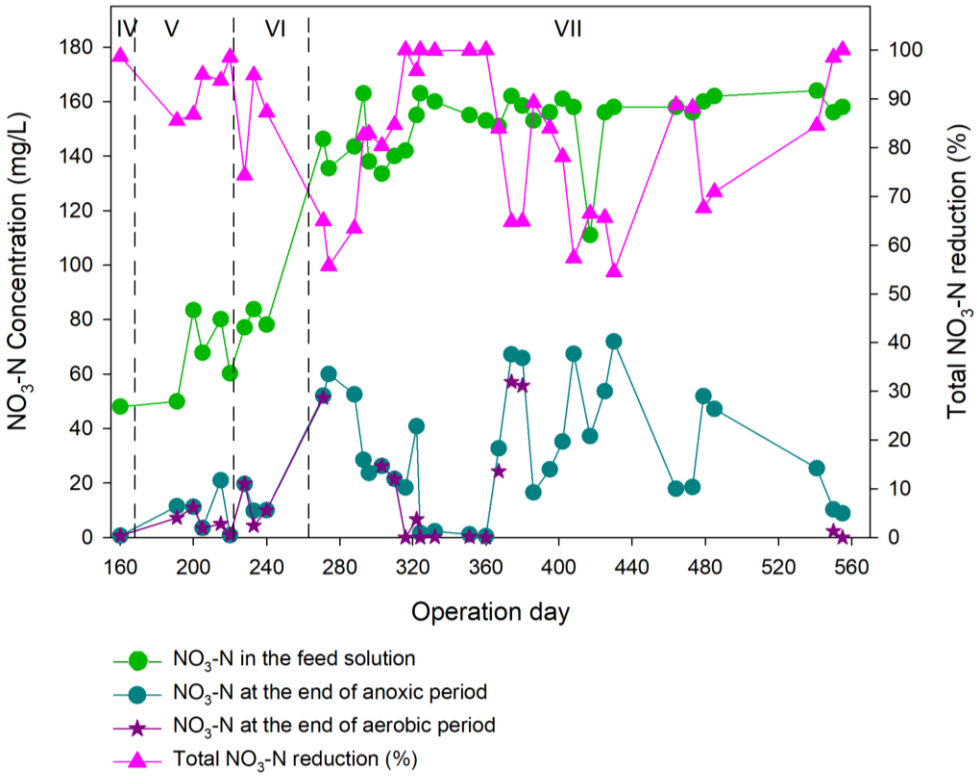

Figure 4.11. NO_3-N concentration and NO_3-N reduction efficiencies monitored in the reactor (100 $mg.L^{-1}$ NO_3-N during Stage IV, V, and VI, 185 $mg.L^{-1}$ NO_3-N during Stage VII).

Typically, no significant difference was observed between of the NO_3-N concentrations measured at the end of the aerobic period and the anoxic period (Figure 4.11). In some days, it was determined that the nitrate remaining in the anoxic phase was slightly further reduced during the aerobic period. Denitrification under aerobic conditions has been observed in many granular sludge studies [191,192]. This is because even under aerobic conditions, the concentration of dissolved oxygen in the environment may not be sufficient for oxygen transfer to bacteria at the center of the granules, and with the transport of nitrate to the center of the granules, anaerobic conditions are established and allowing denitrification to occur [69,143,191]. In addition, some species capable of aerobic denitrification could be present among the dominant bacterial genera such as *Hyphomicrobium* sp, *Chryseobacterium* sp, *Aquamicrobium* sp, *Anoxybacillus* sp, *Brevundimonas* sp and *Pseudofulvimonas* sp [193–197]. This also made the reduction of nitrate under aerobic conditions meaningful.

Urea Hydrolysis

In order to determine urea hydrolysis efficiencies, total ammonium nitrogen was measured at regular intervals and corresponding urea hydrolysis efficiencies were presented in Table 4.4 and Figure 4.12.

In the bioreactor operation, the cross-inoculation process was conducted primarily to enhance the enrichment of heat- and alkali-resilient bacteria as well as to increase urea hydrolysis. The cross-inoculation increased urea hydrolysis performance to levels around 30% at the end of the second stage (6 $g.L^{-1}$ urea in the feed solution) and 70% at the end of the third stage (1 $g.L^{-1}$ urea in the feed solution). However, urea hydrolysis performance decreased to around 40% at the fourth stage (1 $g.L^{-1}$ urea in the feed solution). Two main reasons led to this situation: (i) Cross-inoculation disrupted the biomass's settling characteristics in the reactor, resulting in VSS values dropping below 2000 $mg.L^{-1}$, and (ii) increased urea hydrolysis in the third stage led to microbial-induced $CaCO_3$ precipitation in the reactor and thus a severe increase in TSS levels resulting in the decrease of VSS:TSS ratio below 25%.

Following the termination of cross-inoculation at the beginning of Stage V, a noticeable recovery in anoxic urea hydrolysis efficiency was observed until the end of Stage VI (Figure 4.12). In this stage, the average anoxic urea hydrolysis efficiency increased from 19±7% to 27±7% (Table 4.4). Interestingly, there was no significant change in the average aerobic urea hydrolysis efficiency during this recovery period. Therefore, the observed recovery in urea hydrolysis efficiency could be attributed to two main reasons: (i) stopping the loss of biomass in the system, resulting in VSS levels rising above 2000 $mg.L^{-1}$, and (ii) discontinuing Ca^{2+} supplementation, leading to the VSS:TSS ratio reaching levels around 40%. At the beginning of stage V, 6 grams of powder containing denitrifying spores were added to the system. However, as no evidence existed that denitrifying spores performed urea hydrolysis, it was believed that the recovery was not attributable to their presence.

Table 4.4. Urea hydrolysis performances in different operational stages

Stages	Days	TAN Concentration (mg.L^{-1})		Urea Hydrolysis Efficiency (%)		
		At the end of the anoxic period	At the end of the aerobic period	Anoxic	Aerobic	Total
I	0-31	183±90	256±120	4±2	6±2	9±4
II	32-40	469±52	775±64	5±2	23±2	27±3
III	41-106	184±88	242±107	25±21	35±22	49±28
IV	107-168	181±25	259±41	20±3	44±10	55±9
V	169-222	158±35	243±47	19±7	46±12	56±10
VI	223-263	195±24	274±30	27±7	48±11	63±6
VII	264-560	215±33	300±44	34±8	56±15	71±12

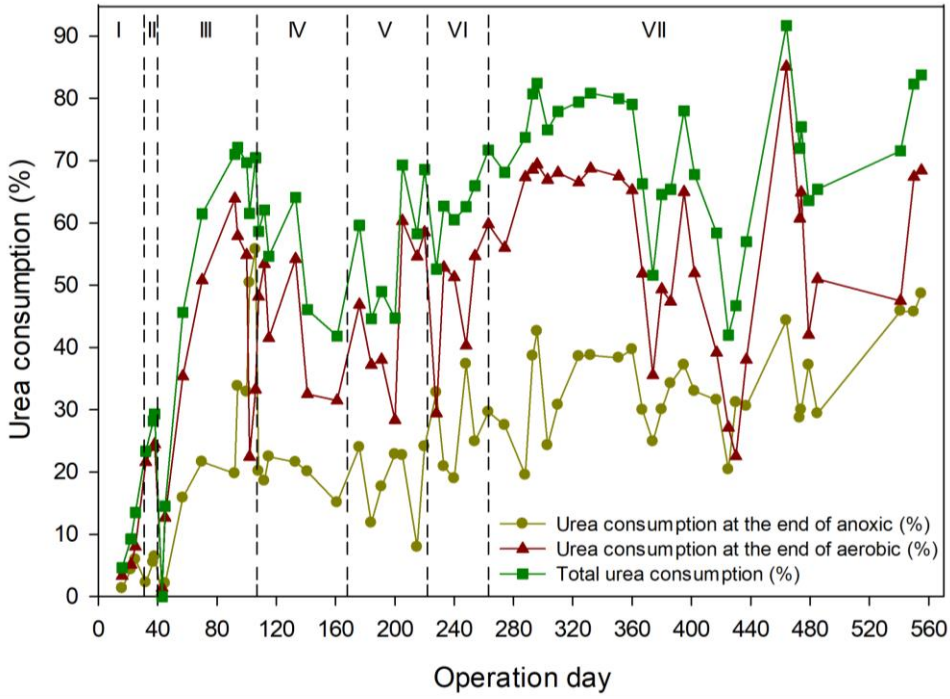

Figure 4.12. Urea hydrolysis efficiencies monitored in the reactor

At the beginning of Stage VII, on the 263rd day, the COD and NO_3-N concentrations in the nutrient solution were increased while maintaining the COD:NO_3-N ratio at ~7.5. This adjustment was made to promote the growth of the microbial community which can simultaneously conduct denitrification and urea hydrolysis. Following this modification, the VSS amount was raised, and the average urea hydrolysis efficiency of the reactor increased from 63±6% to 71±12% until the 362nd day when granule harvesting began. Additionally, the average cycle efficiency increased from 63±6% to 78±3%. A decrease in standard deviations was observed compared to previous operational stages. Because of

the significant granule harvesting from the system on the 362nd, 402nd, 417th, and 470th day, there was a decrease in VSS in the system (Figure 4.3), resulting in temporary declines in urea hydrolysis activities. Despite regular granule harvesting from the system, the urea hydrolysis efficiency in the reactor was calculated to be an average of 71% during Stage VII (Table 4.4).

The ability to achieve urea hydrolysis in both anoxic and aerobic periods with the produced granules indicated the presence of a community capable of performing denitrification and urea hydrolysis within the granules. After the bioreactor was operated steadily for a period, metagenomic analyses were conducted on biogranule samples to confirm the presence of urea hydrolyzing nitrate-reducing microbial community.

Another notable result extracted from the urea hydrolysis performances achieved in the reactor was the influence of yeast extract on urea hydrolysis performance. An increase in urea hydrolysis performance was observed during Stage III when the concentration of yeast extract in the feed was increased from 4 mg.L^{-1} to 100 mg.L^{-1}. However, during Stage VI, reducing the concentration of yeast extract in the feed from 100 mg.L^{-1} to 50 mg.L^{-1} did not have a detrimental effect on urea hydrolysis performance. It has been reported that the use of yeast extract is not desired in biomineralization applications as it causes some compatibility issues with base materials such as concrete, limestone, and soil [198–200]. For instance, it has been reported that yeast extract has a detrimental effect on fresh concrete properties in self-healing concrete produced using 5 g.L^{-1} yeast extract and 20 g.L^{-1} urea [199]. Therefore, in biomineralization applications, reliance on the performance of the microbial community on the presence of yeast extract is not a desired trait. The biogranules produced in this thesis study could perform urea hydrolysis at yeast extract concentrations as low as 50 mg.L^{-1} which was 100 times lower than those reported in the literature [201]. Therefore, the use of these biogranules can provide advantages in terms of both cost and compatibility in some biomineralization applications such as the development of microbial self-healing concrete. Further analysis on the reliance of urea hydrolysis performance of biogranules on the presence of yeast extract was conducted at higher urea concentrations. Those results revealed that at high VSS levels, yeast extract had no significant effect on the urea hydrolysis. Further details were presented in Section 4.2.1.

Investigation of the Existence of Dissimilatory Nitrate Reduction to Ammonia

In Stage VII, the produced amount of Total Ammoniacal Nitrogen (TAN) and the reduced amount of NO_3-N during the anoxic period were examined. It was observed that on certain days (288, 303, and 310), the amount of reduced nitrate nitrogen was very close to the amount of TAN produced (Table 4.5). This situation raised suspicions about whether the Dissimilatory Nitrate Reduction to Ammonium (DNRA) was occurring during the anoxic period. Additionally, Özbay [39] reported that *Petrimonas* sp., which is known to be capable of DNRA, was abundant in the microbial community of biogranules produced by Sekercioglu [147]. As those granules were also used as inoculum in this thesis study, it became crucial to check potential DNRA occurrence in the anoxic period. Therefore, a separate batch reactor was prepared to test the presence of DNRA in the reactor. This reactor was fed with a urea-free nutrient solution containing 90 $mg.L^{-1}$ NO_3-N and 730 $mg.L^{-1}$ COD and operated under anoxic conditions. The concentrations of TAN and NO_3-N during this process were presented in Table 4.5.

Table 4.5. The amount of reduced NO_3-N and produced TAN in Stage VII

Operational Days	Reduced NO_3-N in the anoxic period (mg)	Produced TAN in the anoxic period (mg)
288	51	52
293	84	105
296	76	117
303	66	66
310	73	83

According to the results of the TAN and NO_3-N analyses conducted on samples taken from the batch reactor, it was observed that in the absence of urea, TAN production did not occur during the anoxic period, while nitrate reduction did occur (Figure 4.3). Therefore, it was confirmed that the observed TAN production during the anoxic period was due to urea hydrolysis. The latter validated that the produced granules were composed of a microbial community that could reduce nitrate and hydrolyze urea.

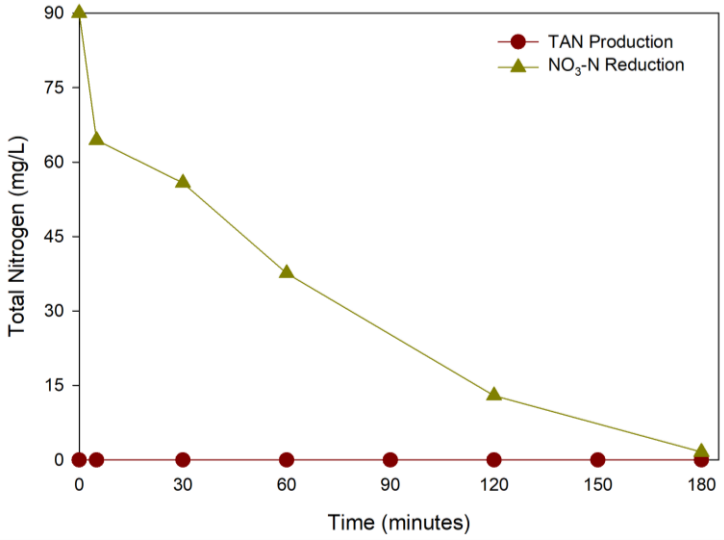

Figure 4.13. Analysis results in the DNRA test reactor

Carbon Consumption

Soluble COD concentration in the reactor was monitored to confirm heterotrophic denitrification activity and the occurrence of feast/famine conditions. The measured sCOD values were presented in Figure 4.14. The COD consumption in the reactor was always over 75% following the recovery period in operational Stage V. After doubling the COD concentration in Stage VII, the consumption efficiency gradually increased to 94% (Figure 4.12). (Figure 4.14). The average organic carbon consumption efficiency was measured as 92±4% in Stage VII.

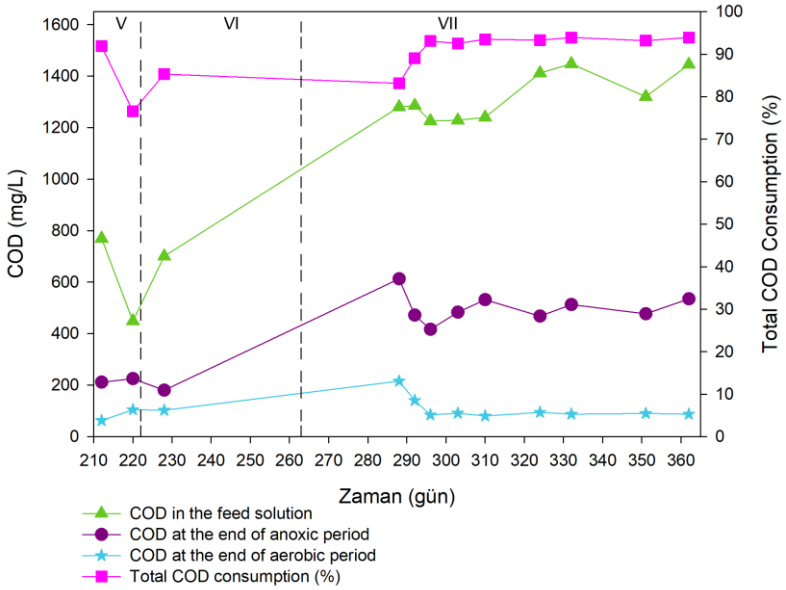

Figure 4.14. COD concentrations and consumption efficiencies monitored in the reactor (740 mg.L^{-1} COD during Stage V and VI; 1460 mg.L^{-1} COD during Stage VII)

During the stable stage of the reactor (324-362 days), the ratio of COD consumed during the anoxic period to the consumed NO_3-N was determined to be 5.76. This confirmed that the conditions were favorable for the growth and multiplication of denitrifying bacteria, rather than bacteria involved in nitrate ammonification during operation [148,156].

Furthermore, in Stage VII, the average dissolved oxygen (DO) value was below 5 $mg.L^{-1}$. This low DO level indirectly confirmed the presence of organic carbon in the system during the aerobic period.

Monitoring of Nutrient Consumption of a single SBR cycle

After achieving stable urea hydrolysis and denitrification efficiency with biogranules produced in the reactor, a single SBR cycle was monitored in shorter intervals to assess the nutrient consumption and determine the specific NO_3-N reduction and urea hydrolysis activities. The single cycle was monitored at 15-minute intervals with samples collected from the reactor. The change in NO_3-N concentration during the monitored single cycle was presented in Figure 4.15. According to the analysis results, 80% of the NO_3-N was reduced within the first 120 minutes of the anoxic period (Figure 4.15). It was observed that the NO_3-N consumption mostly followed zero-order reaction kinetics and the specific nitrate reduction activity was calculated as 7.26 mg NO_3-N. $h^{-1}.g^{-1}$ VSS (Figure Annex 2). By the end of the anoxic period, all NO_3-N in the reactor was reduced by microbial biomass. Throughout denitrification, NO_2-N accumulation in the system did not exceed 15 $mg.L^{-1}$ of NO_2-N, and it was determined that there was no NO_2-N remaining in the system at the end of the anoxic period.

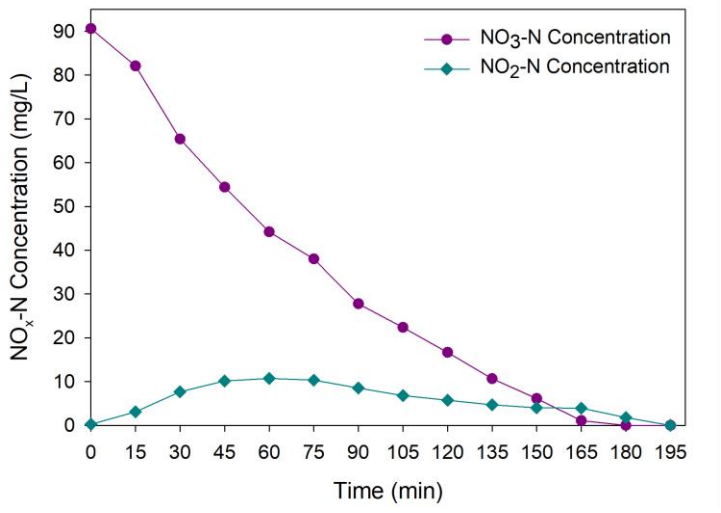

Figure 4. 15. The monitoring of denitrification activity in the produced biogranules within a single cycle

As shown in Figure 4.16, the NH_4-N concentration rapidly increased during the initial anoxic period of the cycle (first 180 min). As observed in Figure 4.16, while 80% of urea was hydrolyzed during the anoxic period, 94% of urea was hydrolyzed by the end of the cycle. It was observed that urea hydrolysis mostly followed zero-order reaction kinetics and the specific urea hydrolysis activity in the anoxic period was calculated as 32.1 mg urea. $h^{-1}g^{-1}$ VSS (Figure Annex 3).

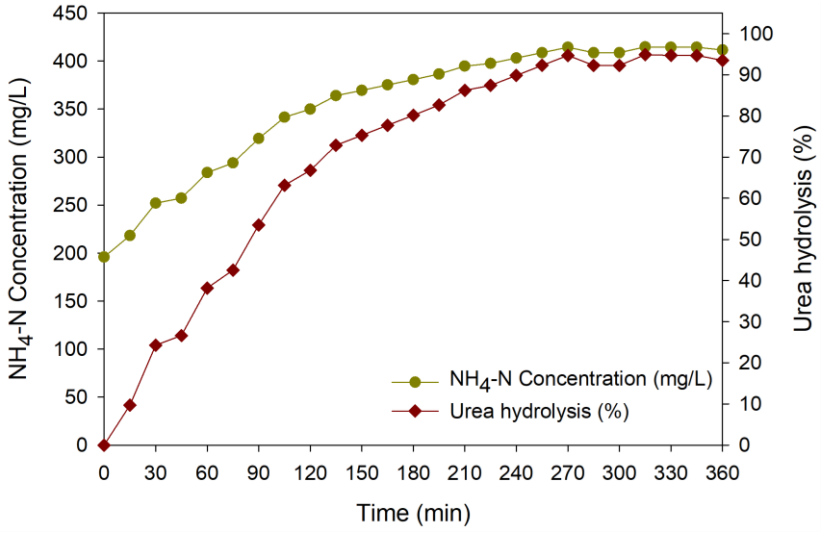

Figure 4.16. The monitoring of urea hydrolysis activity in the produced biogranules within a single cycle

As shown in Figure 4.17, 50% of the organic carbon (576 mg COD) was consumed within the first 180 minutes of the cycle. By the end of the cycle, 95% of the total COD was consumed, leaving only ~35 mg/L COD in the reactor. Based on this carbon consumption, the COD:N consumption ratio during the anoxic period was determined to be 5.64. It can be inferred that the majority of the supplied carbon was consumed within 285 minutes, resulting in a 75-minute period of nutrient limitation. The achievement of compact and stable granules indicated that the duration of the famine period was sufficient. It has also been noted in the literature that long famine periods are not required for granulation [114,202]. It was observed that organic carbon consumption followed zero-order reaction kinetics and the specific carbon consumption activities in anoxic and aerobic periods were calculated as 40.67 and 41.66 mg COD. h^{-1} g^{-1} VSS. (Figure Annex 4).

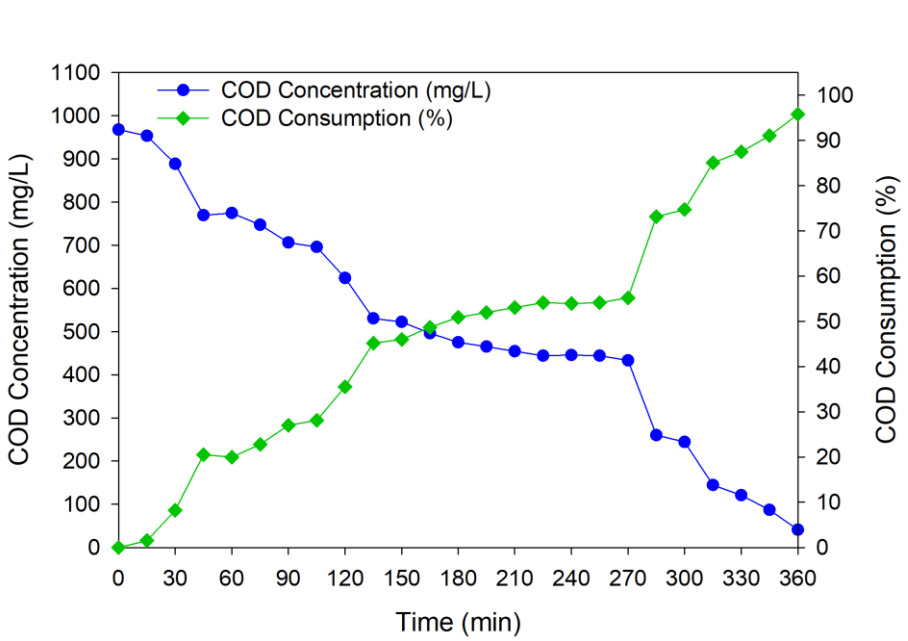

Figure 4.17. The monitoring of carbon consumption activity in the produced biogranules within a single cycle

4.2 Evaluation of microbial activity and biomineralization performance of biogranules via batch tests

4.2.1 Detecting Whether the Urease Enzyme in Biogranules Is Suppressive or Non-Suppressive

There are suppressive and non-suppressive types of the urease enzyme and urea values such as 10 $g.L^{-1}$ and 20 $g.L^{-1}$ are commonly used in biomineralization applications. Since granule production utilized 1 $g.L^{-1}$ of urea in this study, it was critical to ascertain the type of urease in the granules. Moreover, high nitrate concentrations, particularly under alkaline conditions have the potential to adversely affect denitrification activity through nitrite accumulation. Therefore, it was essential to test biogranules under high urea and nitrate conditions. In order to determine any inhibition of urease enzymes by the accumulated ammonium and whether the denitrification activity might be affected at high nitrate concentrations, the biogranules were tested in batch reactors at a urea concentration of 10 $g.L^{-1}$ and a nitrate concentration of 0.5 $g.L^{-1}$. In order to observe the effect of the VSS amount on the same nutrient input, high (6.5 $g.L^{-1}$ VSS) and low (2.0 $g.L^{-1}$ VSS) VSS values were used in the tests considering the reactor operation process. Additionally, to elucidate the effect of yeast extract on activity, two different yeast extract concentrations were used in the nutrient solution (0.05 $g.L^{-1}$ and 5.0 $g.L^{-1}$). A total of 30

hours of operation were conducted for the batch reactors, with access to air restricted for the first 12 hours to achieve anoxic conditions, while air access was not restricted for the remaining 18 hours.

Considering the TAN results from samples taken from the batch reactors in the first 12 hours, it was observed that there was no difference between Group A (6.5 $g.L^{-1}$ VSS, 5.0 $g.L^{-1}$ yeast extract) and B (6.5 $g.L^{-1}$ VSS, 0.05 $g.L^{-1}$ yeast extract). These results revealed that at high VSS levels, yeast extract had no significant effect on the urea hydrolysis activity of the wet biogranules. On the other hand, when comparing Group A (6.5 $g.L^{-1}$ VSS, 5.0 $g.L^{-1}$ yeast extract) and Group C (2.0 $g.L^{-1}$ VSS, 5.0 $g.L^{-1}$ yeast extract), it was determined that at different VSS values with the same yeast extract concentration, urea hydrolysis achieved over 85% in both groups (Figure 4.16). Obtaining similar urea hydrolysis under both VSS conditions indicated that 10 $g.L^{-1}$ urea could be hydrolyzed at a maximum rate with 2 $g.L^{-1}$ VSS, and the presence of additional granules in the environment did not have any impact on the activity. Therefore, the maximum specific urea hydrolysis activity of the granules was determined to be 90 mg $Urea.h^{-1}.g^{-1}$ VSS under anoxic conditions and 233 mg $urea.h^{-1}.g^{-1}$ VSS under air-contact conditions (Table 4.6).

Table 4.6. The observed specific urea consumption activities of biogranules under high nutrient input

	Specific Activities (mg urea. $h^{-1}.g^{-1}$ VSS)		
Batch groups	**A***	**B***	**C***
Anoxic condition (0-12 hours)	51.1	50.9	90.3
Air-contact condition (12-30 hours)	58.6	57.4	232.8

* A: 6.5 $g.L^{-1}$ VSS, 5.0 $g.L^{-1}$ yeast extract; B: 6.5 $g.L^{-1}$ VSS, 0.05 $g.L^{-1}$ yeast extract; C: 2.0 $g.L^{-1}$ VSS, 5.0 $g.L^{-1}$ yeast extract

The obtained results initially demonstrated that the presence of high ammonium nitrogen did not exert an adverse effect on urea hydrolysis. Thus, it was determined that the urease enzyme in the produced biogranules belonged to the non-suppressive type, remaining unaffected under high TAN conditions. Moreover, when examining the urea hydrolysis efficiencies under anoxic and air-contact conditions, an increase in urea hydrolysis activity was observed in all groups when air contact was not restricted (Table 4.6). Considering the majority of reported ureolytic bacteria are aerobic [15,58], contact with

air likely facilitated the urease enzyme produced by bacteria. The DO values measured at the end of the anoxic and air-contact conditions were 0.00 and 0.23±0.05 mg.L^{-1}, respectively, for all groups. At this point, it was observed that air-contact conditions had a positive effect on urea hydrolysis (Figure 4.18b). Furthermore, when comparing the data from the 30th hour with those from the 27th hour, no statistical difference was found between the datasets (p=0.05).

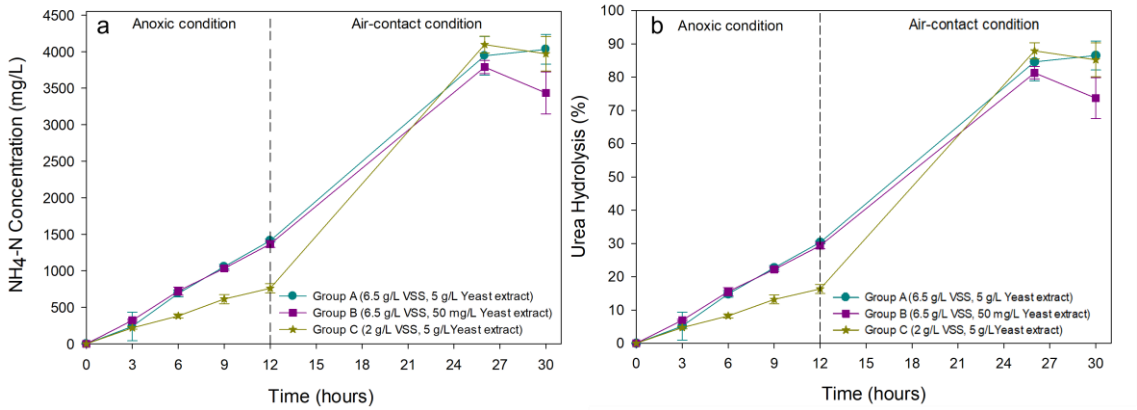

Figure 4.18. The time-dependent variations of a) TAN concentrations and b) urea hydrolysis of biogranules under high nutrient input

Comparison of groups with different yeast extract content under the same VSS value (Groups A and B) based on nitrate analyses revealed that higher specific activity was achieved under conditions of high yeast extract content (6.5 g.L^{-1} VSS, 5.0 g.L^{-1} yeast extract). Similarly, achieving nitrate reduction at the same rate in the batch reactor with low VSS and low yeast extract content (Group C) indicated that 2 g.L^{-1} VSS could achieve a maximum reduction of 0.5 g.L^{-1} nitrate, and the presence of additional granules in the environment did not contribute to the activity. Consequently, the maximum specific nitrate reduction activity of the granules was determined to be 9.25 mg NO_3-N.h^{-1}.g^{-1} VSS under anoxic conditions and 3.06 mg NO_3-N.h^{-1}.g^{-1} VSS under air-contact conditions (Table 4.7). In a study conducted at high nitrate concentration, employing an inoculum adapted to elevated nitrate levels achieved complete denitrification in 6 hours, with a denitrification rate of 22.8 mg NO_3-N.h^{-1}.g^{-1} VSS. In this study, methanol was used as the carbon source at a COD/N ratio of 4, and the wastewater had a nitrate nitrogen content of 700 mg.L^{-1} and calcium content of 150 mg.L^{-1} [203]. This result was approximately 2.5 times higher compared to the maximum activity of the biogranules. In our test, the

COD/N ratio was 4.63 and no calcium was present in the nutrient solution. Also, biogranules were not acclimated to high nitrate concentrations.

Table 4.7. The observed specific nitrate reduction activities of biogranules under high nutrient input

	Specific Activities (mg NO_3-N. $h^{-1}.g^{-1}$ VSS)		
Batch groups	**A***	**B***	**C***
Anoxic condition (0-12 hours)	3.70	3.41	9.25
Air-contact condition (12-30 hours)	1.42	0.85	3.06

* A: 6.5 $g.L^{-1}$ VSS, 5.0 $g.L^{-1}$ yeast extract; B: 6.5 $g.L^{-1}$ VSS, 0.05 $g.L^{-1}$ yeast extract; C: 2.0 $g.L^{-1}$ VSS, 5.0 $g.L^{-1}$ yeast extract

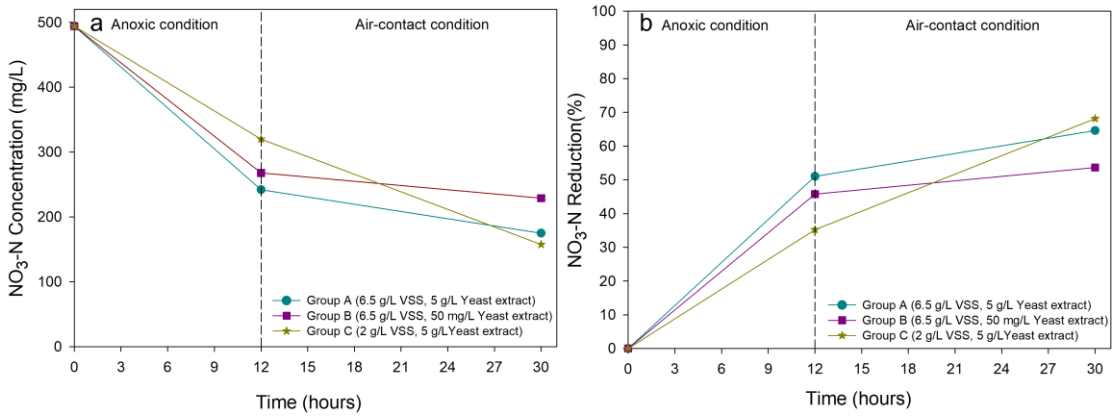

Figure 4.19. The time-dependent variations of a) NO_3-N concentrations and b) nitrate reduction of biogranules under high nutrient input

In all groups, at 0.5 $g.L^{-1}$ NO_3-N concentration, nitrate reduction efficiencies exceeded 50% by the 30th hour (Figure 4.19b). In this test, biogranules extracted from the currently operational reactor were subjected to approximately five and a half times higher initial NO_3-N concentration (500 $mg.L^{-1}$) compared to the initial NO_3-N concentration (90 $mg.L^{-1}$) in the reactor operation. When comparing specific nitrate reduction activities under anoxic conditions, there was a reduction of 49% and 53% in Groups A (3.70 mg NO_3-N. $h^{-1}.g^{-1}$ VSS) and B (3.40 mg NO_3-N. $h^{-1}.g^{-1}$ VSS), respectively, relative to the activity in the bioreactor (7.26 mg NO_3-N. $h^{-1}.g^{-1}$ VSS). Conversely, in Group C, which had low VSS and high yeast content, specific activity under anoxic conditions increased by 27% compared to the bioreactor.

4.2.2 Comparison of Microbial Activity of Produced Biogranules and Reference Granular Culture for MICP

In order to compare microbial activities, produced biogranules and the reference nitrate-reducing granular culture (ACDC) were tested in batch reactors containing 10 $g.L^{-1}$ urea and 0.11 $g.L^{-1}$ NO_3-N.

The produced biogranules were tested in both wet and desiccated forms, while ACDC was tested only in desiccated form. Considering biomineralization applications the yeast extract concentration in all tests was adjusted to 0.05 $g.L^{-1}$. The use of yeast extract in MICP applications is not desirable due to its high cost and its potentially negative effects on material properties in some applications. Moreover, it is unnecessary in soil applications due to the existing organic matter in the environment. In concrete applications, yeast extract is undesirable because it is not compatible with mortar and prolongs the setting time, making it unsuitable for microbial self-healing concrete [153,199]. Therefore, the yeast extract concentration in the microbial activity test was deliberately kept low (0.05 $g.L^{-1}$).

In the microbial activity test, batch reactors were operated for 24 hours under anoxic conditions, followed by an additional 24 hours under air-contact conditions. The initial bacterial concentration in the tests was set to 0.5 $g.L^{-1}$ VSS.

The initial pH value of the nutrient solution was measured to be 7.5. The pH values measured at the 48th hour of the test are presented in Table 4.8. Due to the production of alkalinity by both urea hydrolysis and denitrification metabolic pathways, the pH increased in all batch reactors compared to the initial measurement.

Table 4.8. The pH values of the batch reactors at the end of 48 hours in microbial activity test

Batch Groups*	pH at the end of 48 hour
A	9,3
B	9,3
C	8,7

*A: Produced biogranules in wet form, B: Produced biogranules in desiccated form, C: ACDC in desiccated form

Urea Hydrolysis Activities of The Produced Biogranules and Reference Granular Culture

The changes in TAN concentrations over time obtained from the tests with biogranules were presented in Figure 4.20. The urea hydrolysis efficiencies of the biogranules at the end of the 48th hour were recorded as 41%, 80%, and 1% for groups A (Wet biogranules), B (Desiccated biogranules), and C (Desiccated ACDC), respectively (Figure 4.20). In batch reactors testing the wet form of the produced biogranules (Group A), the specific urea consumption activity was determined to be 125.1 mg urea.h^{-1}.g^{-1} VSS and 120.6 mg urea.h^{-1}.g^{-1} VSS under anoxic and aerobic conditions, respectively. No significant difference in urea hydrolysis activity was observed between anoxic and aerobic conditions. However, in the group testing the desiccated form of the produced biogranules (Group B), the specific urea consumption activity under anoxic conditions was recorded as 97.1 mg urea.h^{-1}.g^{-1} VSS, slightly lower than that of the wet form. This difference was thought to be influenced by the resuscitation time of the dry biogranules. When passing through to aerobic conditions, the activity reached 410 mg urea.h^{-1}.g^{-1} VSS, showing the highest activity (Table 4.9). The reference nitrate-reducing granular culture (ACDC) did not exhibit urea hydrolysis activity as they were produced solely for denitrification purposes. Considering that the resuscitation times of the ACDC might be longer, the TAN value was also measured on the seventh day in group C. However, upon determining the urea hydrolysis amount as 2%, it was confirmed that ACDC did not exhibit urea hydrolysis activity.

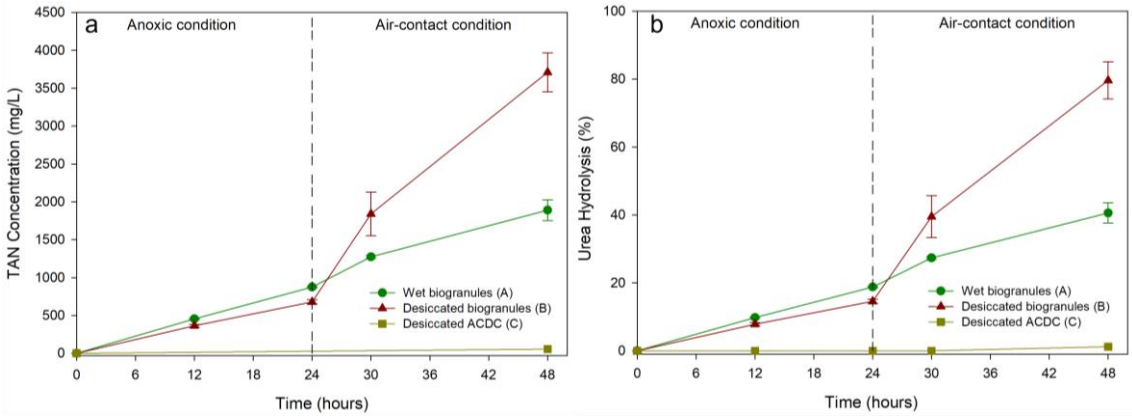

Figure 4.20. The time-dependent TAN concentrations (a) and urea hydrolysis efficiencies (b) of the biogranules throughout the microbial activity test

Table 4.9. The specific urea consumption activities of the granular cultures in microbial activity test

Conditions	Specific urea consumption activity (mg urea.day^{-1}.g^{-1} VSS)		
	A*	B*	C*
Anoxic	125,1	97,1	0,0
Aerobic	120,6	410,0	3,3

*A: Produced biogranules in wet form, B: Produced biogranules in desiccated form, C: ACDC in desiccated form

After oxygen access was provided, the urea hydrolysis activity of the desiccated biogranules (Group B) increased significantly. This increase was not observed in the biogranules tested in wet form (Group A). The primary reason for this difference was cell debris during desiccation. In the desiccation process, some bacteria form spores while others die. The cellular contents of these dead bacteria create an activity-enhancing effect similar to yeast extract for those capable of forming spores and resuscitation. In tests conducted with low yeast extract concentrations, it can be said that the revived bacteria achieved higher activity by also utilizing the cellular contents from the dead bacteria after access to oxygen. In the granules tested in wet form, there was no temporal change in activity because there was no dead cell debris present in the medium.

Nitrate Reduction Activities of The Produced Biogranules and Reference Granular Culture

The changes in nitrate concentrations over time obtained from the tests with biogranules were presented in Figure 4.21. The nitrate reduction efficiencies of the biogranules at the end of 24 hours were recorded as 71%, 8%, and 13% for groups A (Wet biogranules), B (Desiccated biogranules), and C (Desiccated ACDC), respectively, while at the 48th hour, these efficiencies were recorded as 78%, 9%, and 17%, respectively (Figure 4.21). Considering that the activity of the desiccated biogranules and ACDC continued despite being low at the end of the second day of testing and recognizing that the duration of the experiment might be insufficient for resuscitation from the desiccated form, the test duration was extended up to 7 days. According to measurements taken on the seventh day, the nitrate reduction efficiency reached 92% in group B (Desiccated biogranules) and 98% in group C (Desiccated ACDC). Thus, it can be said that biogranules and ACDC

could resuscitate in one week. This result was consistent with the reported ones for ACDC [14].

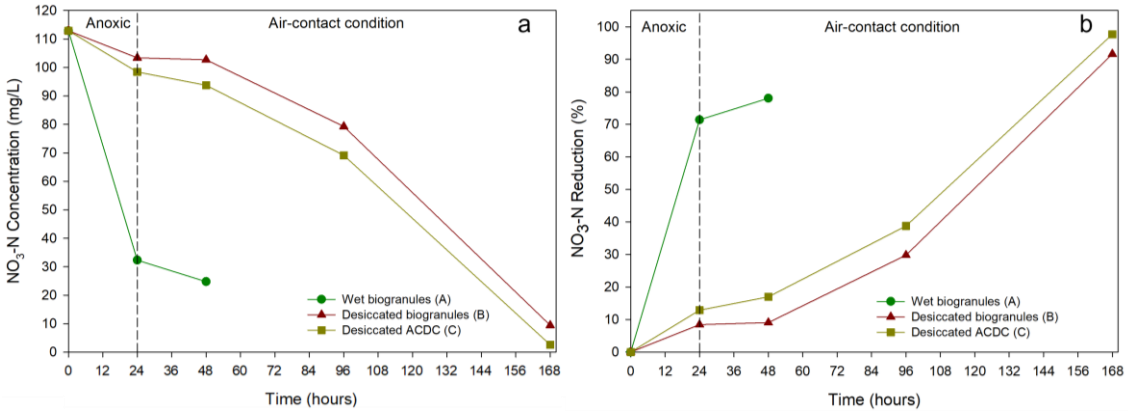

Figure 4.21. The time-dependent nitrate concentrations (a) and nitrate reduction efficiencies (b) of the granular cultures throughout the microbial activity test

In the anoxic period (first 24 hours), the specific nitrate reduction activities for groups A (Wet biogranules), B (Desiccated biogranules), and C (Desiccated ACDC), respectively were calculated as 161 mg NO_3-N $day^{-1}.g^{-1}$ VSS, 19 mg NO_3-N $day^{-1}.g^{-1}$ VSS, and 29 mg NO_3-N $day^{-1}.g^{-1}$ VSS, respectively (Table 4.11). Under air-contact conditions, the specific nitrate reduction activities for groups A (Wet biogranules), B (Desiccated biogranules), and C (Desiccated ACDC), respectively were determined as 17 mg NO_3-N $day^{-1}.g^{-1}$ VSS, 40 mg NO_3-N $day^{-1}.g^{-1}$ VSS, and 41 mg NO_3-N $day^{-1}.g^{-1}$ VSS, respectively (Table 4.11). Upon examining the NO_3-N and NO_2-N values at the 48^{th} hour, it can be observed that the reduced nitrate was not accumulated as nitrite at high concentrations, indicating that denitrification occurred through the reduction of nitrite as well (Table 4.10).

Table 4.10. The NO_x concentrations in batch reactors at the end of 48 hours in microbial activity test

Batch Groups*	Feed NO_x-N ($mg.L^{-1}$)	NO_3-N ($mg.L^{-1}$)	NO_2-N Accumulation ($mg.L^{-1}$)	Total NO_x-N ($mg.L^{-1}$)
A	113	24.8	2.5	27.3
B		102.7	0.0	102.7
C		93.8	4.9	98.6
*A: Produced biogranules in wet form, B: Produced biogranules in desiccated form, C: ACDC in desiccated form				

Specific denitrification activities were calculated as 87 mg NO_x-N $day^{-1}.g^{-1}$ VSS S, 29 mg NO_x-N $day^{-1}.g^{-1}$ VSS, and 31 mg NO_x-N $day^{-1}.g^{-1}$ VSS for groups A (Wet biogranules), B (Desiccated biogranules), and C (Desiccated ACDC), respectively, in batch reactors (Table 4.11).

Table 4.11. The specific nitrate reduction, nitrite accumulation, and denitrification activities recorded during the microbial activity test

Conditions	**A***	**B***	**C***
	Specific nitrate reduction activity (mg NO_3-N.$day^{-1}.g^{-1}$ VSS)		
Anoxic	161	19	29
Air-contact	17	40	41
Throughout the experiment	**Specific nitrite accumulation activity (mg NO_3-N.$day^{-1}.g^{-1}$ VSS)**		
	2	0	5
	Specific denitrification activity (mg NOx-N.$day^{-1}.g^{-1}$ VSS)		
	87	29	31
*A: Produced biogranules in wet form, B: Produced biogranules in desiccated form, C: ACDC in desiccated form			

Among the tested granular cultures, produced biogranules in the wet form exhibited the highest denitrification activity under both anoxic conditions and throughout the entire test duration. This outcome can be attributed to the utilization of biogranules already exhibiting activity and not necessitate an activation period. Conversely, the resuscitation periods of the produced biogranules and ACDC in desiccated form led to delays in nitrate reduction. Nonetheless, both granular culture types demonstrated comparable activity levels following the resuscitation period (Figure 4.21, Table 4.11).

4.2.3 Comparison of Biomineralization Capacity of Produced Biogranules and Reference Granular Culture

Batch reactors were set up to determine and compare the biomineralization activities of the produced biogranules and nitrate-reducing reference granular culture (ACDC). Considering the resuscitation period of the desiccated cultures, the tests were conducted over a total of nine days, with an anoxic period of six days followed by an air-contact period of three days. In the biomineralization test, a nutrient solution containing 6 $g.L^{-1}$

Ca^{2+}, 10 $g.L^{-1}$ urea, 0.25 $g.L^{-1}$ NO_3-N, and 1.9 $g.L^{-1}$ COD was used. The granular cultures were tested both with and without 0.05 $g.L^{-1}$ yeast extract. The tests were conducted using 0.5 $g.L^{-1}$ VSS.

One of the important factors in the microbial precipitation of calcium carbonate is the pH value. Under alkaline pH conditions, the bicarbonate-carbonate equilibrium shifts towards carbonate ion formation, resulting in the precipitation of $CaCO_3$ when free calcium ions are present. In this context, pH values were measured at the end of each period in the batch reactors and are presented in Table 4.12.

Table 4.12. End-of-period pH values in batch reactors in biomineralization test

Batch Groups*	Anoxic	Air-contact
A	9.1	9.0
B1	8.8	7.8
B3	8.9	7.9
C1	7.3	7.4
C3	7.9	7.6

A* : Wet biogranules (0.5 $g.L^{-1}$ VSS, 50 $mg.L^{-1}$ Yeast Extract), B1:Desiccated biogranules (0.5 $g.L^{-1}$ VSS, 50 $mg.L^{-1}$ Yeast extract), B3: Desiccated biogranules (0.5 $g.L^{-1}$ VSS, No Yeast Extract), C1: Desiccated ACDC (0.5 $g.L^{-1}$ VSS, 50 $mg.L^{-1}$ Yeast Extract), C3: Desiccated ACDC (0.5 $g.L^{-1}$ VSS, No Yeast Extract)

Urea Hydrolysis Activities in Biomineralization Test

The TAN concentrations and urea hydrolysis efficiencies recorded at the end of the ninth day in the biomineralization test were presented in Table 4.13. The urea hydrolysis efficiencies recorded at the end of the ninth day for groups A (Wet Biogranules, 0.05 $g.L^{-1}$ yeast extract), B1 (Desiccated Biogranules, 0.05 $g.L^{-1}$ yeast extract), B3 (Desiccated Biogranules, no yeast extract), C1 (Desiccated ACDC, 0.05 $g.L^{-1}$ yeast extract), and C3 (Desiccated ACDC, no yeast extract) were 83%, 65%, 69%, 2%, and 3%, respectively (Table 4.13). The highest urea hydrolysis efficiency was observed in group A, which consisted of already active biogranules. As in the microbial activity tests, the reference nitrate-reducing granular culture (ACDC) did not perform urea hydrolysis (Table 4.13).

Table 4.13. The recorded TAN concentrations and urea hydrolysis efficiencies in the biomineralization test

Batch Groups*	TAN ($mg.L^{-1}$)	Urea Hydrolysis (%)
A	3878	83
B1	3038	65
B3	3206	69
C1	91	2
C3	126	3

A* : Wet biogranules (0.5 $g.L^{-1}$ VSS, 50 $mg.L^{-1}$ Yeast Extract), B1:Desiccated biogranules (0.5 $g.L^{-1}$ VSS, 50 $mg.L^{-1}$ Yeast extract), B3: Desiccated biogranules (0.5 $g.L^{-1}$ VSS, No Yeast Extract), C1: Desiccated ACDC (0.5 $g.L^{-1}$ VSS, 50 $mg.L^{-1}$ Yeast Extract), C3: Desiccated ACDC (0.5 $g.L^{-1}$ VSS, No Yeast Extract)

Nitrate Reduction Activities in Biomineralization Test

The NO_3-N concentrations and nitrate reduction efficiencies recorded at the end of the ninth day in the biomineralization test were presented in Table 4.14. The nitrate reduction efficiencies of the biogranules recorded at the end of the ninth day were measured as 98%, 74%, 28%, 71%, and 40% for A (Wet Biogranules, 0.05 $g.L^{-1}$ yeast extract), B1 (Desiccated Biogranules, 0.05 $g.L^{-1}$ yeast extract), B3 (Desiccated Biogranules, no yeast extract), C1 (Desiccated ACDC, 0.05 $g.L^{-1}$ yeast extract), and C3 (Desiccated ACDC, no yeast extract) respectively (Table 4.14). Consistent with the results of the microbial activity tests, the already active biogranules used in wet form (A) demonstrated the highest activity in the biomineralization tests.

On the other hand, when examining the nitrate reduction efficiency of the desiccated biogranules (B) and desiccated ACDC (C), it was observed that the presence of yeast extract positively influenced nitrate reduction in both types of granular cultures. Nitrite accumulation increased in both the B and C groups compared to the microbial activity tests. Nonetheless, it was observed that the B and C granules, which were capable of reducing nitrate to nitrite, were also able to further reduce nitrite, thereby completing the denitrification process comprehensively. The lower denitrification activity compared to the microbial activity test can be explained by the high calcium concentration. Exposure to high calcium levels adversely affects the denitrification rate.

Table 4.14. The recorded NO_x-N concentrations and nitrate reduction efficiencies in the biomineralization test

Batch Groups*	Feed NO_x-N ($mg.L^{-1}$)	NO_3-N ($mg.L^{-1}$)	Nitrate reduction (%)	NO_2-N Accumulation ($mg.L^{-1}$)	Total NO_x-N ($mg.L^{-1}$)
A	250	3.9	98	0.0	3.9
B1		63.8	74	97.0	160.8
B3		181.0	28	28.0	209.0
C1		73.7	71	118.0	191.7
C3		148.8	40	66.3	215.1
A* : Wet biogranules (0.5 $g.L^{-1}$ VSS, 50 $mg.L^{-1}$ Yeast Extract), B1:Desiccated biogranules (0.5 $g.L^{-1}$ VSS, 50 $mg.L^{-1}$ Yeast extract), B3: Desiccated biogranules (0.5 $g.L^{-1}$ VSS, No Yeast Extract), C1: Desiccated ACDC (0.5 $g.L^{-1}$ VSS, 50 $mg.L^{-1}$ Yeast Extract), C3: Desiccated ACDC (0.5 $g.L^{-1}$ VSS, No Yeast Extract)					

In a study [203], it was reported that the optimum calcium concentration for achieving the highest specific denitrification rate was 150 $mg.L^{-1}$, with a rate of 22.8 mg NO_3-N $h^{-1}.g^{-1}$ VSS. However, higher calcium concentrations lead to a significant decline in denitrification efficiency, with specific rates decreasing to 15.5 mg NO_3-N $h^{-1}.g^{-1}$ VSS at 450 $mg.L^{-1}$ Ca^{2+} and 11.0 mg NO_3-N $h^{-1}.g^{-1}$ VSS at 550 $mg.L^{-1}$ Ca^{2+}.

Comparison of precipitated $CaCO_3$ amounts

The precipitated $CaCO_3$ amounts were determined and shown in Figure 4.22. In parallel with the microbial activity results in the biomineralization test, the highest amount of $CaCO_3$ precipitation was observed in Group A which contained biogranules in wet form. According to the results, 642.5±4.4 mg $CaCO_3$ was precipitated in Group A which indicated that all the dissolved calcium was precipitated. In Group B, which contains the produced biogranules in desiccated form, the total amount of precipitated calcium carbonate was 590.3±88.2 mg for B1 (Desiccated biogranules, 50 $mg.L^{-1}$ Yeast extract), and 590.5±20.5 mg for B3 (Desiccated biogranules, No Yeast Extract) (Figure 4.22). Based on these results, it was observed that the presence of yeast extract did not significantly influence biomineralization performance. Furthermore, the desiccating of biogranules resulted in a 5.3% reduction in $CaCO_3$ precipitation performance.

In Group C, which contains the reference nitrate-reducing granular culture (ACDC) in desiccated form total precipitated $CaCO_3$ amounts were measured as 137.1±46 mg and

82.2 mg for C1(Desiccated ACDC, 50 mg.L^{-1} Yeast Extract) and C3 (Desiccated ACDC, No Yeast Extract) respectively (Figure 4.22). Based on the observed nitrate reduction activity in ACDCs, the level of MICP was lower than expected. In this group, where ACDC had been dried and stored for 1.5 years before use, it was observed that the yeast extract positively influenced biomineralization performance.

From these results, it can be inferred that biogranules demonstrated a higher $CaCO_3$ precipitation performance compared to the reference nitrate-reducing granular culture (ACDC). However, it was crucial to note that the ACDC was used after being stored for 1.5 years, whereas the biogranules were utilized immediately after drying. To conclusively establish that biogranules exhibited superior performance compared to ACDC, it was necessary to conduct further testing on the biogranules following a similar storage period.

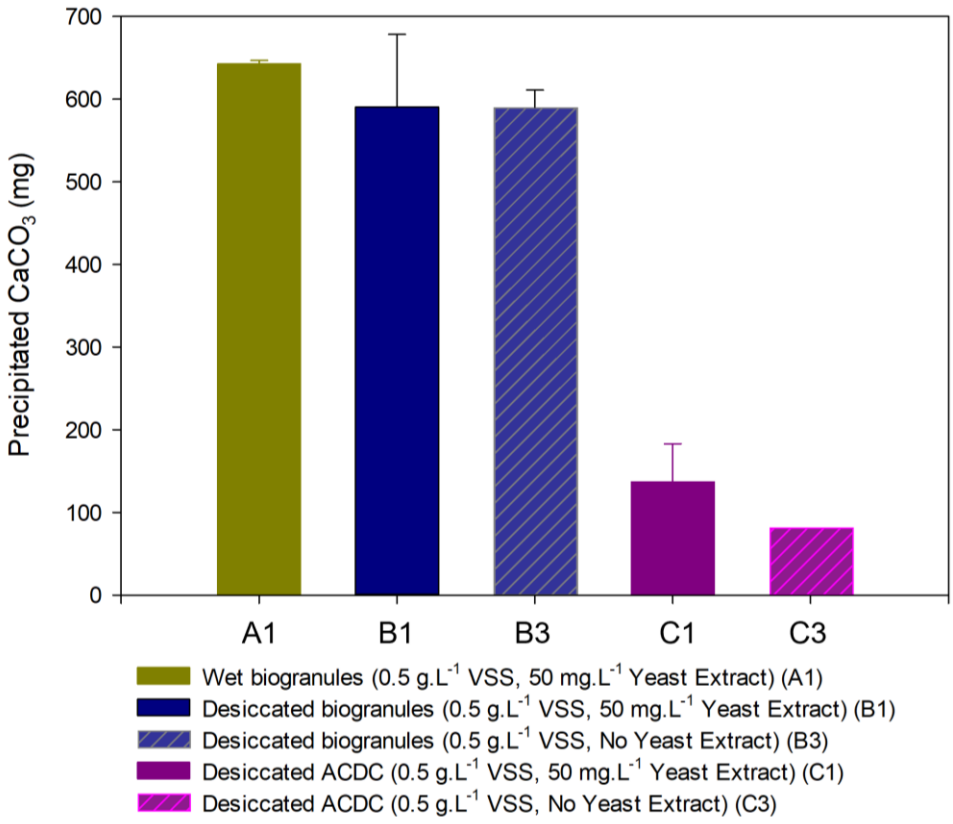

Figure 4.22. Amounts of calcium carbonate precipitated by the produced biogranules and ACDC at the end of nine days

Mineral Composition Obtained by using the produced Biogranules in Biomineralization Tests

In order to ascertain whether the dissolved calcium precipitated as $CaCO_3$ in the biomineralization tests, an additional batch reactor was set by using produced biogranules in this study. Alongside measuring $CaCO_3$, the precipitate obtained from this reactor underwent visual examination under a scanning electron microscope. Elemental composition analysis of the precipitate was conducted through Energy Dispersive X-ray Spectroscopy (EDX) on the obtained images. Micrographs showing the precipitates obtained with the biogranules were presented in Figure 4.23, while the EDX analysis and results were provided in Figure 4.24. Both micrographs and EDX analysis revealed that the precipitates obtained in the biomineralization tests predominantly consisted of the calcite form of $CaCO_3$ (Figure 4.23, Figure 4.24).

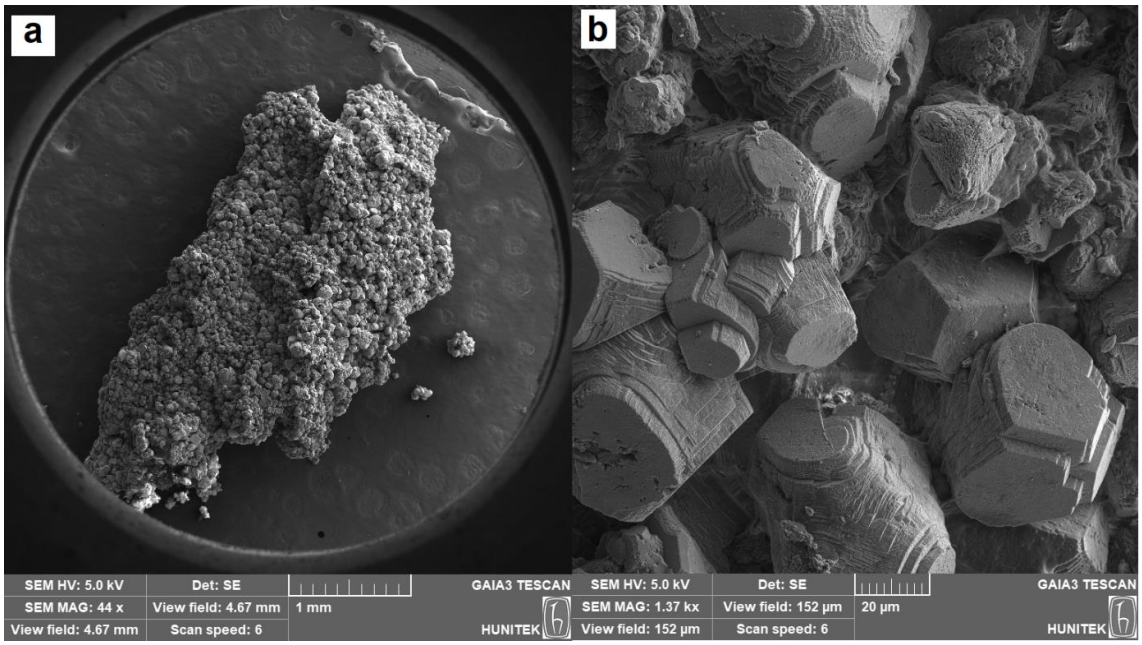

Figure 4.23. SEM micrographs of $CaCO_3$ minerals obtained in biomineralization tests with produced biogranules a) appearance of the mineral precipitate; b) precipitated calcite minerals

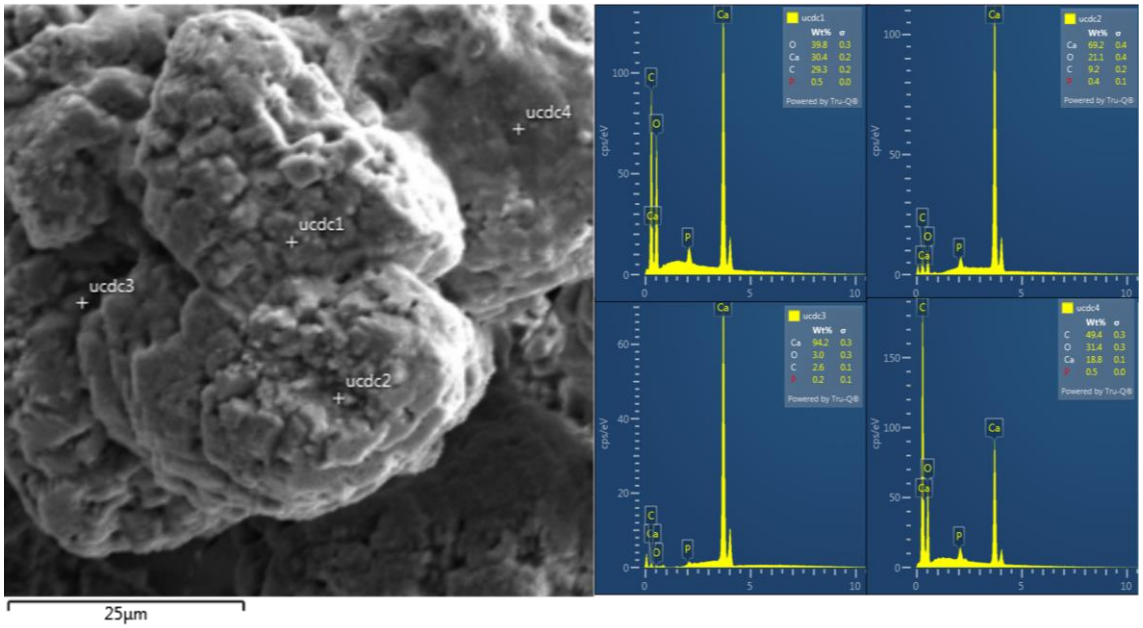

Figure 4.24. Results of EDX analysis conducted at four different points on the obtained minerals

4.2.4 Determination of the Impact of Shelf Life of Biogranules on Biomineralization Performance

The produced biogranules were desiccated and stored for 1.5 years and the reference nitrate-reducing granular culture (ACDC) was stored for 3 years. A biomineralization test was conducted again by using stored biogranules and ACDC with the same procedure. After nine days of operation, the precipitated $CaCO_3$ amounts were recorded as 386.34± 53.4 mg $CaCO_3$, 264.9± 13.7 mg $CaCO_3$, 296.7±19.3 mg $CaCO_3$ and 100.3±7.7 mg $CaCO_3$ for B1 (Desiccated biogranules, 50 $mg.L^{-1}$ Yeast extract), B3 (Desiccated biogranules, No Yeast Extract), C1(Desiccated ACDC, 50 $mg.L^{-1}$ Yeast Extract) and C3 (Desiccated ACDC, No Yeast Extract) respectively in the test (Figure 4.25).

According to the results from Group B, it was observed that the storage period negatively impacted $CaCO_3$ precipitation performance, with reductions of 35% for B1 and 55% for B3. In Group C, which contained ACDC, similar biomineralization performance results were obtained for C3, while a 116% increase was observed for C1. In Group C1, the denitrification activities revealed that nitrate reduction activity decreased from 71% to 60% compared to the previous test (Table 4.14 and Table 4.15). The pH values measured at the end of the periods were also very similar in both tests. Despite the decreased nitrate reduction activity, the reason for the increased mineral precipitation remained unclear.

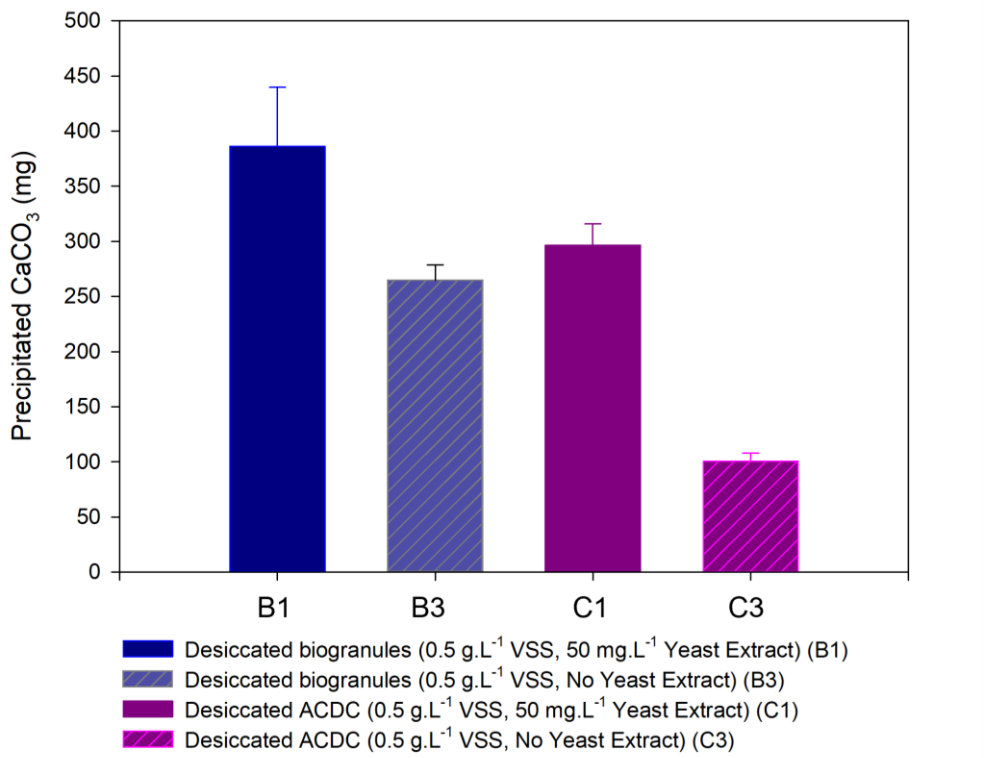

Figure 4.25. Amounts of calcium carbonate precipitated by the produced biogranules and ACDC at the end of nine days in the second biomineralization test

Upon evaluating all the results, it was determined that the positive effect of yeast extract on biomineralization became more pronounced as the shelf life increased. Comparing the yeast-containing batches B1 and C1, and the yeast-free batches B3 and C3, it was concluded that biogranules exhibited a higher MICP performance compared to ACDC.

Table 4.15. The recorded NO_x-N concentrations and nitrate reduction efficiencies in the second biomineralization test

Batch Groups*	**Feed NO_x-N ($mg.L^{-1}$)**	**NO_3-N ($mg.L^{-1}$)**	**Nitrate reduction (%)**	**NO_2-N Accumulation ($mg.L^{-1}$)**	**Total NO_x-N ($mg.L^{-1}$)**
B1	250	109.4	56.2	53.6	163.0
B3		186.8	26.8	63.9	246.9
C1		99.9	60.1	128.8	228.7
C3		208.4	16.6	34.5	242.9
A* : Wet biogranules (0.5 $g.L^{-1}$ VSS, 50 $mg.L^{-1}$ Yeast Extract), B1:Desiccated biogranules (0.5 $g.L^{-1}$ VSS, 50 $mg.L^{-1}$ Yeast extract), B3: Desiccated biogranules (0.5 $g.L^{-1}$ VSS, No Yeast Extract), C1: Desiccated ACDC (0.5 $g.L^{-1}$ VSS, 50 $mg.L^{-1}$ Yeast Extract), C3: Desiccated ACDC (0.5 $g.L^{-1}$ VSS, No Yeast Extract)					

5. CONCLUSION

In this study, it was aimed to optimize the granulation of an enrichment culture capable of urea hydrolysis and nitrate reduction, under minimal nutrient conditions. The production process was tailored and optimized for further use of biogranules in biomineralization applications. An optimization study was conducted to develop granules with enhanced characteristics, including resistance to alkaline conditions, functionality in the absence of micronutrients, minimal sensitivity to yeast extract, and the ability to be desiccated and resuscitated. Following the evaluation of seven different operating conditions, biogranules were successfully produced. These granules demonstrated the capability to perform both urea hydrolysis and denitrification in highly alkaline environments (pH > 9.5), grow in minimal nutrient media containing 0.05 $g.L^{-1}$ yeast extract and moderate osmotic stress (2000 $mg.L^{-1}$ NaCl) and maintain stable and predictable microbial communities both in wet conditions and after drying and reactivation. Then the microbial activity and $CaCO_3$ precipitation performance of these produced biogranules was comprehensively evaluated.

The key findings of this study are as follows:

Dissolved calcium concentration, VSS: TSS ratio, and selection pressure were found to be critical in the granulation of the bacteria under minimal nutrient conditions and the steady production of biogranules for biomineralization applications. The optimized operational conditions included only 50 $mg.L^{-1}$ calcium ions coming from tap water on the grounds that calcium levels than this value caused intense mineral precipitation in the reactor and a decrease in the VSS:TSS ratio. It is essential that the VSS:TSS ratio remains above 50% to ensure the operational stability of the reactor and achieve granulation. Additionally, there was no settling period in the optimized conditions and extra selective pressure was applied to the system once a week. Based on the findings applied extra selective pressure can be increased to achieve large granules.

Initial microscopic examinations revealed the formation of baby granules around day 200, with a gradual increase in size and compactness over time. According to the size distribution analysis, 82±7% of the granules were larger than 200 µm between days 324-362. Analysis of samples collected from the reactor on days 362 and 560 showed that 94% and 54% of the granules were larger than 200 µm respectively. Under minimal nutrient conditions, the granule sizes were smaller, and granules smaller than 200 microns

were also present in the system. Also, between days 362 and 560, a total of 10.8 grams of biogranules were harvested from the reactor, resulting in the formation of new baby granules during the recovery process. As selective pressure was applied weekly, smaller aggregates were able to remain in the system.

Metagenomic analyses revealed a consistent microbial community dominated by bacteria capable of urea hydrolysis and denitrification. In granule samples taken at different times, the dominance of the denitrifying community ranged from 51.7% to 70.7%, while the ureolytic community ranged from 34.2% to 49.4%. The beta diversity analysis results, along with the predominant genera in granules collected at different intervals, showed a high degree of similarity in the microbial community over the granule production period. This indicated that stable granule production of consistent quality is achievable in the bioreactor with optimized operational parameters.

The microbial community exhibited significant resilience and activity under alkaline pH (~9.75) and osmotic stress (2000 $mg.L^{-1}$ NaCl). Anoxic and aerobic periods were effectively managed to support denitrification and urea hydrolysis. According to the kinetic analysis, it was observed that nitrate reduction, COD, and urea consumption mostly followed zero-order reaction kinetics. The recorded specific activities of nitrate reduction, urea hydrolysis, and COD consumption under anoxic conditions were recorded as 7.26 mg NO_3-N. $h^{-1}.g^{-1}$ VSS, 32.1 mg urea. $h^{-1}g^{-1}$ VSS and 40.67 mg COD. h^{-1} g^{-1} VSS respectively.

Under 10 $g.L^{-1}$ urea and 0.5 $g.L^{-1}$ NO_3-N concentrations, the biogranules showed maximum activities of 232.8 mg urea. $h^{-1}.g^{-1}$ VSS for urea hydrolysis and 9.25 mg NO_3-N. $h^{-1}.g^{-1}$ VSS for nitrate reduction. The results showed that high ammonium nitrogen did not adversely affect urea hydrolysis, indicating that the urease enzyme in the biogranules was of the non-suppressive type and remained effective under high TAN conditions.

The comparative analysis of microbial activity between the produced biogranules and the nitrate-reducing reference granular culture (ACDC) for MICP revealed significant insights into their performance. According to the nitrate reduction performances, dried biogranules and ACDC could resuscitate in one week. At the end of seven days of the resuscitation period, specific denitrification activities of the desiccated biogranules and ACDC were recorded as 29 and 31 mg NOx-N.$day^{-1}.g^{-1}$ VSS respectively. It was observed that the biogranules achieved a nitrate reduction activity very similar to that of the ACDC.

Since ACDC was produced with a focus on denitrification, it did not exhibit urea hydrolysis activity. The maximum specific urea hydrolysis activity of the biogranules was recorded as 410 mg urea.day^{-1}.g^{-1} VSS. In light of all these results, biogranules were found to be more advantageous than ACDC, as they exhibited both denitrification and urea hydrolysis activities, whereas ACDC demonstrated only denitrification activity.

In the biomineralization test, Group A (wet biogranules (0.5 g.L^{-1} VSS, 50 mg.L^{-1} Yeast Extract) precipitated the highest amount of $CaCO_3$ (642.5±4.4 mg), indicating complete dissolved calcium precipitation. For the desiccated groups, the precipitated $CaCO_3$ amounts were measured as 590.3±88.2 mg for B1 (Desiccated biogranules, 50 mg.L^{-1} Yeast extract), 590.5±20.5 mg for B3 (Desiccated biogranules, No Yeast Extract) 137.1±46 mg for C1(Desiccated ACDC, 50 mg.L^{-1} Yeast Extract) and 82.2 mg for C3 (Desiccated ACDC, No Yeast Extract). However, since ACDC was stored for 1.5 years before use while biogranules were used immediately after drying, a further test was conducted. In the second biomineralization test, 1.5 years of stored biogranules and 4 years of stored ACDC were used. The precipitated $CaCO_3$ amounts were recorded as 386.34± 53.4 mg $CaCO_3$, 264.9± 13.7 mg $CaCO_3$, 296.7±19.3 mg $CaCO_3$, and 100.3±7.7 mg $CaCO_3$ for B1 (Desiccated biogranules, 50 mg.L^{-1} Yeast extract), B3 (Desiccated biogranules, No Yeast Extract), C1(Desiccated ACDC, 50 mg.L^{-1} Yeast Extract) and C3 (Desiccated ACDC, No Yeast Extract) respectively in the second test. It was observed that the storage period negatively impacted $CaCO_3$ precipitation performance in Group B. Upon evaluating all the results, it was determined that the positive effect of yeast extract on biomineralization became more pronounced as the shelf life increased.

Comparing the yeast-containing batches B1 and C1, and the yeast-free batches B3 and C3, it was concluded that biogranules exhibited 30% and 164% higher MICP performance compared to nitrate-reducing reference granular culture (ACDC) in the second biomineralization test. Additionally, SEM micrographs and EDX analysis revealed that the $CaCO_3$ precipitates of the biogranules obtained in the biomineralization tests predominantly consisted of the calcite form of $CaCO_3$.

The biogranules' ability to maintain high microbial activity under both anoxic and aerobic conditions, with low yeast extract concentrations, indicated their potential for effective biomineralization applications, including self-healing concrete and soil stabilization. This study demonstrated that optimizing microbial cultures for dual metabolic activities significantly enhanced biomineralization performance, making the produced biogranules

a more versatile and efficient solution compared to ACDC for various environmental and industrial applications. Future research should test these biogranules in applications such as self-healing bioconcrete, soil stabilization, and heavy metal removal, comparing their effectiveness to pure cultures.

In this study, synthetic nutrients were used but to reduce costs exploring alternative nutrient sources such as process waters from the food industry is essential. The biogranules produced in this study were found to perform urea hydrolysis and facilitate a rapid MICP process. However, the ammonium nitrogen released from urea hydrolysis is a pollutant and remains unutilized, representing a significant drawback of this process. Therefore, identifying optimal biomineralization conditions that enhance the dominance of the denitrification process without reducing biomineralization capacity is crucial to minimizing the amount of ammonium released. In this regard, future studies should focus on optimizing the ratios of urea, nitrate, and carbon required during biomineralization applications to improve the sustainability of the process.

Due to the observed decline in MICP performance of desiccated biogranules after two years, advanced storage methods to maintain microbial viability and activity over longer periods should be developed. These methods are essential to ensure that the biogranules remain effective for extended durations, facilitating consistent biomineralization performance in various applications. Additionally, studies should be conducted to determine the shelf life for both wet and dry forms of the biogranules.

6. REFERENCES

[1] I. Justo-Reinoso, A. Heath, S. Gebhard, K. Paine, Aerobic non-ureolytic bacteria-based self-healing cementitious composites: A comprehensive review, Journal of Building Engineering 42 (2021) 102834. https://doi.org/10.1016/J.JOBE.2021.102834.

[2] S. Jain, D.N. Arnepalli, Biochemically Induced Carbonate Precipitation in Aerobic and Anaerobic Environments by Sporosarcina pasteurii, Geomicrobiol J 36 (2019) 443–451. https://doi.org/10.1080/01490451.2019.1569180.

[3] M. Naveed, J. Duan, S. Uddin, M. Suleman, Y. Hui, H. Li, Application of microbially induced calcium carbonate precipitation with urea hydrolysis to improve the mechanical properties of soil, Ecol Eng 153 (2020) 105885. https://doi.org/10.1016/J.ECOLENG.2020.105885.

[4] N.K. Dhami, M. Sudhakara Reddy, A. Mukherjee, Application of calcifying bacteria for remediation of stones and cultural heritages, Front Microbiol 5 (2014). https://doi.org/10.3389/fmicb.2014.00304.

[5] V. Achal, A. Mukherjee, D. Kumari, Q. Zhang, Biomineralization for sustainable construction-A review of processes and applications, (2015). https://doi.org/10.1016/j.earscirev.2015.05.008.

[6] Á.E. Torres-Aravena, C. Duarte-Nass, L. Azócar, R. Mella-Herrera, M. Rivas, D. Jeison, Can Microbially Induced Calcite Precipitation (MICP) through a Ureolytic Pathway Be Successfully Applied for Removing Heavy Metals from Wastewaters?, Crystals 2018, Vol. 8, Page 438 8 (2018) 438. https://doi.org/10.3390/CRYST8110438.

[7] S.E. Lambert, D.G. Randall, Manufacturing bio-bricks using microbial induced calcium carbonate precipitation and human urine, Water Res 160 (2019) 158–166. https://doi.org/10.1016/J.WATRES.2019.05.069.

[8] M.J. Castro-Alonso, L.E. Montañez-Hernandez, M.A. Sanchez-Muñoz, M.R. Macias Franco, R. Narayanasamy, N. Balagurusamy, Microbially induced calcium carbonate precipitation (MICP) and its potential in bioconcrete: Microbiological and molecular concepts, Front Mater 6 (2019). https://doi.org/10.3389/fmats.2019.00126.

[9] M.M. Rahman, R.N. Hora, I. Ahenkorah, S. Beecham, M.R. Karim, A. Iqbal, State-of-the-art review of microbial-induced calcite precipitation and its sustainability in engineering applications, Sustainability (Switzerland) 12 (2020). https://doi.org/10.3390/SU12156281.

[10] M. Li, K. Wen, Y. Li, L. Zhu, Impact of Oxygen Availability on Microbially Induced Calcite Precipitation (MICP) Treatment, Geomicrobiol J 35 (2018) 15–22. https://doi.org/10.1080/01490451.2017.1303553.

[11] Y. Gao, L. Wang, • Jia He, • Jie Ren, Y. Gao, Denitrification-based MICP for cementation of soil: treatment process and mechanical performance, Acta Geotech 17 (2022) 3799–3815. https://doi.org/10.1007/s11440-022-01489-6.

[12] Y.Ç. Erşan, N. de Belie, N. Boon, Microbially induced CaCO3 precipitation through denitrification: An optimization study in minimal nutrient environment, Biochem Eng J 101 (2015) 108–118. https://doi.org/10.1016/j.bej.2015.05.006.

[13] L.A. Van Paassen, C.M. Daza, M. Staal, D.Y. Sorokin, W. Van Der Zon, M.C.M. Van Loosdrecht, Potential soil reinforcement by biological denitrification, Ecol Eng 36 (2010) 168–175. https://doi.org/10.1016/j.ecoleng.2009.03.026.

[14] Y.Ç. Erşan, H. Verbruggen, I. De Graeve, W. Verstraete, N. De Belie, N. Boon, Nitrate reducing CaCO3 precipitating bacteria survive in mortar and inhibit steel corrosion, Cem Concr Res 83 (2016) 19–30. https://doi.org/10.1016/j.cemconres.2016.01.009.

[15] X. Zhu, J. Wang, N. De Belie, N. Boon, Complementing urea hydrolysis and nitrate reduction for improved microbially induced calcium carbonate precipitation, Appl Microbiol Biotechnol 103 (2019) 8825–8838. https://doi.org/10.1007/s00253-019-10128-2.

[16] Y. Wu, H. Li, Y. Li, Biomineralization induced by cells of sporosarcina pasteurii: Mechanisms, applications and challenges, Microorganisms 9 (2021). https://doi.org/10.3390/microorganisms9112396.

[17] R.S. Perry, N. Mcloughlin, B.Y. Lynne, M.A. Sephton, J.D. Oliver, C.C. Perry, K. Campbell, M.H. Engel, J.D. Farmer, M.D. Brasier, J.T. Staley, Defining biominerals and organominerals: Direct and indirect indicators of life, Sediment Geol 201 (2007) 157–179. https://doi.org/10.1016/j.sedgeo.2007.05.014.

[18] C. Dupraz, R.P. Reid, O. Braissant, A.W. Decho, R.S. Norman, P.T. Visscher, Processes of carbonate precipitation in modern microbial mats, Earth Sci Rev 96 (2009) 141–162. https://doi.org/10.1016/j.earscirev.2008.10.005.

[19] N.K. Dhami, M.S. Reddy, M.S. Mukherjee, Biomineralization of calcium carbonates and their engineered applications: A review, Front Microbiol 4 (2013). https://doi.org/10.3389/fmicb.2013.00314.

[20] E. Ortega-Villamagua, M. Gudiño-Gomezjurado, A. Palma-Cando, Microbiologically induced carbonate precipitation in the restoration and conservation of cultural heritage materials, Molecules 25 (2020). https://doi.org/10.3390/molecules25235499.

[21] Y. Wu, H. Li, Y. Li, Biomineralization induced by cells of sporosarcina pasteurii: Mechanisms, applications and challenges, Microorganisms 9 (2021). https://doi.org/10.3390/microorganisms9112396.

[22] O. Reinhardt, S. Ihmann, M. Ahlhelm, M. Gelinsky, 3D bioprinting of mineralizing cyanobacteria as novel approach for the fabrication of living building materials, Front Bioeng Biotechnol 11 (2023). https://doi.org/10.3389/fbioe.2023.1145177.

[23] M. Seifan, A.K. Samani, A. Berenjian, Bioconcrete: next generation of self-healing concrete, (n.d.). https://doi.org/10.1007/s00253-016-7316-z.

[24] S. Mondal, A. (Dey) Ghosh, Review on microbial induced calcite precipitation mechanisms leading to bacterial selection for microbial concrete, Constr Build Mater 225 (2019) 67–75. https://doi.org/10.1016/j.conbuildmat.2019.07.122.

[25] W. Lin, W. Lin, X. Cheng, G. Chen, Y.C. Ersan, Microbially induced desaturation and carbonate precipitation through denitrification: A review, Applied Sciences (Switzerland) 11 (2021). https://doi.org/10.3390/app11177842.

[26] D.J. Tobler, M.O. Cuthbert, R.B. Greswell, M.S. Riley, J.C. Renshaw, S. Handley-Sidhu, V.R. Phoenix, Comparison of rates of ureolysis between Sporosarcina pasteurii and an indigenous groundwater community under conditions required to precipitate large volumes of calcite, Geochim Cosmochim Acta 75 (2011) 3290–3301. https://doi.org/10.1016/j.gca.2011.03.023.

[27] T. Zhu, M. Dittrich, Carbonate precipitation through microbial activities in natural environment, and their potential in biotechnology: A review, Front Bioeng Biotechnol 4 (2016). https://doi.org/10.3389/fbioe.2016.00004.

[28] M. Alazhari, T. Sharma, A. Heath, R. Cooper, K. Paine, Application of expanded perlite encapsulated bacteria and growth media for self-healing concrete, Constr Build Mater 160 (2018) 610–619. https://doi.org/10.1016/J.CONBUILDMAT.2017.11.086.

[29] M.T. González-Muñoz, C. Rodriguez-Navarro, F. Martínez-Ruiz, J.M. Arias, M.L. Merroun, M. Rodriguez-Gallego, Bacterial biomineralization: New insights from Myxococcus-induced mineral precipitation, Geol Soc Spec Publ 336 (2010) 31–50. https://doi.org/10.1144/SP336.3.

[30] V. Nežerka, P. Holeček, M. Somr, P. Tichá, M. Domonkos, H. Stiborová, On the possibility of using bacteria for recycling finest fractions of concrete waste: a critical review, Rev Environ Sci Biotechnol 22 (2023) 427–450. https://doi.org/10.1007/s11157-023-09654-3.

[31] W. Mwandira, M. Mavroulidou, M.J. Gunn, D. Purchase, H. Garelick, J. Garelick, Concurrent Carbon Capture and Biocementation through the Carbonic Anhydrase (CA) Activity of Microorganisms -a Review and Outlook, Environmental Processes 10 (2023). https://doi.org/10.1007/s40710-023-00667-2.

[32] J.T. DeJong, B.M. Mortensen, B.C. Martinez, D.C. Nelson, Bio-mediated soil improvement, Ecol Eng 36 (2010) 197–210. https://doi.org/10.1016/J.ECOLENG.2008.12.029.

[33] L. Jiang, H. Xia, W. Wang, Y. Zhang, Z. Li, Applications of microbially induced calcium carbonate precipitation in civil engineering practice: A state-of-the-art review, Constr Build Mater 404 (2023) 133227. https://doi.org/10.1016/j.conbuildmat.2023.133227.

[34] G. Ganendra, W.D. De Muynck, A. Ho, E.C. Arvaniti, B. Hosseinkhani, J.A. Ramos, H. Rahier, N. Boon, Formate oxidation-driven calcium carbonate precipitation by Methylocystis parvus OBBP, Appl Environ Microbiol 80 (2014) 4659–4667. https://doi.org/10.1128/AEM.01349-14.

[35] G. Ganendra, J. Wang, J.A. Ramos, H. Derluyn, H. Rahier, V. Cnudde, A. Ho, N. Boon, Biogenic concrete protection driven by the formate oxidation by Methylocystis parvus OBBP, Front Microbiol 6 (2015). https://doi.org/10.3389/fmicb.2015.00786.

[36] M. Seifan, A. Berenjian, Microbially induced calcium carbonate precipitation: a widespread phenomenon in the biological world, Appl Microbiol Biotechnol 103 (2019) 4693–4708. https://doi.org/10.1007/s00253-019-09861-5.

[37] K. Kappaun, A.R. Piovesan, C.R. Carlini, R. Ligabue-Braun, Ureases: Historical aspects, catalytic, and non-catalytic properties-A review, J Adv Res 13 (2018) 3–17. https://doi.org/10.1016/j.jare.2018.05.010.

[38] C. Zhang, H. Chen, G. Xue, Fe 0-induced multifunctional effect of aerobic denitrification, autotrophic denitrification and chemically enhanced phosphorus removal in oxic/ anoxic process for low C/N wastewater, Chemical Engineering Journal 483 (2024) 149218. https://doi.org/10.1016/j.cej.2024.149218.

[39] B. Özbay, Complementing Urea Hydrolysis and Nitrate Reduction Metabolisms to Enhance Microbial Self-Healing Performance in Cementitious Composites, Hacettepe University, 2023.

[40] X. Zhu, M. Sakarika, R. Ganigué, K. Van Tittelboom, Y.Ç. Erşan, N. Boon, N. De Belie, Production of calcium carbonate-precipitating biomass powder as self-healing additive in concrete and performance evaluation in mortar, Cem Concr Compos 138 (2023). https://doi.org/10.1016/j.cemconcomp.2023.104952.

[41] K. Chetty, S. Xie, Y. Song, T. McCarthy, U. Garbe, X. Li, G. Jiang, Self-healing bioconcrete based on non-axenic granules: A potential solution for concrete wastewater infrastructure, Journal of Water Process Engineering 42 (2021). https://doi.org/10.1016/j.jwpe.2021.102139.

[42] W.J. Shin, S.H. Choi, J.S. Ryu, K. Ha, J.Y. Lee, K.S. Lee, Factors affecting diurnal dissolved inorganic carbon and its isotopic composition in a small stream on a volcanic island in South Korea, Geosciences Journal 24 (2020) 73–83. https://doi.org/10.1007/s12303-019-0013-z.

[43] D.C. Bakker, H.J. de Baar, E. de Jong, The dependence on temperature and salinity of dissolved inorganic carbon in East Atlantic surface waters, 1999.

[44] L. Merlivat, J. Boutin, D. Antoine, L. Beaumont, M. Golbol, V. Vellucci, Increase of dissolved inorganic carbon and decrease in pH in near-surface waters in the Mediterranean Sea during the past two decades, Biogeosciences 15 (2018) 5653–5662. https://doi.org/10.5194/bg-15-5653-2018.

[45] Y. Li, Q. He, X. Ma, H. Wang, C. Liu, D. Yu, Plant traits interacting with sediment properties regulate sediment microbial composition under different aquatic DIC levels caused by rising atmospheric CO2, Plant Soil 445 (2019) 497–512. https://doi.org/10.1007/s11104-019-04312-6.

[46] M. Wu, B. Johannesson, M. Geiker, A review: Self-healing in cementitious materials and engineered cementitious composite as a self-healing material, Constr Build Mater 28 (2012) 571–583. https://doi.org/10.1016/j.conbuildmat.2011.08.086.

[47] K. DArunachalam, K. Sathyanarayanan, B. Darshan, Rb. Raja, Studies on the characterisation of Biosealant properties of Bacillus sphaericus, 2010.

[48] K.D. Mutitu, M.O. Munyao, M.J. Wachira, R. Mwirichia, K.J. Thiong'o, M.J. Marangu, Effects of biocementation on some properties of cement-based materials incorporating Bacillus Species bacteria–a review, J Sustain Cem Based Mater 8 (2019) 309–325. https://doi.org/10.1080/21650373.2019.1640141.

[49] W. De Muynck, K. Verbeken, N. De Belie, W. Verstraete, Influence of temperature on the effectiveness of a biogenic carbonate surface treatment for limestone conservation, Appl Microbiol Biotechnol 97 (2013) 1335–1347. https://doi.org/10.1007/s00253-012-3997-0.

[50] M.A. Rivadeneyra, J. Párraga, R. Delgado, A. Ramos-Cormenzana, G. Delgado, Biomineralization of carbonates by Halobacillus trueperi in solid and liquid media with different salinities, FEMS Microbiol Ecol 48 (2004) 39–46. https://doi.org/10.1016/j.femsec.2003.12.008.

[51] N. De Belie, J. Wang, Bacteria-based repair and self-healing of concrete, J Sustain Cem Based Mater 5 (2015) 35–56. https://doi.org/10.1080/21650373.2015.1077754.

[52] B. Kardogan, K. Sekercioglu, Y.Ç. Erşan, Compatibility and biomineralization oriented optimization of nutrient content in nitrate-reducing-biogranules-based

microbial self-healing concrete, Sustainability (Switzerland) 13 (2021). https://doi.org/10.3390/su13168990.

[53] J. Li, W. Bi, Y. Yao, Z. Liu, State-of-the-Art Review of Utilization of Microbial-Induced Calcite Precipitation for Improving Moisture-Dependent Properties of Unsaturated Soils, Applied Sciences (Switzerland) 13 (2023). https://doi.org/10.3390/app13042502.

[54] D. Mujah, L. Cheng, M.A. Shahin, Microstructural and Geomechanical Study on Biocemented Sand for Optimization of MICP Process, Journal of Materials in Civil Engineering 31 (2019). https://doi.org/10.1061/(asce)mt.1943-5533.0002660.

[55] L.S. Wong, Microbial cementation of ureolytic bacteria from the genus Bacillus: A review of the bacterial application on cement-based materials for cleaner production, J Clean Prod 93 (2015) 5–17. https://doi.org/10.1016/j.jclepro.2015.01.019.

[56] S. Liang, X. Xiao, Z. Li, D. Feng, Effect of Nutrient Solution Composition on Bio-Cemented Sand, Crystals (Basel) 11 (2021). https://doi.org/10.3390/cryst11121572.

[57] B.M. Mortensen, M.J. Haber, J.T. Dejong, L.F. Caslake, D.C. Nelson, Effects of environmental factors on microbial induced calcium carbonate precipitation, J Appl Microbiol 111 (2011) 338–349. https://doi.org/10.1111/j.1365-2672.2011.05065.x.

[58] D. Martin, K. Dodds, B.T. Ngwenya, I.B. Butler, S.C. Elphick, Inhibition of sporosarcina pasteurii under anoxic conditions: Implications for subsurface carbonate precipitation and remediation via ureolysis, Environ Sci Technol 46 (2012) 8351–8355. https://doi.org/10.1021/es3015875.

[59] A. Robles-Fernández, C. Areias, D. Daffonchio, V.C. Vahrenkamp, M. Sánchez-Román, The Role of Microorganisms in the Nucleation of Carbonates, Environmental Implications and Applications, Minerals 12 (2022). https://doi.org/10.3390/min12121562.

[60] A. Bains, N.K. Dhami, A. Mukherjee, M.S. Reddy, Influence of Exopolymeric Materials on Bacterially Induced Mineralization of Carbonates, Appl Biochem Biotechnol 175 (2015) 3531–3541. https://doi.org/10.1007/s12010-015-1524-3.

[61] Z. Zeng, M.M. Tice, Promotion and nucleation of carbonate precipitation during microbial iron reduction, Geobiology 12 (2014) 362–371. https://doi.org/10.1111/gbi.12090.

[62] T.D. Hoffmann, B.J. Reeksting, S. Gebhard, Bacteria-induced mineral precipitation: A mechanistic review, Microbiology (United Kingdom) 167 (2021). https://doi.org/10.1099/mic.0.001049.

[63] Z. Gu, Q. Chen, L. Wang, S. Niu, J. Zheng, M. Yang, Y. Yan, Morphological Changes of Calcium Carbonate and Mechanical Properties of Samples during Microbially Induced Carbonate Precipitation (MICP), Materials 15 (2022). https://doi.org/10.3390/ma15217754.

[64] R. Murugan, G.K. Suraishkumar, A. Mukherjee, N.K. Dhami, Insights into the influence of cell concentration in design and development of microbially induced calcium carbonate precipitation (MICP) process, PLoS One 16 (2021). https://doi.org/10.1371/journal.pone.0254536.

[65] H. Fazeli, M. Masoudi, R.A. Patel, P. Aagaard, H. Hellevang, Pore-Scale Modeling of Nucleation and Growth in Porous Media, ACS Earth Space Chem 4 (2020) 249–260. https://doi.org/10.1021/acsearthspacechem.9b00290.

[66] S.C. Chuo, S.F. Mohamed, S.H.M. Setapar, A. Ahmad, M. Jawaid, W.A. Wani, A.A. Yaqoob, M.N.M. Ibrahim, Insights into the current trends in the utilization of bacteria for microbially induced calcium carbonate precipitation, Materials 13 (2020) 1–28. https://doi.org/10.3390/ma13214993.

[67] S. Maheswaran, S.S. Dasuru, A. Rama, C. Murthy, B. Bhuvaneshwari, V.R. Kumar, G.S. Palani, N.R. Iyer, S. Krishnamoorthy, S. Sandhya, Strength improvement studies using new type wild strain Bacillus cereus on cement mortar, Jstor 106 (2014) 50–57. https://about.jstor.org/terms (accessed May 15, 2024).

[68] Y.Ç. Erşan, E. Hernandez-Sanabria, N. Boon, N. De Belie, Enhanced crack closure performance of microbial mortar through nitrate reduction, Cem Concr Compos 70 (2016) 159–170. https://doi.org/10.1016/j.cemconcomp.2016.04.001.

[69] Y. Ersan, E. Gruyaert, G. Louis, C. Lors, N. De Belie, N. Boon, Self-protected nitrate reducing culture for intrinsic repair of concrete cracks, Front Microbiol 6 (2015). https://doi.org/10.3389/fmicb.2015.01228.

[70] E. Tziviloglou, V. Wiktor, H.M. Jonkers, E. Schlangen, Bacteria-based self-healing concrete to increase liquid tightness of cracks, Constr Build Mater 122 (2016) 118–125. https://doi.org/10.1016/j.conbuildmat.2016.06.080.

[71] W. Khaliq, M.B. Ehsan, Crack healing in concrete using various bio influenced self-healing techniques, Constr Build Mater 102 (2016) 349–357. https://doi.org/10.1016/j.conbuildmat.2015.11.006.

[72] D. Palin, V. Wiktor, H.M. Jonkers, A Bacteria-Based Self-Healing Cementitious Composite for Application in Low-Temperature Marine Environments, Biomimetics 2 (2017). https://doi.org/10.3390/biomimetics2030013.

[73] D. Mujah, M.A. Shahin, L. Cheng, State-of-the-Art Review of Biocementation by Microbially Induced Calcite Precipitation (MICP) for Soil Stabilization, Geomicrobiol J 34 (2017) 524–537. https://doi.org/10.1080/01490451.2016.1225866.

[74] V.S. Whiffin, L.A. van Paassen, M.P. Harkes, Microbial carbonate precipitation as a soil improvement technique, Geomicrobiol J 24 (2007) 417–423. https://doi.org/10.1080/01490450701436505.

[75] N. Hamdan, E. Kavazanjian, B.E. Rittmann, I. Karatas, Carbonate Mineral Precipitation for Soil Improvement Through Microbial Denitrification, Geomicrobiol J 34 (2017) 139–146. https://doi.org/10.1080/01490451.2016.1154117.

[76] V. Achal, X. Pan, D. Zhang, Remediation of copper-contaminated soil by Kocuria flava CR1, based on microbially induced calcite precipitation, Ecol Eng 37 (2011) 1601–1605. https://doi.org/10.1016/J.ECOLENG.2011.06.008.

[77] N. Shahidah, A. Ali, K. Muda, M. Faiz, M. Amin, M. Zuhaili, M. Najib, H. Ezechi, M.S.J. Darwish, Initialization, enhancement and mechanisms of aerobic granulation in wastewater treatment, Sep Purif Technol 260 (2021) 118220. https://doi.org/10.1016/j.seppur.2020.118220.

[78] E. Morgenroth, T. Sherden I, M.C.M. Van Loosdrecht @2, J.J. Heijnen, P.A. Wllderer, RAPID COMMUNICATION AEROBIC GRANULAR SLUDGE IN A SEQUENCING BATCH REACTOR, Wat. Res 31 (1997) 3191–3194.

[79] A.C. Trego, S. Mills, G. Collins, Granular biofilms: Function, application, and new trends as model microbial communities, Crit Rev Environ Sci Technol 51 (2021) 1702–1725. https://doi.org/10.1080/10643389.2020.1769433.

[80] B.-M. Wilén, R. Liébana, F. Persson, O. Modin, M. Hermansson, The mechanisms of granulation of activated sludge in wastewater treatment, its optimization, and impact on effluent quality, Appl Microbiol Biotechnol 102 (2018) 5005–5020. https://doi.org/10.1007/s00253-018-8990-9.

[81] Y.Q. Liu, Y. Liu, J.H. Tay, The effects of extracellular polymeric substances on the formation and stability of biogranules, Appl Microbiol Biotechnol 65 (2004) 143–148. https://doi.org/10.1007/s00253-004-1657-8.

[82] M. Geng, S. You, H. Guo, F. Ma, X. Xiao, X. Ma, Co-existence of flocs and granules in aerobic granular sludge system: Performance, microbial community and proteomics, Chemical Engineering Journal 451 (2023) 1385–8947. https://doi.org/10.1016/j.cej.2022.139011.

[83] L. van den Berg, C.M. Kirkland, J.D. Seymour, S.L. Codd, M.C.M. van Loosdrecht, M.K. de Kreuk, Heterogeneous diffusion in aerobic granular sludge, Biotechnol Bioeng 117 (2020) 3809–3819. https://doi.org/10.1002/bit.27522.

[84] Q. He, W. Zhang, S. Zhang, H. Wang, Enhanced nitrogen removal in an aerobic granular sequencing batch reactor performing simultaneous nitrification, endogenous denitrification and phosphorus removal with low superficial gas velocity, Chemical Engineering Journal 326 (2017) 1223–1231. https://doi.org/10.1016/J.CEJ.2017.06.071.

[85] M.K. De Kreuk, J.J. Heijnen, M.C.M. Van Loosdrecht, Simultaneous COD, nitrogen, and phosphate removal by aerobic granular sludge, Biotechnol Bioeng 90 (2005) 761–769. https://doi.org/10.1002/BIT.20470.

[86] N. Hubaux, G. Wells, E. Morgenroth, Impact of coexistence of flocs and biofilm on performance of combined nitritation-anammox granular sludge reactors, (2014). https://doi.org/10.1016/j.watres.2014.09.036.

[87] A. Elahinik, L. Li, M. Pabst, B. Abbas, D. Xevgenos, M.C.M. van Loosdrecht, M. Pronk, Aerobic granular sludge phosphate removal using glucose, Water Res 247 (2023) 120776. https://doi.org/10.1016/J.WATRES.2023.120776.

[88] W.P. Kovacik, J.C.M. Scholten, D. Culley, R. Hickey, W. Zhang, F.J. Brockman, Microbial dynamics in upflow anaerobic sludge blanket (UASB) bioreactor granules in response to short-term changes in substrate feed, (n.d.). https://doi.org/10.1099/mic.0.036715-0.

[89] M. Sonmez, Y.C. Ersan, Production of concrete compatible biogranules for self-healing concrete applications, MATEC Web of Conferences 289 (2019) 01002. https://doi.org/10.1051/matecconf/201928901002.

[90] A. Makalesi, / Research, A. Yusuf, Ç. Erşan, Self-Healing Performance of Biogranule Containing Microbial Self-Healing Concrete Under Intermittent Wet/Dry Cycles, Journal of Polytechnic 24 (2021) 323–332. https://doi.org/10.2339/POLITEKNIK.742210.

[91] X. Tan, G.J. Xie, W.B. Nie, D.F. Xing, B.F. Liu, J. Ding, N.Q. Ren, High value-added biomaterials recovery from granular sludge based wastewater treatment process, Resour Conserv Recycl 169 (2021). https://doi.org/10.1016/j.resconrec.2021.105481.

[92] Y.C. Ersan, D. Palin, S.B. Yengec Tasdemir, K. Tasdemir, H.M. Jonkers, N. Boon, N. De Belie, Volume fraction, thickness, and permeability of the sealing layer in microbial self-healing concrete containing biogranules, Front Built Environ 4 (2018) 404643. https://doi.org/10.3389/FBUIL.2018.00070/BIBTEX.

[93] Y. Liu, Chapter 5 Factors affecting aerobic granulation, in: Waste Management Series, Elsevier, 2006: pp. 99–114. https://doi.org/10.1016/S0713-2743(06)80107-8.

[94] B.Y.P. Moy, J.H. Tay, S.K. Toh, Y. Liu, S.T.L. Tay, High organic loading influences the physical characteristics of aerobic sludge granules, Lett Appl Microbiol 34 (2002) 407–412. https://doi.org/10.1046/j.1472-765X.2002.01108.x.

[95] L. Cha, Y.Q. Liu, W. Duan, C.E.W. Sternberg, Q. Yuan, F. Chen, Fluctuation and re-establishment of aerobic granules properties during the long-term operation period with low-strength and low c/n ratio wastewater, Processes 9 (2021). https://doi.org/10.3390/pr9081290.

[96] L. Wu, C. Peng, Y. Peng, L. Li, S. Wang, Y. Ma, Effect of wastewater COD/N ratio on aerobic nitrifying sludge granulation and microbial population shift,

Journal of Environmental Sciences 24 (2012) 234–241. https://doi.org/10.1016/S1001-0742(11)60719-5.

[97] J. Luo, T. Hao, L. Wei, H.R. Mackey, Z. Lin, G.H. Chen, Impact of influent COD/N ratio on disintegration of aerobic granular sludge, Water Res 62 (2014) 127–135. https://doi.org/10.1016/J.WATRES.2014.05.037.

[98] I. Kocaturk, T.H. Erguder, Influent COD/TAN ratio affects the carbon and nitrogen removal efficiency and stability of aerobic granules, Ecol Eng 90 (2016) 12–24. https://doi.org/10.1016/J.ECOLENG.2016.01.077.

[99] J.Y. Wang, B. Zhao, Q. An, Q. Dan, J.S. Guo, Y.P. Chen, The acceleration of aerobic sludge granulation by alternating organic loading rate: Performance and mechanism, J Environ Manage 347 (2023) 119047. https://doi.org/10.1016/J.JENVMAN.2023.119047.

[100] L. Wang, X. Liu, Z. Li, C. Wan, Y. Zhang, Filamentous aerobic granular sludge: A critical review on its cause, impact, control and reuse, J Environ Chem Eng 11 (2023) 110039. https://doi.org/10.1016/J.JECE.2023.110039.

[101] R. Tang, X. Han, Y. Jin, J. Yu, Do increased organic loading rates accelerate aerobic granulation in hypersaline environment?, J Environ Chem Eng 10 (2022) 108775. https://doi.org/10.1016/J.JECE.2022.108775.

[102] M. Ali, Z. Wang, K.W. Salam, A.R. Hari, M. Pronk, M.C.M. Van Loosdrecht, P.E. Saikaly, Importance of species sorting and immigration on the bacterial assembly of different-sized aggregates in a full-scale Aerobic granular sludge plant, Environ Sci Technol 53 (2019) 8291–8301. https://doi.org/10.1021/ACS.EST.8B07303/SUPPL_FILE/ES8B07303_SI_001.PDF.

[103] E.I.P. Volcke, C. Picioreanu, B. De Baets, M.C.M. van Loosdrecht, The granule size distribution in an anammox-based granular sludge reactor affects the conversion-Implications for modeling, Biotechnol Bioeng 109 (2012) 1629–1636. https://doi.org/10.1002/bit.24443.

[104] Y. Li, Y. Liu, H. Xu, Is sludge retention time a decisive factor for aerobic granulation in SBR?, Bioresour Technol 99 (2008) 7672–7677. https://doi.org/10.1016/J.BIORTECH.2008.01.073.

[105] J.J. Beun, M.C.M. Van Loosdrecht, J.J. Heijnen, Aerobic granulation, Water Science and Technology 41 (2000) 41–48. https://doi.org/10.2166/wst.2000.0423.

[106] Z. Zhang, Z. Yu, Z. Wang, K. Ma, X. Xu, P.J.J. Alvarezc, L. Zhu, Understanding of aerobic sludge granulation enhanced by sludge retention time in the aspect of quorum sensing, Bioresour Technol 272 (2019) 226–234. https://doi.org/10.1016/J.BIORTECH.2018.10.027.

[107] B. Kończak, J. Karcz, K. Miksch, Influence of Calcium, Magnesium, and Iron Ions on Aerobic Granulation, Appl Biochem Biotechnol 174 (2014) 2910–2918. https://doi.org/10.1007/s12010-014-1236-0.

[108] G. Yilmaz, U. Bozkurt, K.A. Magden, Effect of iron ions (Fe2+, Fe3+) on the formation and structure of aerobic granular sludge, Biodegradation 28 (2017) 53–68. https://doi.org/10.1007/s10532-016-9777-2.

[109] C. Ye, X. Yang, F.J. Zhao, L. Ren, The shift of the microbial community in activated sludge with calcium treatment and its implication to sludge settleability, Bioresour Technol 207 (2016) 11–18. https://doi.org/10.1016/J.BIORTECH.2016.01.135.

[110] S. Wang, W. Shi, T. Tang, Y. Wang, L. Zhi, J. Lv, J. Li, Function of quorum sensing and cell signaling in the formation of aerobic granular sludge, Rev Environ Sci Biotechnol 16 (2017). https://doi.org/10.1007/s11157-017-9420-7.

[111] T. Peng, Y. Wang, J. Wang, F. Fang, P. Yan, Z. Liu, Effect of different forms and components of EPS on sludge aggregation during granulation process of aerobic granular sludge, Chemosphere 303 (2022) 135116. https://doi.org/10.1016/J.CHEMOSPHERE.2022.135116.

[112] Y. Sun, B. Angelotti, M. Brooks, Z.W. Wang, Feast/famine ratio determined continuous flow aerobic granulation, Science of The Total Environment 750 (2021) 141467. https://doi.org/10.1016/J.SCITOTENV.2020.141467.

[113] S. López-Palau, A. Pinto, N. Basset, J. Dosta, J. Mata-Álvarez, ORP slope and feast–famine strategy as the basis of the control of a granular sequencing batch reactor treating winery wastewater, Biochem Eng J 68 (2012) 190–198. https://doi.org/10.1016/J.BEJ.2012.08.002.

[114] Y.Q. Liu, J.H. Tay, Influence of starvation time on formation and stability of aerobic granules in sequencing batch reactors, Bioresour Technol 99 (2008) 980–985. https://doi.org/10.1016/J.BIORTECH.2007.03.011.

[115] Y. V. Nancharaiah, G. Kiran Kumar Reddy, Aerobic granular sludge technology: Mechanisms of granulation and biotechnological applications, Bioresour Technol 247 (2018) 1128–1143. https://doi.org/10.1016/J.BIORTECH.2017.09.131.

[116] D. Gao, L. Liu, H. liang, W.M. Wu, Comparison of four enhancement strategies for aerobic granulation in sequencing batch reactors, J Hazard Mater 186 (2011) 320–327. https://doi.org/10.1016/J.JHAZMAT.2010.11.006.

[117] Y.Q. Liu, X. Zhang, R. Zhang, W.T. Liu, J.H. Tay, Effects of hydraulic retention time on aerobic granulation and granule growth kinetics at steady state with a fast start-up strategy, Appl Microbiol Biotechnol 100 (2016) 469–477. https://doi.org/10.1007/s00253-015-6993-3.

[118] Y.Q. Liu, J.H. Tay, Variable aeration in sequencing batch reactor with aerobic granular sludge, J Biotechnol 124 (2006) 338–346. https://doi.org/10.1016/J.JBIOTEC.2005.12.037.

[119] S. Lochmatter, C. Holliger, Optimization of operation conditions for the startup of aerobic granular sludge reactors biologically removing carbon, nitrogen, and phosphorous, Water Res 59 (2014) 58–70. https://doi.org/10.1016/J.WATRES.2014.04.011.

[120] Z. Song, Y. Pan, K. Zhang, N. Ren, A. Wang, Effect of seed sludge on characteristics and microbial community of aerobic granular sludge, Journal of Environmental Sciences 22 (2010) 1312–1318. https://doi.org/10.1016/S1001-0742(09)60256-4.

[121] X. chun Wang, Z. lin Chen, J. Kang, X. Zhao, J. min Shen, L. Yang, The key role of inoculated sludge in fast start-up of sequencing batch reactor for the domestication of aerobic granular sludge, Journal of Environmental Sciences 78 (2019) 127–136. https://doi.org/10.1016/J.JES.2018.08.008.

[122] S. Kosar, O. Isik, Y. Akdag, H. Gulhan, I. Koyuncu, H. Ozgun, M.E. Ersahin, Impact of seed sludge characteristics on granulation and performance of aerobic

granular sludge process, J Clean Prod 363 (2022) 132424. https://doi.org/10.1016/J.JCLEPRO.2022.132424.

[123] G. ping Sheng, A. jie Li, X. yan Li, H. qing Yu, Effects of seed sludge properties and selective biomass discharge on aerobic sludge granulation, Chemical Engineering Journal 160 (2010) 108–114. https://doi.org/10.1016/J.CEJ.2010.03.017.

[124] J. Zou, J. Yang, H. He, X. Wang, R. Mei, L. Cai, J. Li, Effect of Seed Sludge Type on Aerobic Granulation, Pollutant Removal and Microbial Community in a Sequencing Batch Reactor Treating Real Textile Wastewater, Int J Environ Res Public Health 19 (2022). https://doi.org/10.3390/ijerph191710940.

[125] P. Dangcong, N. Bernet, J.P. Delgenes, R. Moletta, Aerobic granular sludge—a case report, Water Res 33 (1999) 890–893. https://doi.org/10.1016/S0043-1354(98)00443-6.

[126] Y. Hou, C. Gan, R. Chen, Y. Chen, S. Yuan, Y. Chen, Structural characteristics of aerobic granular sludge and factors that influence its stability: A mini review, Water (Switzerland) 13 (2021). https://doi.org/10.3390/w13192726.

[127] Y. Liu, Z.W. Wang, L. Qin, Y.Q. Liu, J.H. Tay, Selection pressure-driven aerobic granulation in a sequencing batch reactor, Appl Microbiol Biotechnol 67 (2005) 26–32. https://doi.org/10.1007/s00253-004-1820-2.

[128] J.P. Bassin, Aerobic granular sludge technology, in: Advanced Biological Processes for Wastewater Treatment: Emerging, Consolidated Technologies and Introduction to Molecular Techniques, Springer International Publishing, 2017: pp. 75–142. https://doi.org/10.1007/978-3-319-58835-3_4.

[129] E.J.H. Van Dijk, V.A. Haaksman, M.C.M. Van Loosdrecht, M. Pronk, On the mechanisms for aerobic granulation-model based evaluation, Water Res 216 (2022). https://doi.org/10.1016/j.watres.2022.118365.

[130] M.C.M. Van Loosdrecht, J.J. Heijnen, H. Eberl, J. Kreft, & C. Picioreanu, Mathematical modelling of biofilm structures, Antonie Van Leeuwenhoek 81 (2002) 245–256.

[131] M.K. de Kreuk, M.C.M. van Loosdrecht, Selection of slow growing organisms as a means for improving aerobic granular sludge stability, Water Science and Technology 49 (2004) 9–17. https://doi.org/10.2166/wst.2004.0792.

[132] E.J.H. van Dijk, M. Pronk, M.C.M. van Loosdrecht, A settling model for full-scale aerobic granular sludge, Water Res 186 (2020). https://doi.org/10.1016/j.watres.2020.116135.

[133] M. Pronk, M.K. De Kreuk, B. De Bruin, P. Kamminga, R. Kleerebezem, M.C.M. Van Loosdrecht, Full scale performance of the aerobic granular sludge process for sewage treatment, (2015). https://doi.org/10.1016/j.watres.2015.07.011.

[134] D.R. de Graaff, E.J.H. van Dijk, M.C.M. van Loosdrecht, M. Pronk, Strength characterization of full-scale aerobic granular sludge, Environmental Technology (United Kingdom) 41 (2020) 1637–1647. https://doi.org/10.1080/09593330.2018.1543357.

[135] R.D.G. Franca, H.M. Pinheiro, M.C.M. van Loosdrecht, N.D. Lourenço, Stability of aerobic granules during long-term bioreactor operation, Biotechnol Adv 36 (2018) 228–246. https://doi.org/10.1016/j.biotechadv.2017.11.005.

[136] K.S. Shameem, P.C. Sabumon, A Review on the Stability, Sustainability, Storage and Rejuvenation of Aerobic Granular Sludge for Wastewater Treatment, Water (Basel) 15 (2023) 950. https://doi.org/10.3390/w15050950.

[137] S.S. Adav, D.J. Lee, K.Y. Show, J.H. Tay, Aerobic granular sludge: Recent advances, Biotechnol Adv 26 (2008) 411–423. https://doi.org/10.1016/j.biotechadv.2008.05.002.

[138] K. Milferstedt, J. Hamelin, C. Park, J. Jung, Y. Hwang, S.K. Cho, K.W. Jung, D.H. Kim, Biogranules applied in environmental engineering, Int J Hydrogen Energy 42 (2017) 27801–27811. https://doi.org/10.1016/j.ijhydene.2017.07.176.

[139] S.J. Sarma, J.H. Tay, A. Chu, Finding Knowledge Gaps in Aerobic Granulation Technology, Trends Biotechnol 35 (2017) 66–78. https://doi.org/10.1016/j.tibtech.2016.07.003.

[140] Y. Liu, S.F. Yang, J.H. Tay, Q.S. Liu, L. Qin, Y. Li, Cell hydrophobicity is a triggering force of biogranulation, Enzyme Microb Technol 34 (2004) 371–379. https://doi.org/10.1016/j.enzmictec.2003.12.009.

[141] Y. Liu, S.F. Yang, Q.S. Liu, J.H. Tay, The role of cell hydrophobicity in the formation of aerobic granules, Curr Microbiol 46 (2003) 270–274. https://doi.org/10.1007/s00284-002-3878-3.

[142] J.-H. Tay, V. Ivanov, S. Pan, T.-L. Tay, Specific layers in aerobically grown microbial granules, Lett Appl Microbiol 34 (2002) 254–257. https://academic.oup.com/lambio/article/34/4/254/6704306.

[143] D. Gao, L. Liu, H. Liang, W.M. Wu, Aerobic granular sludge: Characterization, mechanism of granulation and application to wastewater treatment, Crit Rev Biotechnol 31 (2011) 137–152. https://doi.org/10.3109/07388551.2010.497961.

[144] S.P. Wei, H.D. Stensel, B. Nguyen Quoc, D.A. Stahl, X. Huang, P.H. Lee, M.K.H. Winkler, Flocs in disguise? High granule abundance found in continuous-flow activated sludge treatment plants, Water Res 179 (2020). https://doi.org/10.1016/j.watres.2020.115865.

[145] C. Sanchez-Sanchez, E. Moreno-Rodríguez, J.A. Ortiz-Cruz, G.E. Moeller-Chávez, Development of aerobic granular sludge for real industrial/municipal wastewater treatment, Water Science and Technology 87 (2023) 2328–2344. https://doi.org/10.2166/wst.2023.121.

[146] L. Wang, X. Liu, D.J. Lee, J.H. Tay, Y. Zhang, C.L. Wan, X.F. Chen, Recent advances on biosorption by aerobic granular sludge, J Hazard Mater 357 (2018) 253–270. https://doi.org/10.1016/J.JHAZMAT.2018.06.010.

[147] K. Şekercioğlu, Investigation of Nickel Recovery by Biogranules Tailored for Metal Recovery Through Biomineralization, Hacettepe University, 2022.

[148] M. Sonmez, Y.Ç. Erşan, Production and compatibility assessment of denitrifying biogranules tailored for self-healing concrete applications, Cem Concr Compos 126 (2022) 104344. https://doi.org/10.1016/j.cemconcomp.2021.104344.

[149] F.B. Da Silva, N. De Belie, N. Boon, W. Verstraete, Production of non-axenic ureolytic spores for self-healing concrete applications, Constr Build Mater 93 (2015) 1034–1041. https://doi.org/10.1016/j.conbuildmat.2015.05.049.

[150] Y. Song, K. Chetty, U. Garbe, J. Wei, H. Bu, L. O'moore, X. Li, Z. Yuan, T. McCarthy, G. Jiang, A novel granular sludge-based and highly corrosion-resistant

bio-concrete in sewers, Science of The Total Environment 791 (2021) 148270. https://doi.org/10.1016/J.SCITOTENV.2021.148270.

[151] W.C. Lipps, E.B. Braun-Howland, T.E. Baxter, eds., Standard Methods for the Examination of Water and Wastewater, 24th ed., American Waterworks Association, 2016.

[152] Y.Q. Liu, B. Moy, Y.H. Kong, J.H. Tay, Formation, physical characteristics and microbial community structure of aerobic granules in a pilot-scale sequencing batch reactor for real wastewater treatment, Enzyme Microb Technol 46 (2010) 520–525. https://doi.org/10.1016/J.ENZMICTEC.2010.02.001.

[153] F. Silva, Up-scaling the production of bacteria for self-healing concrete application, Ghent University, 2015.

[154] X. Li, Y. Li, H. Liu, Z. Hua, G. Du, J. Chen, Characteristics of aerobic biogranules from membrane bioreactor system, J Memb Sci 287 (2007) 294–299. https://doi.org/10.1016/j.memsci.2006.11.005.

[155] J. Wan, Y. Bessière, M. Spérandio, Alternating anoxic feast/aerobic famine condition for improving granular sludge formation in sequencing batch airlift reactor at reduced aeration rate, Water Res 43 (2009) 5097–5108. https://doi.org/10.1016/j.watres.2009.08.045.

[156] M. Jia, M.K.H. Winkler, E.I.P. Volcke, Elucidating the Competition between Heterotrophic Denitrification and DNRA Using the Resource-Ratio Theory, Environ Sci Technol 54 (2020) 13953–13962. https://doi.org/10.1021/acs.est.0c01776.

[157] T.T. Ren, L. Liu, G.P. Sheng, X.W. Liu, H.Q. Yu, M.C. Zhang, J.R. Zhu, Calcium spatial distribution in aerobic granules and its effects on granule structure, strength and bioactivity, Water Res 42 (2008) 3343–3352. https://doi.org/10.1016/J.WATRES.2008.04.015.

[158] J. Wan, M. Sperandio, Possible role of denitrification on aerobic granular sludge formation in sequencing batch reactor, Chemosphere 75 (2009) 220–227. https://doi.org/10.1016/j.chemosphere.2008.11.069.

[159] J. Czarnota, A. Masłoń, Biogranulation and physical properties of aerobic granules in reactors at low organic loading rate and with powdered ceramsite added, Journal of Ecological Engineering 20 (2019). https://doi.org/10.12911/22998993/112489.

[160] J. Li, L. Bin Ding, A. Cai, G.X. Huang, H. Horn, Aerobic sludge granulation in a full-scale sequencing batch reactor, Biomed Res Int 2014 (2014). https://doi.org/10.1155/2014/268789.

[161] Y. Wan, D. Zhang, H. Liu, Y. Li, B. Hou, Influence of sulphate-reducing bacteria on environmental parameters and marine corrosion behavior of Q235 steel in aerobic conditions, Electrochim Acta 55 (2010) 1528–1534. https://doi.org/10.1016/j.electacta.2009.10.009.

[162] J.J. Beun, A. Hendriks, M.C.M. Van Loosdrecht, E. Morgenroth, P.A. Wilderer, J.J. Heijnen, Aerobic Granulation in a Sequencing Batch Reactor, Water Res 33 (1999) 2283–2290.

[163] Y. Liu, J.H. Tay, State of the art of biogranulation technology for wastewater treatment, Biotechnol Adv 22 (2004) 533–563. https://doi.org/10.1016/j.biotechadv.2004.05.001.

[164] O.T. Iorhemen, Y. Liu, Effect of feeding strategy and organic loading rate on the formation and stability of aerobic granular sludge, Journal of Water Process Engineering 39 (2021) 101709. https://doi.org/10.1016/J.JWPE.2020.101709.

[165] Y. Chen, W. Jiang, D.T. Liang, J.H. Tay, Aerobic granulation under the combined hydraulic and loading selection pressures, Bioresour Technol 99 (2008) 7444–7449. https://doi.org/10.1016/J.BIORTECH.2008.02.028.

[166] T. Urakami, J. Sasaki, K. Suzuki, K. Komagata, Characterization and description of Hyphomicrobium denitrificans sp. nov., Int J Syst Bacteriol (1995) 528–532.

[167] T. Osaka, S. Yoshie, S. Tsuneda, A. Hirata, N. Iwami, Y. Inamori, Identification of acetate- or methanol-assimilating bacteria under nitrate-reducing conditions by stable-isotope probing, Microb Ecol 52 (2006) 253–266. https://doi.org/10.1007/s00248-006-9071-7.

[168] C. Martineau, F. Mauffrey, R. Villemur, Comparative analysis of denitrifying activities of Hyphomicrobium nitrativorans, Hyphomicrobium denitrificans, and

Hyphomicrobium zavarzinii, Appl Environ Microbiol 81 (2015) 5003–5014. https://doi.org/10.1128/AEM.00848-15.

[169] J.-Y. Moon, J.-M. Lim, J.-H. Ahn, H.-Y. Weon, S.-W. Kwon, S.-J. Kim, C. Soo-Jin Kim, Paenalcaligenes suwonensis sp. nov., isolated from spent mushroom compost, Int J Syst Evol Microbiol (2014) 882–886. https://doi.org/10.1099/ijs.0.058412-0.

[170] J. Mitzscherling, J. Maclean, D. Lipus, A. Bartholomäus, K. Mangelsdorf, A. Lipski, V. Roddatis, S. Liebner, D. Wagner, Paenalcaligenes niemegkensis sp. nov., a novel species of the family Alcaligenaceae isolated from plastic waste, Int. J. Syst. Evol. Microbiol 72 (2022) 5333. https://doi.org/10.1099/ijsem.0.005333.

[171] A.S. Grabowski, B.J. Tindall, V. Ronique Bardin, D. Blanchet, C. Jeanthon, Petrimonas sulfuriphila gen. nov., sp. nov., a mesophilic fermentative bacterium isolated from a biodegraded oil reservoir, 55 (2005). https://doi.org/10.1099/ijs.0.63426-0.

[172] J. Booth, Chryseobacterium and Related Genera Infections, Elsevier (2007). http://www.dobugsneeddrugs.org/about.html (accessed May 5, 2024).

[173] P. Herzog, I. Winkler, D. Wolking, P. Kämpfer, A. Lipski, Chryseobacterium ureilyticum sp. nov., chryseobacterium gambrini sp. nov., chryseobacterium pallidum sp. nov. and chryseobacterium molle sp. nov., isolated from beer-bottling plants, Int J Syst Evol Microbiol 58 (2008) 26–33. https://doi.org/10.1099/ijs.0.65362-0.

[174] B. Andreas, F.A. Rainey, E. Stackebrandt, J. Winter, Characterization of Aquamicrobium defluvii gen. nov. sp. nov., a thiophene-2-carboxylate-metabolizing bacterium from activated sludge, (n.d.).

[175] H.M. Jin, J.M. Kim, C. Ok, J. Correspondence, C.O. Jeon, Aquamicrobium aestuarii sp. nov., a marine bacterium isolated from a tidal flat, Int J Syst Evol Microbiol 63 (2013). https://doi.org/10.1099/ijs.0.048561-0.

[176] S.-H. Yoo, H.-Y. Weon, B.-Y. Kim, J.-H. Kim, Y.-K. Baek, S.-W. Kwon, S.-J. Go, E. Stackebrandt, Pseudoxanthomonas yeongjuensis sp. nov., isolated from soil cultivated with Korean ginseng, Int J Syst Evol Microbiol 57 (2007) 646–649. https://doi.org/10.1099/ijs.0.64427-0.

[177] B.R. Mohapatra, A. Mazumder, Comparative efficacy of five different rep-PCR methods to discriminate Escherichia coli populations in aquatic environments, Water Science and Technology 58 (2008) 537–547. https://doi.org/10.2166/WST.2008.424.

[178] K. Kumari, P. Sharma, K. Tyagi, R.L. Correspondence, R. Lal, Pseudoxanthomonas indica sp. nov., isolated from a hexachlorocyclohexane dumpsite, Int J Syst Evol Microbiol (2011) 2107–2111. https://doi.org/10.1099/ijs.0.017624-0.

[179] K.A. Bernard, A. Vachon, A.L. Pacheco, T. Burdz, D. Wiebe, D.R. Beniac, S.L. Hiebert, T. Booth, D.A. Doyle, P. Lawson, A.M. Bernier, Pseudoxanthomonas winnipegensis sp. nov., derived from human clinical materials and recovered from cystic fibrosis and other patient types in canada, and emendation of pseudoxanthomonas spadix Young et al. 2007, Int J Syst Evol Microbiol 70 (2020) 6313–6322. https://doi.org/10.1099/ijsem.0.004533.

[180] Z. Sun, F. Dai, Y. Yan, L. Guo, H. Gu, J. Xu, Q. Ren, Pseudoxanthomonas beigongshangi sp. nov., a novel bacteria with predicted nitrite and nitrate reduce ability isolated from pit mud of Baijiu, Antonie van Leeuwenhoek, International Journal of General and Molecular Microbiology 114 (2021) 1307–1314. https://doi.org/10.1007/S10482-021-01603-W/TABLES/2.

[181] B. La Scola, M.N. Mallet, P.A.D. Grimont, D. Raoult, Bosea eneae sp. nov., Bosea massiliensis sp. nov. and Bosea vestrisii sp. nov., isolated from hospital water supplies, and emendation of the genus Bosea (Das et al. 1996), Int J Syst Evol Microbiol 53 (2003) 15–20. https://doi.org/10.1099/ijs.0.02127-0.

[182] A.L. Sazanova, V.I. Safronova, I.G. Kuznetsova, D.S. Karlov, A.A. Belimov, E.E. Andronov, E.R. Chirak, J.P. Popova, A. V Verkhozina, A. Willems, I.A. Tikhonovich, Bosea caraganae sp. nov. a new species of slow-growing bacteria isolated from root nodules of the relict species Caragana jubata (Pall.) Poir. originating from Mongolia, Int J Syst Evol Microbiol 69 (2019) 2687–2695. https://doi.org/10.1099/ijsem.0.003509.

[183] K.M. Goh, H.M. Gan, K.-G. Chan, G.F. Chan, S. Shahar, Analysis of Anoxybacillus Genomes from the Aspects of Lifestyle Adaptations, Prophage

Diversity, and Carbohydrate Metabolism, PLoS One 9 (2014) 90549. https://doi.org/10.1371/journal.pone.0090549.

[184] W. Hassan, Y. Jaf, M. Emre Erez, M. Ertas, Determination of extracellular hydrolytic enzyme capabilities of some Anoxybacillus isolated from hot spring environments, (2022). https://doi.org/10.51753/flsrt.1094629.

[185] L. Liu, Y. Feng, L. Wei, Z. Zong, Genome-Based Taxonomy of Brevundimonas with Reporting Brevundimonas huaxiensis sp. nov. , Microbiol Spectr 9 (2021). https://doi.org/10.1128/SPECTRUM.00111-21.

[186] L. Zhang, Q. Li, C. Chen, X. Li, M. Li, J. Hu, X. Shen, Propioniciclava sinopodophylli sp. nov., isolated from leaves of Sinopodophyllum hexandrum (Royle) Ying TAXONOMIC DESCRIPTION, Int J Syst Evol Microbiol 67 (2017) 4111–4115. https://doi.org/10.1099/ijsem.0.002265.

[187] M.H. Zainudin, N. Asyifah Mustapha, T. Maeda, N. Ramli, K. Sakai, M. Hassan, Biochar enhanced the nitrifying and denitrifying bacterial communities during the composting of poultry manure and rice straw, (2020). https://doi.org/10.1016/j.wasman.2020.03.029.

[188] A. van Belkum, COGEM RESEARCH REPORT CLASSIFICATION OF BACTERIAL PATHOGENS, 2011.

[189] Commissie Genetische Modificatie (COGEM) Classification of Organisms: Pathogenicity classification of Bacteria, 2023. https://wetten.overheid.nl/BWBR0035072/2023-10-01.

[190] R. Du, Y. Peng, J. Ji, L. Shi, R. Gao, X. Li, Partial denitrification providing nitrite: Opportunities of extending application for anammox, Environ Int 131 (2019). https://doi.org/10.1016/j.envint.2019.105001.

[191] G. Yilmaz, R. Lemaire, J. Keller, Z. Yuan, Simultaneous nitrification, denitrification, and phosphorus removal from nutrient-rich industrial wastewater using granular sludge, Biotechnol Bioeng 100 (2008) 529–541. https://doi.org/10.1002/bit.21774.

[192] J. Wang, X. Wang, Z. Zhao, J. Li, Organics and nitrogen removal and sludge stability in aerobic granular sludge membrane bioreactor, Appl Microbiol Biotechnol 79 (2008) 679–685. https://doi.org/10.1007/s00253-008-1466-6.

[193] J. Zhao, J. Wu, X. Li, S. Wang, B. Hu, X. Ding, The denitrification characteristics and microbial community in the cathode of an mfc with aerobic denitrification at high temperatures, Front Microbiol 8 (2017). https://doi.org/10.3389/fmicb.2017.00009.

[194] P. Kundu, A. Pramanik, A. Dasgupta, S. Mukherjee, J. Mukherjee, Simultaneous heterotrophic nitrification and aerobic denitrification by Chryseobacterium sp. R31 isolated from abattoir wastewater, Biomed Res Int 2014 (2014). https://doi.org/10.1155/2014/436056.

[195] Z. Qiao, R. Sun, Y. Wu, S. Hu, X. Liu, J. Chan, X. Mi, Characteristics and metabolic pathway of the bacteria for heterotrophic nitrification and aerobic denitrification in aquatic ecosystems, Environ Res 191 (2020). https://doi.org/10.1016/j.envres.2020.110069.

[196] J. Chen, J. Zheng, Y. Li, H. hong Hao, J. meng Chen, Characteristics of a novel thermophilic heterotrophic bacterium, Anoxybacillus contaminans HA, for nitrification–aerobic denitrification, Appl Microbiol Biotechnol 99 (2015) 10695–10702. https://doi.org/10.1007/s00253-015-6870-0.

[197] P. Lv, J. Luo, X. Zhuang, D. Zhang, Z. Huang, Z. Bai, Diversity of culturable aerobic denitrifying bacteria in the sediment, water and biofilms in Liangshui River of Beijing, China, Sci Rep 7 (2017). https://doi.org/10.1038/s41598-017-09556-9.

[198] A.I. Omoregie, G. Khoshdelnezamiha, N. Senian, D.E.L. Ong, P.M. Nissom, Experimental optimisation of various cultural conditions on urease activity for isolated Sporosarcina pasteurii strains and evaluation of their biocement potentials, Ecol Eng 109 (2017) 65–75. https://doi.org/10.1016/j.ecoleng.2017.09.012.

[199] Y.Ç. Erşan, F.B. Da Silva, N. Boon, W. Verstraete, N. De Belie, Screening of bacteria and concrete compatible protection materials, Constr Build Mater 88 (2015) 196–203. https://doi.org/10.1016/j.conbuildmat.2015.04.027.

[200] V. Achal, A. Mukherjee, P.C. Basu, M.S. Reddy, Lactose mother liquor as an alternative nutrient source for microbial concrete production by Sporosarcina pasteurii, J Ind Microbiol Biotechnol 36 (2009) 433–438. https://doi.org/10.1007/s10295-008-0514-7.

[201] J. Zhang, B. Mai, T. Cai, J. Luo, W. Wu, B. Liu, N. Han, F. Xing, X. Deng, Optimization of a binary concrete crack self-healing system containing bacteria and oxygen, Materials 10 (2017). https://doi.org/10.3390/ma10020116.

[202] Y.Q. Liu, W.W. Wu, J.H. Tay, J.L. Wang, Starvation is not a prerequisite for the formation of aerobic granules, Appl Microbiol Biotechnol 76 (2007) 211–216. https://doi.org/10.1007/s00253-007-0979-8.

[203] Y. Fernández-Nava, E. Marañón, J. Soons, L. Castrillón, Denitrification of wastewater containing high nitrate and calcium concentrations, Bioresour Technol 99 (2008) 7976–7981. https://doi.org/10.1016/j.biortech.2008.03.048.

ANNEX

ANNEX 1. COD Calibration Curve

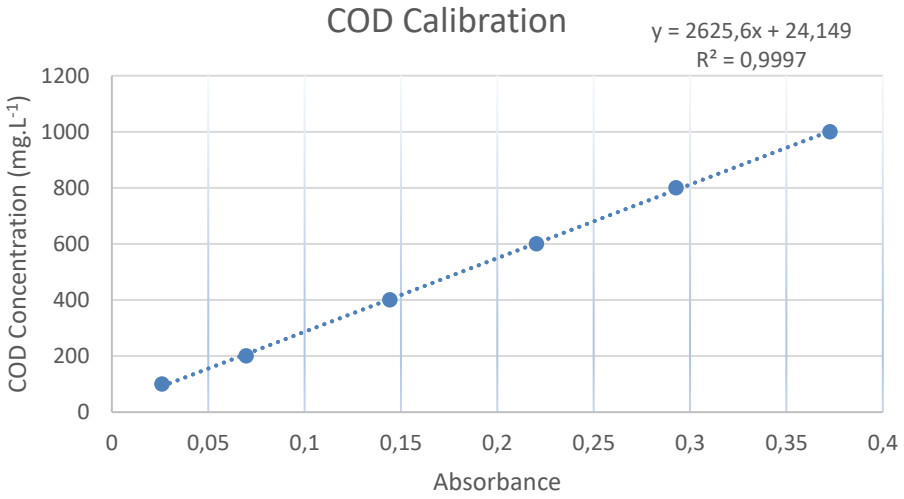

Figure Annex 1. COD Calibration Curve

ANNEX 2. Nitrate Reduction Reaction Kinetics

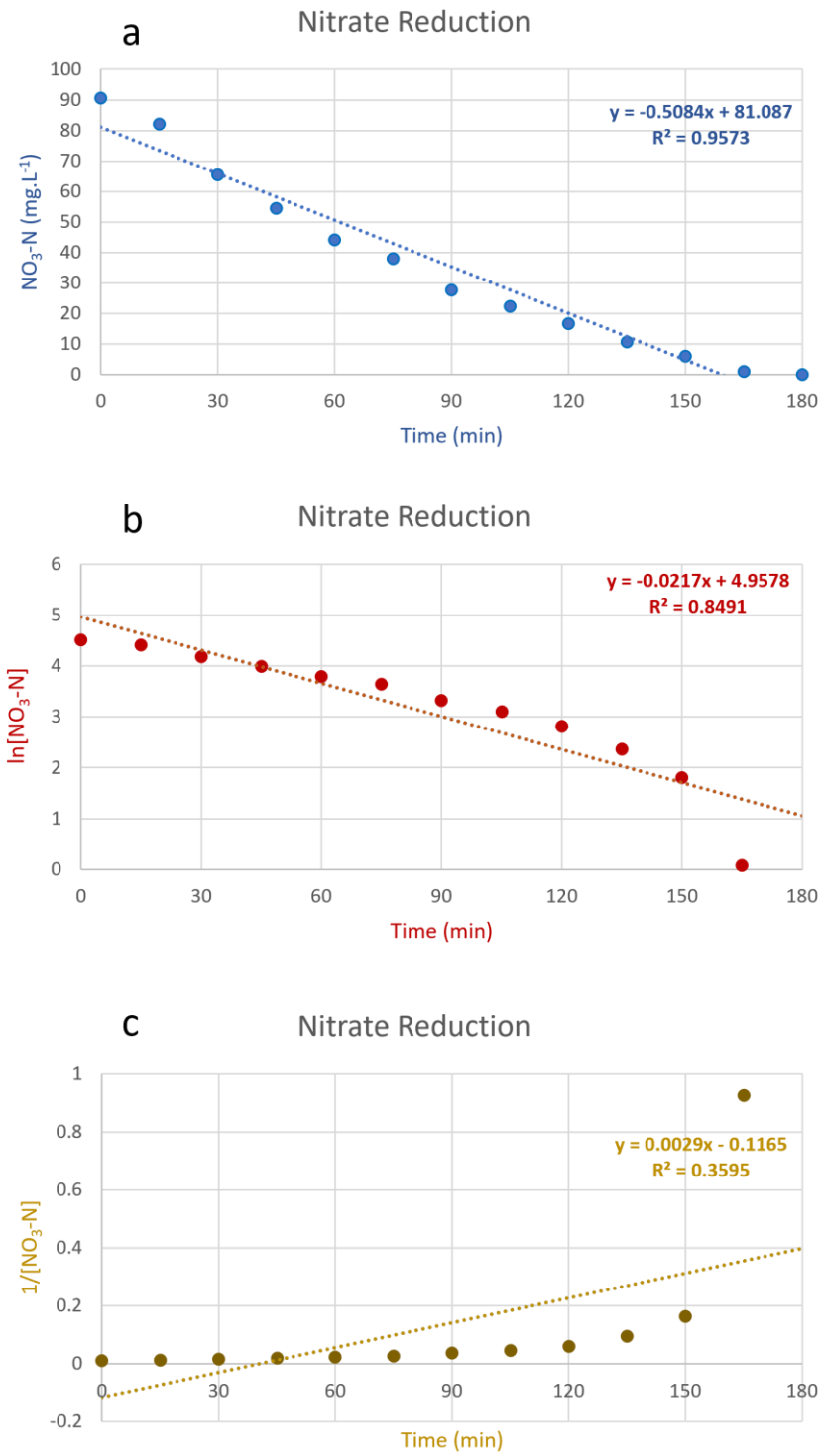

Figure Annex 2. Nitrate reduction of a single cycle a) zero b) first c) second-order reaction kinetics

ANNEX 3. Urea Hydrolysis Reaction Kinetics

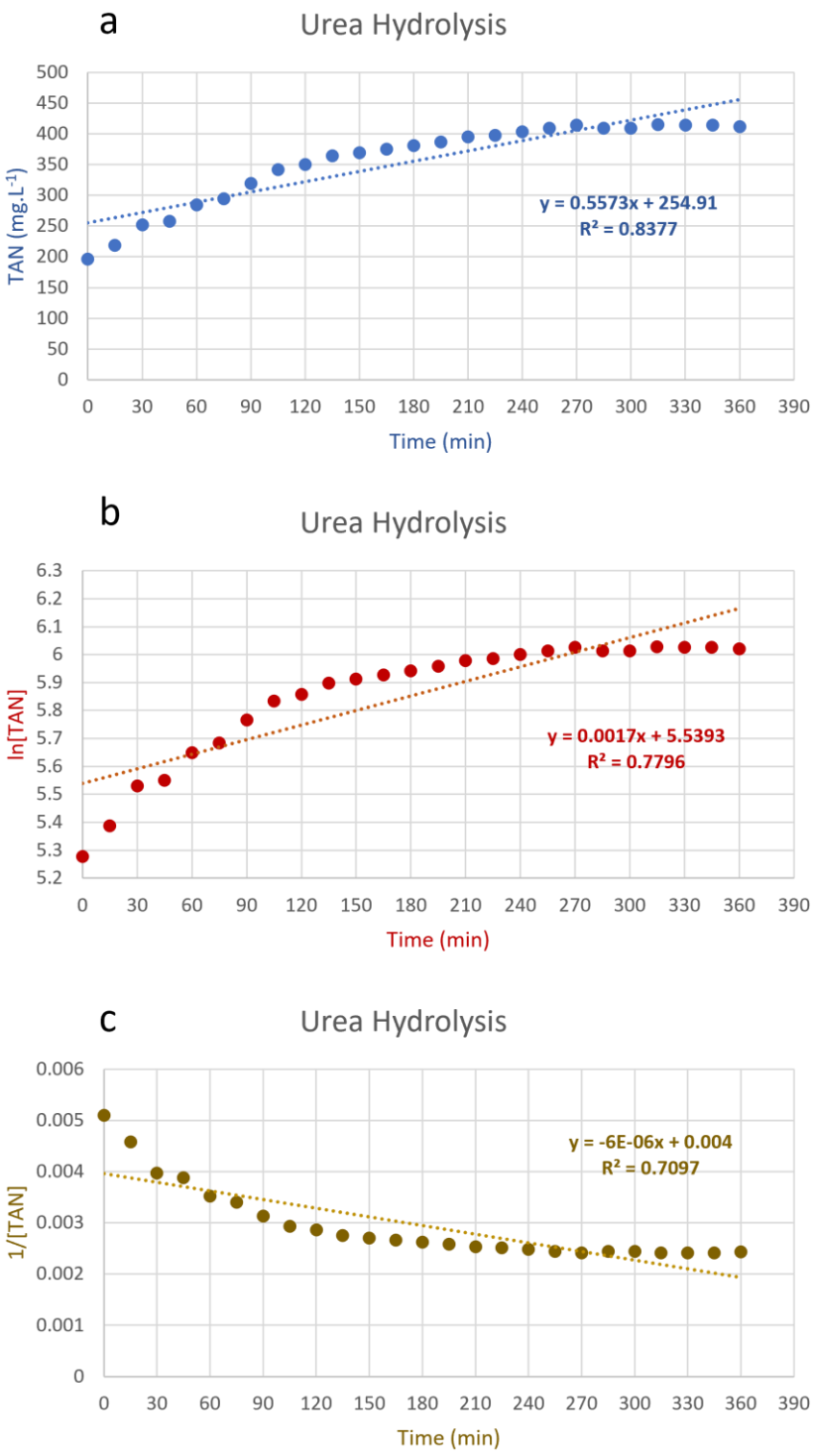

Figure Annex 3. Urea hydrolysis of a single cycle a) zero b) first c) second-order reaction kinetics

ANNEX 4. COD Consumption Reaction Kinetics

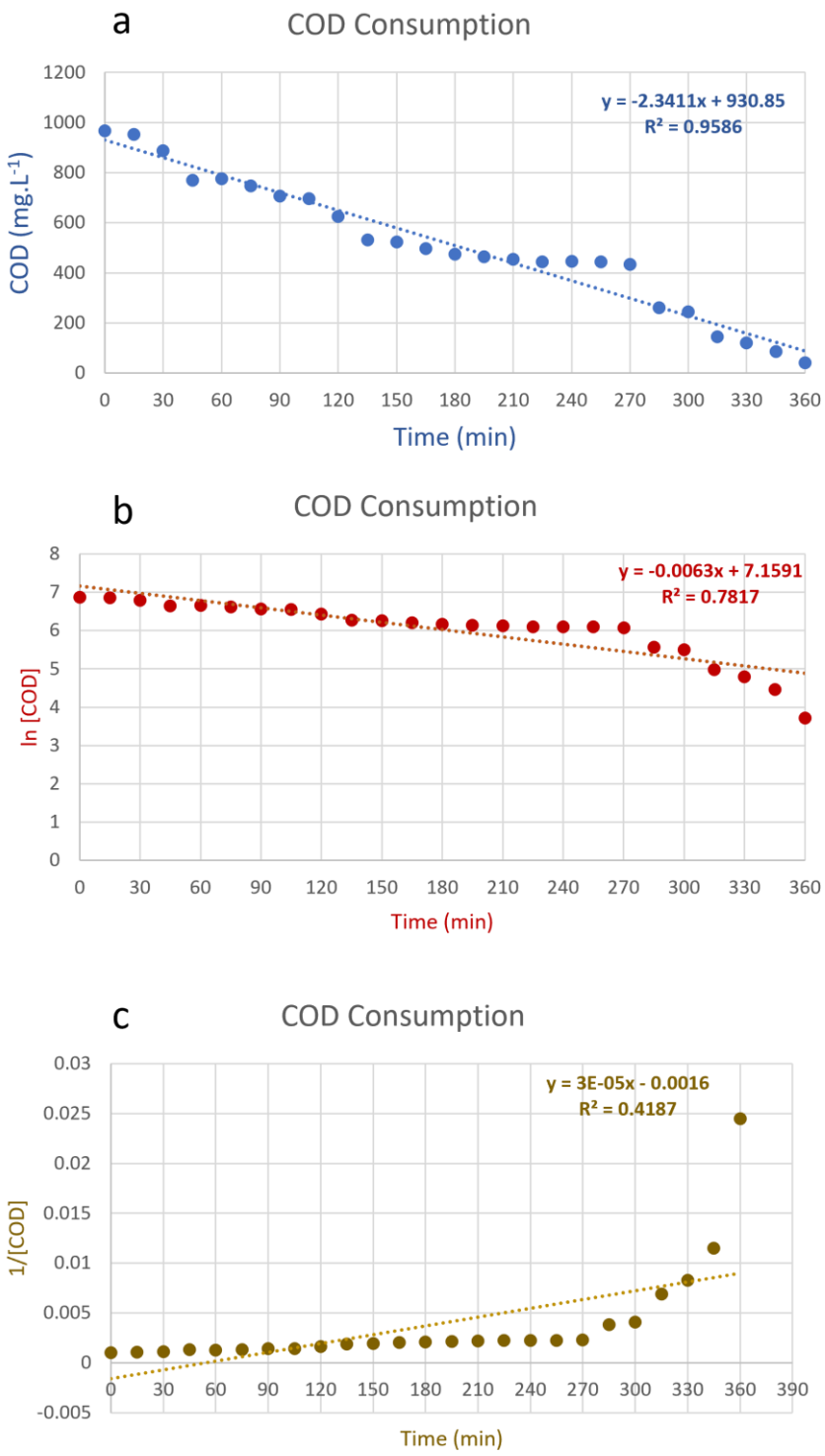

Figure Annex 4. Organic carbon consumption of a single cycle a) zero b) first c) second-order reaction kinetics

ANNEX 5. Conference Papers Derived from Thesis

M. Soluk, B. Kardoğan, Y. Çağatay Erşan, Biogranules Simultaneously Hydrolyzing Urea and Reducing Nitrate and Their Biomineralization Performance, in: 6th Eurasia Waste Management Symposium, İstanbul, 2022.